

Forthcoming Topics in Seminars in Ultrasound, CT, and MRI

Vol 36, No 6, December 2015—Prenatal MRI

Previous Topics

Vol 36, No 4, August 2015 - Magnetic Resonance Imaging in Obstetrics and Gynecology

Vol 36, No 3, June 2015—Imaging of Functional and Dysfunctional Neurologic Systems

Vol 36, No 2, April 2015—Neonatal Imaging-Part II

Vol 36, No 1, February 2015—Foreign Bodies

Vol 35, No 6, December 2014—Neonatal Imaging-Part 1

Vol 35, No 5, October 2014—Brain White Matter Tracts: Functional Anatomy and Pathology

Vol 35, No 4, August 2014—Imaging of Infants and Children: State-of-the-art Dose Reduction Strategies

Vol 35, No 3, June 2014—The Great Mimickers

Vol 35, No 2, April 2014—Toxic and Metabolic Encephalopathic Syndromes

Vol 35, No 1, February 2014—Interstitial Pneumonia and Related Diseases

Vol 34, No 6, December 2013—Radiological Imaging in Hematological Disorders

Vol 34, No 5, October 2013—Central Skull Base

Vol 34, No 4, August 2013—Imaging of Contemporary Gastrointestinal Interventions

Vol 34, No 3, June 2013—Small Parts Ultrasound

Vol 34, No 2, April 2013—Brainstem Part 2

Vol 34, No 1, February 2013—Hepatobiliary Radiology

Vol 33, No 6, December 2012—The Pulmonary Vasculature

Vol 33, No 5, October 2012—Cervical Lymphadenopathy

Vol 33, No 4, August 2012—Errors and Malpractice in Radiology

Vol 33, No 3, June 2012—Imaging of the Aorta

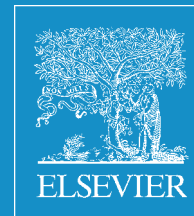
Vol 33, No 2, April 2012—Thyroid and Parathyroid Imaging

Vol 33, No 1, February 2012—Multimodality Imaging of the Pregnant Patient

Vol 32, No 6, December 2011—Congenital/Developmental Brain Abnormalities, Part II

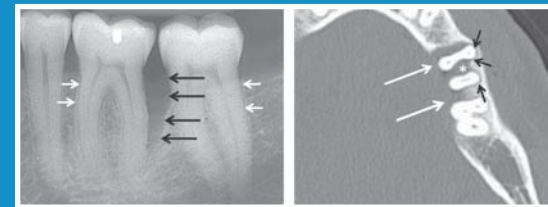
Vol 32, No 5, October 2011—Sarcomas

Vol 32, No 4, August 2011—Breast Cancer Screening and Diagnosis: State of the Art



VOL 36, NO 5
OCTOBER 2015

Seminars in ULTRASOUND CT and MRI



Editors:

Howard W. Raymond, MD

Joel D. Swartz, MD

Gabriela Gayer, MD

Dental Imaging

Guest Editor - James J. Abrahams, MD

- Embryology and Anatomy of the Jaw and Dentition
- Imaging of the jaws
- Dental Implants
- Dental Implant Complications
- Inflammatory Diseases of the Teeth and Jaws
- Lesions of the Jaw

<http://www.sem ultrasoundctmri.com>

Seminars in ULTRASOUND *CT and MRI*

**HOWARD W. RAYMOND, MD, JOEL D. SWARTZ, MD, and
GABRIELA GAYER, MD**

Publication information: *Seminars in Ultrasound, CT and MRI* (ISSN: 0887-2171) is published bimonthly by Elsevier Inc., 360 Park Avenue South, New York, NY 10010-1710. Months of issue are February, April, June, August, October, and December. Periodicals postage paid at New York, NY and additional mailing offices.

USA POSTMASTER: Send address changes to *Seminars in Ultrasound, CT and MRI*, Elsevier Customer Service Department, 3251 Riverport Lane, Maryland Heights, MO 63043, USA.

Editorial correspondence should be addressed to Howard W. Raymond, MD, 50 Lindor Heights, Holyoke, MA 01040; Joel D. Swartz, MD, 1210 Page Terrace, Villanova, PA 19085-2132; and Gabriela Gayer, MD, Assaf Harofeh Medical Center, Zerifin 70300, Israel.

Correspondence regarding subscriptions or change of address should be addressed to Elsevier Health Sciences Division, Subscription Customer Service, 3251 Riverport Lane, Maryland Heights, MO 63043.

Change of address notices, including both the old and new addresses of the subscriber, should be sent to the Publisher at least one month in advance.

Customer Service: Tel: 1-800-654-2452 (U.S. and Canada); 314-447-8871 (outside U.S. and Canada). Fax: 314-447-8029. E-mail: JournalCustomerService-usa@elsevier.com (for print support); JournalsOnlineSupportusa@elsevier.com (for online support).

Yearly subscription rates: United States and possessions: individual, \$368.00; student and resident, \$185.00. All other countries: individual, \$421.00; student and resident, \$241.00. For all areas outside the United States and possessions, there is no additional charge for surface delivery. To receive student/resident rate, orders must be accompanied by name of affiliated institution, date of term, and the *signature* of program/residency coordinator on institution letterhead. Orders will be billed at individual rate until proof of status is received. Prices are subject to change without notice. Current prices are in effect for back volumes and back issues. Single issues, both current and back, exist in limited quantities and are offered for sale subject to availability. Back issues sold in conjunction with a subscription are on a prorated basis.

©2015 Elsevier Inc. All rights reserved.

This journal and the individual contributions contained in it are protected under copyright by Elsevier Inc., and the following terms and conditions apply to their use:

Photocopying

Single photocopies of single articles may be made for personal use as allowed by national copyright laws. Permission of the Publisher and payment of a fee is required for all other photocopying, including multiple or systematic copying, copying for advertising or promotional purposes, resale, and all forms of document delivery. Special rates are available for educational institutions that wish to make photocopies for non-profit educational classroom use.

For information on how to seek permission visit www.elsevier.com/permissions or call: (+44) 1865 843830 (UK)/(+1) 215 239 3804 (USA).

Derivative Works

Subscribers may reproduce tables of contents or prepare lists of articles including abstracts for internal circulation within their institutions. Permission of the Publisher is required for resale or distribution outside the institution. Permission of the Publisher is required for all other derivative works, including compilations and translations (please consult www.elsevier.com/permissions).

Electronic Storage or Usage

Permission of the Publisher is required to store or use electronically any material contained in this journal, including any article or part of an article (please consult www.elsevier.com/permissions).

Except as outlined above, no part of this publication may be reproduced, stored in a retrieval system or transmitted in any form or by any means, electronic, mechanical, photocopying, recording or otherwise, without prior written permission of the Publisher.

Notice

No responsibility is assumed by the Publisher for any injury and/or damage to persons or property as a matter of products liability, negligence or otherwise, or from any use or operation of any methods, products, instructions or ideas contained in the material herein. Because of rapid advances in the medical sciences, in particular, independent verification of diagnoses and drug dosages should be made.

Although all advertising material is expected to conform to ethical (medical) standards, inclusion in this publication does not constitute a guarantee or endorsement of the quality or value of such product or of the claims made of it by its manufacturer.

Advertising representative: Cunningham Associates, 180 Old Tappan Rd, Old Tappan, NJ 07675. Tel: 201-767-4170; Fax: 201-767-2784.

The contents of *Seminars in Ultrasound, CT, and MRI* are indexed and included in *Index Medicus*, *EMBASE/Excerpta Medica*, *RSNA Index to Imaging Literature*, *Science Citation Index*, *Biosis*, *CINAHL® database* and *Current Contents & Clinical Medicine*.

Seminars in ULTRASOUND *CT and MRI*

Dental Imaging

VOL 36, NO 5

OCTOBER 2015

Table of Contents

Letter From the Guest Editor: Imaging of the Jaw	<i>James J. Abrahams</i>	395
Embryology and Anatomy of the Jaw and Dentition.....	<i>Vahe M. Zohrabian, Colin S. Poon, and James J. Abrahams</i>	397
Imaging of the jaws.....	<i>Lisa J Koenig</i>	407
Dental Implants.....	<i>Vahe M. Zohrabian, Michael Sonick, Debby Hwang, and James J. Abrahams</i>	415
Dental Implant Complications	<i>Kevin Liaw, Ronald H. Delfni, and James J. Abrahams</i>	427
Inflammatory Diseases of the Teeth and Jaws	<i>Vahe M. Zohrabian and James J. Abrahams</i>	434
Lesions of the Jaw.....	<i>Kristine M. Moser</i>	444

Seminars in ULTRASOUND *CT and MRI*

EDITORS

HOWARD W. RAYMOND, MD
Holyoke Medical Center
Holyoke, MA, USA

JOEL D. SWARTZ, MD
Germantown Imaging Associates
Gladwyne, PA, USA

GABRIELA GAYER, MD
Assaf Harofeh Medical Center
Zerifin, Israel

EDITORIAL BOARD

JAN WALTHER CASSELMAN
MRI and Head and Neck Radiology
AZ St - Jan Brugge
Bruges, Belgium

HUGH CURTIN, MD
Massachusetts Eye and Ear Infirmary
Boston, MA

NYREE GRIFFIN, MD, FRCR
Guy's and St. Thomas' NHS Foundation Trust
London, UK

H. RIC HARNBERGER, MD
University of Utah School of Medicine
Salt Lake City, UT

OLIVIER HÉLÉNON, MD
Hôpital Necker
Paris, France

ARI LEPPÄNIEMI, MD
Helsinki University Central Hospital
Helsinki, Finland

KOICHI NISHIMURA, MD
National Center for Geriatrics and Gerontology
Obu, Japan

STEPHEN C. O'CONNOR, MD
Department of Radiology
Baystate Medical Center and Children's Hospital
Springfield, MA

ANTONIO PINTO, MD, PhD
Department of Radiology
Cardarelli Hospital
Naples, Italy

MAHESH K. SHETTY, MD, FRCR, FACR, FAIUM
Baylor College of Medicine
Woman's Hospital of Texas
Houston, TX

FRANCIS VEILLON, MD
Hôpital de Hautepierre
Strasbourg, France

Letter From the Guest Editor: Imaging of the Jaw



Why do radiologists find imaging of the jaw and teeth difficult and intimidating? A large part of the reason is because dental professionals traditionally did this imaging in their office using plane radiographs. As a result, radiologists were never involved or trained in this area, making it foreign to them.

So why did this all change? In the mid 1980s dental implants (metallic posts surgically implanted into the jaw to support a dental prosthesis) became quite popular and thus the preoperative evaluation of these patients became common. To determine if sufficient bone existed in the jaw to support an implant, dentists performed panoramic radiographs. Unfortunately, the panoramic radiographs could only give information regarding the height of the bone but not the thickness. As a result, patients that appeared to have enough bone height on the panoramic radiographs were operated on only to find out at surgery that there was insufficient bone thickness to support an implant. Very embarrassing for the dentist to suture the patient closed and has to explain that he could not get the implant in!

In an attempt to find a better method of evaluating these patients radiographically, a dentist in California approached his friend, the radiologist, with this dilemma. The result of this interaction was the development of a computed tomographic (CT) reformatting program called DentaScan that enabled accurate measurements of both the height and width of the jaw.^{1,2}

Interestingly, a former Yale University neuroradiologist named Steven Rothman was one of the initial authors of these articles describing DentaScan. At that time, he was doing innovative work with reformatted CT imaging and was therefore invited back to Yale to give Grand Rounds. Remember, reformatted imaging was almost unheard of then and was in its infancy.

Of course, at the Grand Rounds I was one of the eager Yale junior faculty in the audience. Intrigued by his work, I soon found myself on a plane to California where I spent a week learning the technology to bring it back to Yale. At the same time I was actively getting involved with the dental imaging; Dr Rothman's practice fell apart and DentaScan was sold to

General Electric who had no idea what to do with it and naturally contacted me as a consultant to refine and promote the program.

I submitted multiple radiology abstracts and manuscripts but to no avail. Not one was accepted. Why? Because radiologists had no interest in teeth! So what did I do? I submitted the manuscripts to those who had interest, the dentists. They thought this was the best thing since toothpaste. The next thing I knew I was publishing in the dental literature and getting invited all over the country to talk about dental imaging. Of course, the dentists who did not have CT scanners in their offices began knocking on the door of their radiologists demanding that they start doing this "amazing" imaging. As a result, my manuscripts finally began being accepted into the radiology literature and that opened the door to a new area of imaging for radiologists, the jaw and teeth!

This has had a significant effect on patient care, because patients who previously were only imaged using radiographs in the dentist's office, could now be more appropriately imaged by radiologists using CT and magnetic resonance imaging. Not only patients undergoing dental implant are now evaluated in this fashion, but also patients with tumors, lesions, and other complex issues related to the teeth and jaws.

So I hate to tell you this, but we are stuck with this imaging now. I have therefore dedicated this issue of the Seminars toward educating those that are unfamiliar with imaging this region of the body. Chapter 1, "Embryology and Anatomy of the Jaws & Dentition," is designed to bring the reader up to speed regarding the basic anatomy of the teeth and jaws, which is vital to understanding the pathology of this region. It also familiarizes the reader with some of the terminology used by dentists.

Chapter 2, "Imaging of the Jaws" is written by a dentist and thus provides the dentist's perspective. It covers the various imaging modalities including intraoral bitewing and periapical films, panoramic radiographs, cone-beam CT, and conventional CT. Dental caries is discussed here as well as in chapter 5, "Inflammatory Disease of the Teeth and Jaws" and some pertinent anatomy is reviewed.

Chapter 3, "Dental Implants and Guided Tissue Regeneration" delves into dental implants and discusses the various

types of implants and the components of the root-form implant. The actual surgical procedure is described and illustrated through various clinical cases. This chapter also discusses guided tissue regeneration and the various surgical procedures that are available to increase bone in patients that do not initially have a sufficient amount for implants.

Although dental implants are typically quite successful, there is always the unfortunate patient that has a complication. Chapter 4, "Complications of Dental Implants" categorizes the various complications and reviews their treatment.

Chapter 5, "Inflammatory Disease of the Teeth and Jaws" covers dental caries, periodontal disease and its treatment and periapical (endodontal) disease and its treatment. The extra dental manifestations of these infections would also be discussed.

Finally, no book is complete without a chapter discussing the various tumors and lesions of the jaw. Chapter 6, "Lesions of the Jaw" does just this.

I do suspect that this little editorial I have written is a "mouthful," but the Seminars issue itself should be something you can really get your "teeth" into. Enjoy and do not forget to floss.

James J. Abrahams

Guest Editor

*Department of Diagnostic Radiology, Yale University School
of Medicine, Haven, CT*

References

1. Schwarz MS, Rothman SLG, Rhodes ML, et al: Computed tomography: 1. Preoperative assessment of the mandible for endosseous implant surgery. *Int J Oral Maxillofac Implants* 2:137-141, 1987
2. Schwarz MS, Rothman SLG, Rhodes ML, et al: Computed tomography: 2. Preoperative assessment of the maxilla for endosseous implant surgery. *Int J Oral Maxillofac Implants* 2:142-148, 1987



Embryology and Anatomy of the Jaw and Dentition

Vahe M. Zohrabian, MD, Colin S. Poon, MD, PhD, and James J. Abrahams, MD

Radiologists should possess working knowledge of the embryological development and anatomy of the jaw and dentition in order to aid in the diagnosis of both simple and complex disorders that affect them. Here, we review the elaborate process of odontogenesis, as well as describe in detail the anatomy of a tooth and its surrounding structures.

Semin Ultrasound CT MRI 36:397-406 © 2015 Elsevier Inc. All rights reserved.

With the ever-increasing sophistication of cross-sectional imaging techniques in the evaluation of head and neck pathology, including multidetector computed tomography (CT) and cone-beam CT with improved contrast and spatial resolution, as well as dental CT software programs,^{1,2} radiologists are charged with the accurate identification of abnormalities of the teeth and jaw. A working knowledge of the development and anatomy of teeth is critical in understanding and describing the disease processes that affect them.

Embryology

The structures of the head and neck are derived from the cephalic portion of the neural tube, which gives rise to the 5 pairs of branchial arches. Each arch consists of 3 layers: an outer ectoderm, a middle layer composed of mesenchyme-containing neural crest cells, and an inner layer of endoderm. The development of the face starts at the fourth week of embryonic age with the stomodeum, a ventral depression located just caudal to the developing brain, which develops into the mouth. Surrounding the stomodeum are 5 primordia. These include the single frontonasal process (prominence) located at midline and cranial to the stomodeum, followed caudally by the paired maxillary and mandibular processes lying on each side of the stomodeum. The frontonasal process originates from the forebrain. The maxillary and mandibular processes are derived from the first branchial arch (also referred to as the mandibular arch) and form the lateral wall and base of the stomodeum. By the fifth week, medial and lateral nasal

processes develop on either side of the frontonasal process. The medial nasal processes fuse to form the upper lip. The mandibular processes enlarge and fuse at midline to form the mandible, the lower part of the face, and the tongue. The skeleton of the mandible is derived from the cartilaginous derivative of the first branchial arch called Meckel's cartilage. The mandibular mentum marks the site where the 2 mandibular processes merge in the midline. By the sixth week, the bilateral maxillary and mandibular processes are completely fused, forming the primitive maxilla and the mandible. When the maxillary and mandibular processes fuse laterally, they form the corners of the lips, or commissures. Any interruption or alteration of the development of the face and the jaw can result in congenital anomalies. For example, failure of proper closure at the midline can result in cleft lip, cleft chin, or cleft palate. Interruption of lateral fusion of the maxillary and mandibular processes can result in cleft corners of the mouth or macrostomia (large mouth).

Ectomesenchyme, a derivative of neural crest cells, forms the bony structures of the head and face. The muscles of mastication are formed from the mesenchymal cells of the first branchial arch. The stomodeum, which forms the primitive oral cavity, is lined by stratified squamous epithelium called oral ectoderm. At approximately the sixth week, the oral ectoderm proliferates into a thick band of epithelium called the primary epithelial band. This horseshoe-shaped structure develops into the alveolar processes of the upper and the lower jaws. The primary epithelial band develops into the vestibular lamina and the dental lamina. The vestibular lamina develops into the vestibule between the cheek and the alveolar process. The dental lamina, a thickening of the oral epithelium overlying the jaws, forms the basis of development of dentition.

The process by which the teeth form is called odontogenesis (Fig. 1). Humans have 2 sets of teeth, the temporary baby, or deciduous, teeth and the permanent adult, or succedaneous,

Division of Neuroradiology, Department of Diagnostic Radiology, Yale University School of Medicine, New Haven, CT.

Address reprint requests to Vahe M. Zohrabian, MD, Yale University School of Medicine 333 Cedar St (Room CB-30), P.O. Box 208042, New Haven, CT 06520-8042. E-mail: vahe.zohrabian@yale.edu

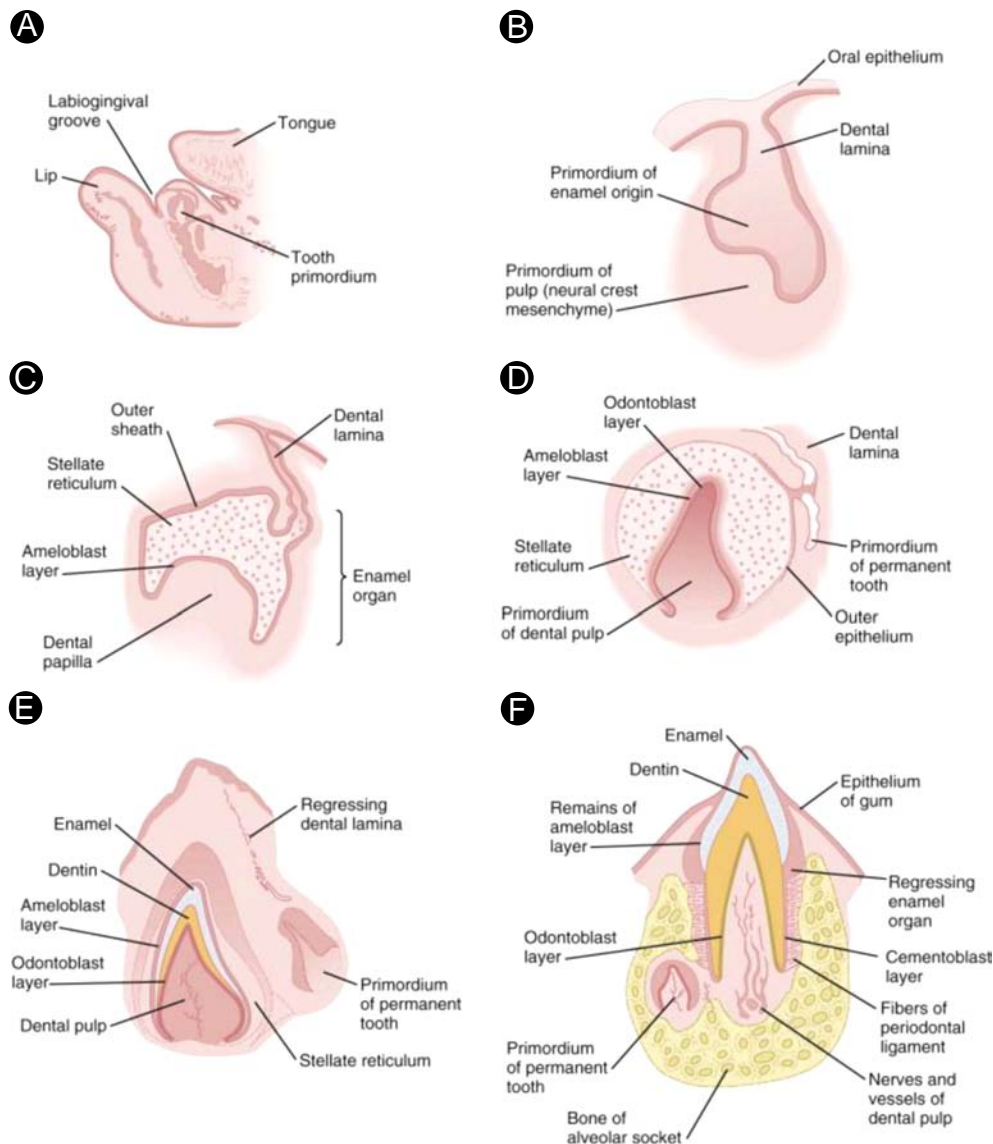


Figure 1 The development of a deciduous tooth. (A) A parasagittal section through the lower jaw of a 14-week-old human embryo showing the relative location of the tooth primordium. (B) Tooth primordium in a 9-week-old embryo. (C) Tooth primordium at the cap stage in an 11-week-old embryo, showing the enamel organ. (D) Central incisor primordium at the bell stage in a 14-week-old embryo before deposition of enamel or dentin. (E) Unerupted incisor tooth in a term fetus. (F) Partially erupted incisor tooth showing the primordium of a permanent tooth near one of its roots. (Adapted with permission from Carlson.⁵) (Color version of figure is available online.)

teeth. There are 20 deciduous teeth (10 maxillary and 10 mandibular) and 32 succedaneous teeth. Deciduous teeth begin development at the sixth- to eighth-week of gestation, and permanent teeth begin development at the twentieth week. Each tooth develops from the ectoderm (enamel) and the ectomesenchyme (dentin, cementum, periodontal ligament, and pulp contents). Ectomesenchyme represents migration of neural crest cells into the developing arches of the mandible and the maxilla. Tooth development begins with the localized proliferation of the primary dental lamina invaginating into the ectomesenchyme, forming focal thickenings of the oral epithelium called placodes in 10 places in each of the mandibular and the maxillary arches.³⁻⁷ These placodes develop into tooth buds, which later develop into individual teeth. The tooth buds and surrounding aggregation of

ectodermal cells constitute the tooth germs. During embryologic development, the deciduous teeth are formed starting from the anterior aspect of the maxilla and the mandible and proceeding posteriorly. Each tooth develops and erupts at a different time, although the pattern of odontogenesis is the same⁵ (Table). The tooth buds of the permanent teeth are arranged in a horseshoe-shaped arch, lingual to the deciduous teeth. All tooth buds, except for the second and third permanent molars, are present and start developing before birth. The major activity of the dental lamina extends over a period of approximately 5 years. However, the dental lamina near the third molar continues to be active until approximately 15 years of age.

As the tooth bud grows, it assumes a cap shape by invagination of the mesenchyme. The ectodermal component

Table The Usual Times of Eruption and Shedding of Deciduous and Permanent Teeth

Teeth	Eruption	Shedding
Deciduous		
Central incisors	6-8 mo	6-7 y
Lateral incisors	7-10 mo	7-8 y
Canines	14-18 mo	10-12 y
First molars	12-16 mo	9-11 y
Second molars	20-24 mo	10-12 y
Permanent		
Central incisors	7-8 y	—
Lateral incisors	8-9 y	—
Canines	12-13 y	—
First premolars	10-11 y	—
Second premolars	11-12 y	—
First molars	6-7 y	—
Second molars	12-13 y	—
Third molars	15-25 y	—

Adapted with permission from Carlson.⁵

of the tooth bud forms the enamel organ, composed of the outer enamel epithelium, the stellate reticulum, and the inner enamel epithelium (Fig. 1C). The stratum intermedium, arising from the stellate reticulum, is a layer of condensed cells along the inner enamel epithelium. Other ectodermal cells surround the enamel organ and the dental papilla, forming the dental, or a fibrous sac that invests the tooth germ and separates it from the adjacent bone. The dental follicle gives rise to the supporting structures of teeth, including the cementum and the periodontal ligament. The enamel organ, dental papilla, and dental follicle together constitute the tooth germ. Ameloblasts are derived from the inner enamel epithelium, which forms the enamel of the tooth.^{4,5} During the bell stage, a concavity along the inner surface of the enamel organ transforms the tooth bud into the shape of a bell (Fig. 1D). The ectomesenchymal cells within the concavity form the dental papilla, and its peripheral-most cells take on a columnar shape and are known as odontoblasts. Odontoblasts form the dentin of the tooth and later the dental pulp, or soft tissue core—containing nerves, blood vessels, and connective tissues (Fig. 1E). Enamel formation is induced by the production of dentin, which begins at the cusp or top of a tooth and progresses toward the tooth apex or root. As an increasing amount of dentin is produced, the dental pulp cavity is filled and narrowed to form the root canal. Enamel formation occurs only in a preruptive tooth, whereas dentin deposition occurs throughout life. Dental lamina starts to disintegrate at the various stages of tooth eruption (Fig. 1F).

A number of anomalies can occur during tooth development. Development of excess dental lamina can lead to an increased number of tooth buds, resulting in too many teeth (supernumerary). Deficient dental lamina can result in a decreased number of teeth (hypodontia), with the third molar being most commonly absent, followed by second premolar and the lateral incisor. Hypodontia is often associated with small teeth (microdontia). Hypodontia and microdontia can also be further influenced by environmental factors such as trauma, infection, chemotherapeutic medications,

and endocrine conditions that can affect the development of dental lamina and tooth buds. Absence of teeth (anodontia) is a rare condition that can be associated with hereditary ectodermal dysplasia. Teeth can also be fused or abnormally located (ectopia). Faulty development of dentin and enamel results in conditions of amelogenesis and dentinogenesis imperfecta, rendering the teeth prone to dental caries and fracture. Other abnormalities include tooth impaction because of impedance of tooth eruption by bone or an adjacent tooth, ankylosis with absence of periodontal ligament and direct attachment of tooth to bone, as well as abnormal timing of tooth eruption. Furthermore, when epithelial cells from dental lamina fail to regress, epithelial rests may persist and develop into cysts (odontogenic cysts). They may also result in the formation of odontomas, or benign tumors or hamartomas of odontogenic origin.

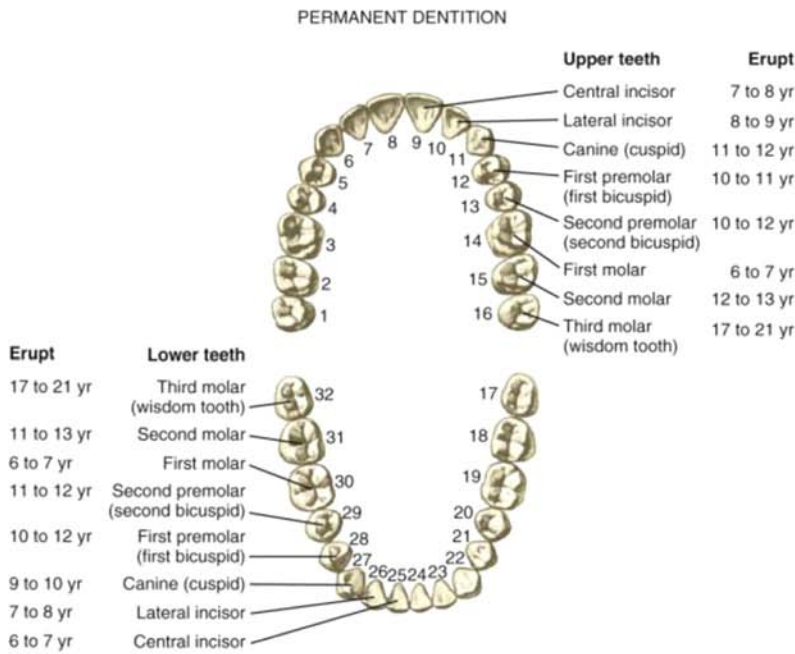
Anatomy of Dentition

The human adult jaw contains 32 teeth: 16 teeth in the maxilla and 16 in the mandible.⁸ From the midline and extending distally, the teeth are named as follows: central incisor, lateral incisor, canine (cuspid), first premolar (first bicuspid), second premolar (second bicuspid), first molar, second molar, and third molar (wisdom tooth). Alternatively, the teeth may be numbered using either of 2 major numbering systems: the Universal/National System and the International Standards Organization System.⁹ According to the Universal/National System used in the United States, permanent adult teeth are numbered 1 through 16 from right to left in the maxilla and 17 through 32 from left to right in the mandible (Fig. 2A). Children possess 20 instead of 32 teeth (10 each in the maxilla and mandible), lacking premolars and third molars. Pediatric teeth are labeled using sequential letters (A through T), starting with tooth letter A in the posterior right maxilla, letter J in the posterior left maxilla, letter K in the posterior left mandible, and letter T in the posterior right mandible (Fig. 2B).

The teeth are individually embedded in bony sockets in an osseous ridge called the alveolar process and are anchored in place by the periodontal ligament, allowing for slight motion of the teeth.¹⁰ The alveolar process divides the oral cavity into central and peripheral portions, with the central oral cavity proper containing the tongue and the peripheral oral vestibule containing the lips and cheeks (Fig. 3). The mucosa lining the oral vestibule reflects onto the alveolar process to create a furrow called the fornix vestibuli, allowing for mobility of the cheeks and lips. The mucosa covering the alveolar process is divided into alveolar mucosa and gingiva below and above the fornix, respectively. The gingiva covers the free border of the alveolar process adjacent to the teeth. The upper and lower labial frenula are vertically oriented mucosal folds that connect the lips to the alveolar processes, and the lingual frenulum anchors the tongue to the floor of the oral cavity (Figs. 3 and 4).

The tooth anatomy, which follows, is best depicted in Figures 4 and 5. A tooth is divided into an enamel-covered anatomical crown projecting into the oral cavity and a root that is embedded into the alveolar process and surrounded by

A



B

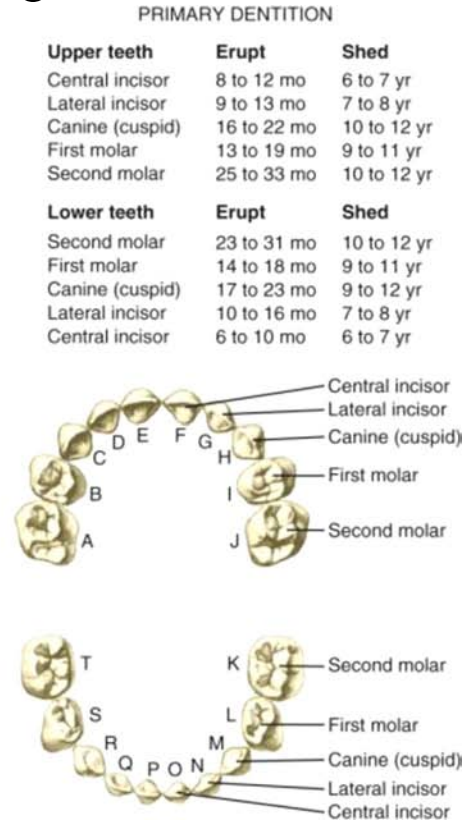


Figure 2 Universal System for tooth numbering in adults (A) and children (B). Approximate age of eruption for primary and permanent teeth and age of shedding of primary teeth are given. (Adapted with permission from Nunez et al.⁹) (Color version of figure is available online.)

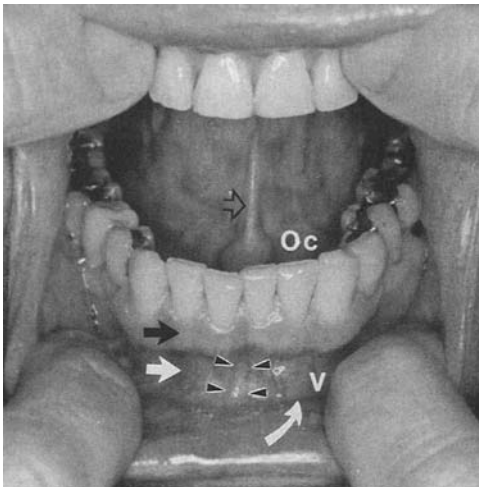


Figure 3 The oral cavity and vestibule. Fingers pulling the lower lip down expose the vestibule (V), which is separated from the oral cavity (Oc) by the alveolar process and teeth. Fornix vestibuli (curved arrow), gingiva (black arrow), alveolar mucosa (white arrow), lingual frenum (open arrow), and labial frenum (arrowheads). (Adapted with permission from Abrahams et al.¹)

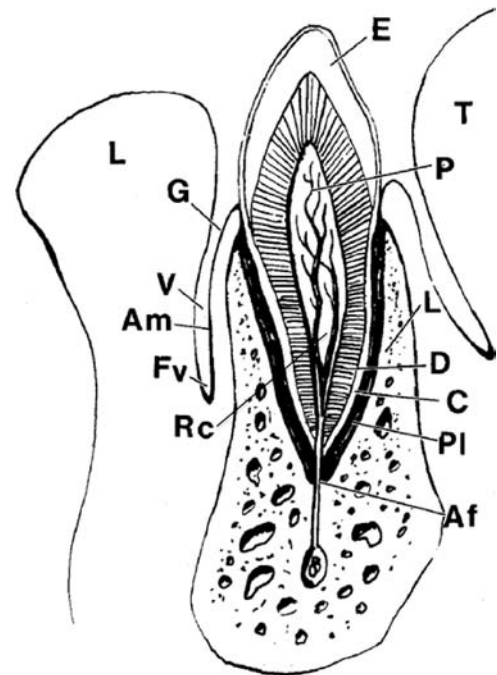


Figure 4 The anatomy of the tooth and mucosa. Am, alveolar mucosa; Af, apical foramen; C, cementum; D, dentin; E, enamel; Fv, fornix vestibuli; G, gingiva; Ld, lamina dura; L, lip; PI, periodontal ligament; P, pulp; Rc, root canal; T, tongue; and V, vestibule. (Adapted with permission from Abrahams et al.¹)

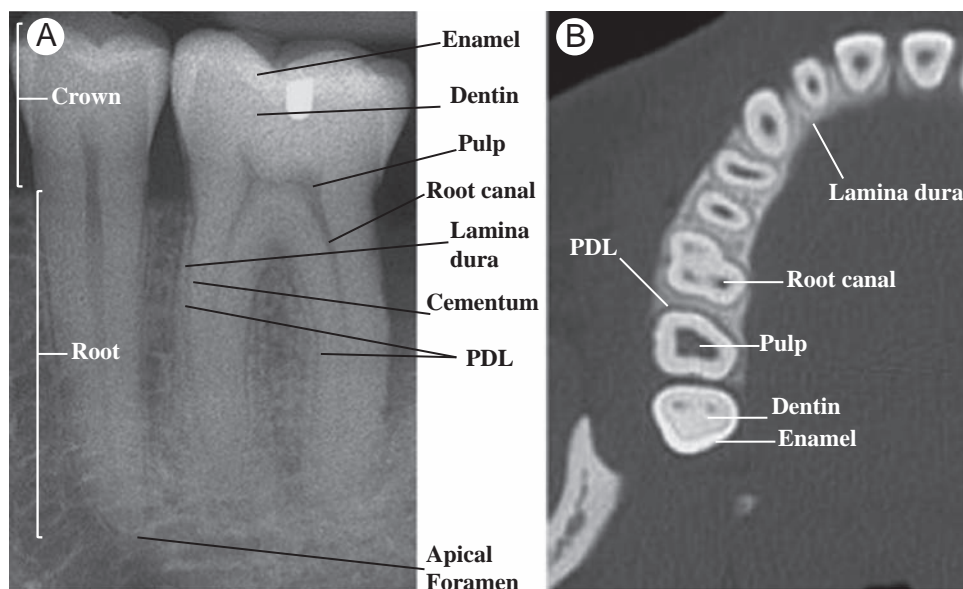


Figure 5 Radiologic anatomy of the tooth. (A) Intraoral radiograph and (B) axial CT image demonstrate anatomy of a tooth. It should be noted that the periodontal ligament (PDL) appears as a thin, radiolucent line deep to the sclerotic lamina dura. Cementum, lining the root, is not actually visible on radiographs. The enamel is extremely radiodense, although most of the tooth is composed of opaque, softer dentin. The pulp chamber and root canals are radiolucent. The root apex is the deepest portion of the tooth.

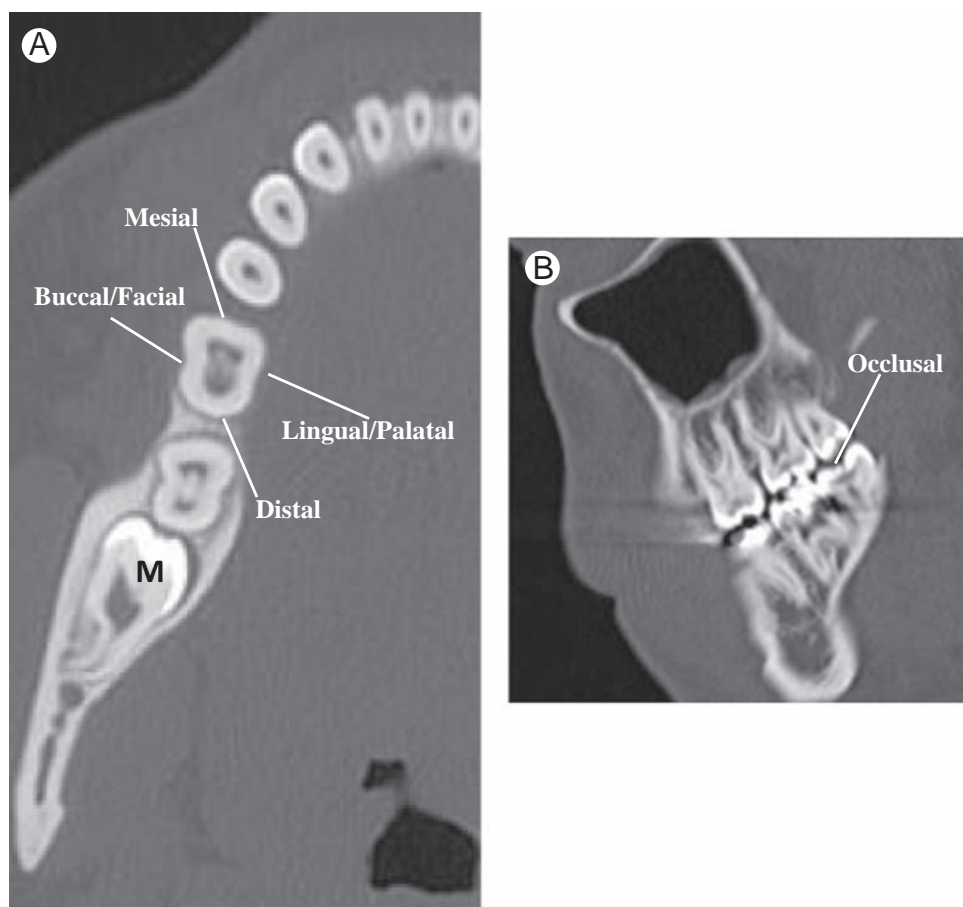


Figure 6 Tooth surfaces. (A) Axial CT and (B) sagittal CT images demonstrate that each crown has 5 free surfaces, as denoted earlier. The same terminology is used to describe directions. Impacted third molar (M).

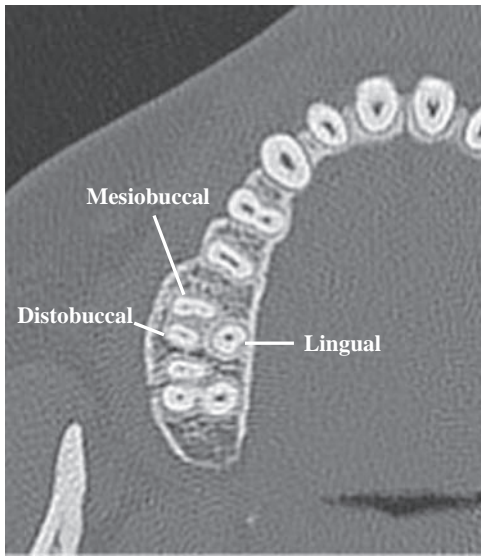


Figure 7 Named roots of molar tooth. An axial CT image from a dental scan demonstrates the 3 roots of a mandibular molar: mesiobuccal, distobuccal, and lingual.

dense cementum. The cemento-enamel junction, or cervical constriction or neck, demarcates the boundary between the anatomical crown and the root. With age, as the gingiva recedes, exposing the root, the portion of tooth exposed in the oral cavity is referred to as the functional crown instead of the

anatomical crown. Radiographically, the enamel appears as an extremely dense, opaque covering over the crown, whereas the cementum surrounding the root is indistinguishable from the underlying dentin and is not visualized on radiographs. Dense cortical bone lining the tooth socket is known as lamina dura, and on radiographs, appears as a thin rim of sclerotic cortical bone lining the socket. The periodontal space, containing the periodontal ligament, appears as a thin, radiolucent line between the lamina dura and the root. The ligament, attaching to both the cementum of the root and the lamina dura, functions to hold the tooth in the bony socket. The core of the tooth is composed of dentin, a modification of bone that appears slightly less dense than the overlying enamel. Deep to the dentin is a radiolucent central compartment known as pulp. The pulp is composed of connective tissue, housing nerves and blood vessels. The neurovascular bundle enters at the root apex via the apical foramen and travels up the root through the root canals to enter the more expanded pulp chamber in the crown of the tooth. The number of roots varies from teeth to teeth, although molars typically have 3 roots.

Each crown has 5 free surfaces¹⁰ (Fig. 6A). The surface facing the lips or cheek is known as the facial surface, also referred to as the labial surface for incisors and canines and buccal surface for premolars and molars. The crown surface on the inside facing the tongue is known as the palatal surface in the maxilla and lingual surface in the mandible. The surfaces abutting adjacent teeth are termed mesial and distal, although

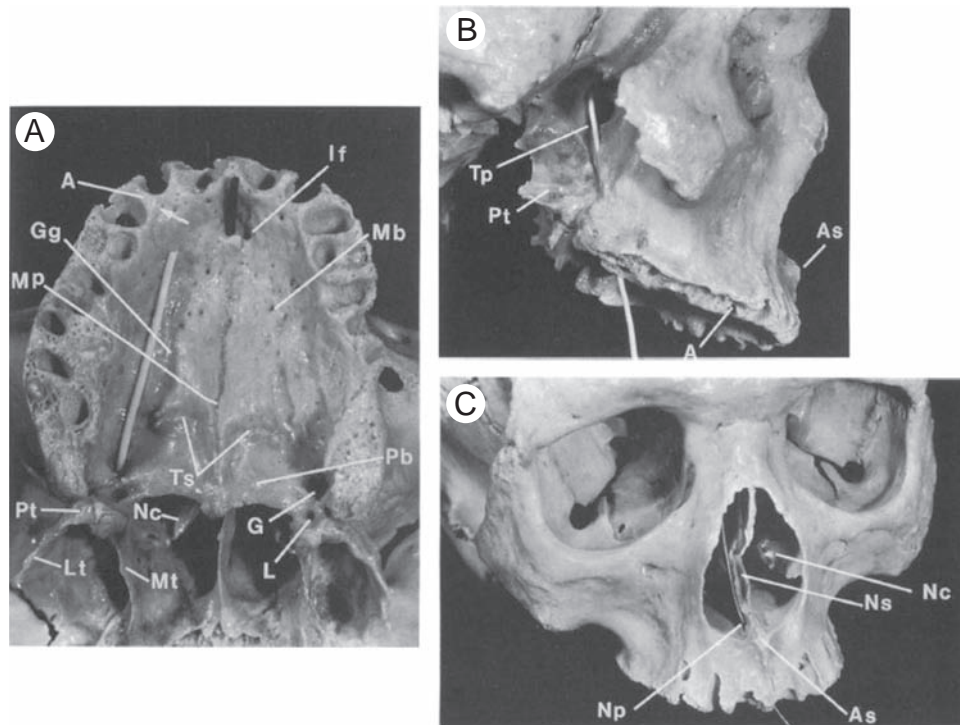


Figure 8 An anatomical specimen demonstrating the inferior (A), lateral (B), and anterior (C) aspects of the maxilla. The white probe demonstrates the course of the greater palatine nerve; the black probe demonstrates the course of the nasopalatine nerve. A, alveolar process; As, anterior nasal spine; G, greater palatine foramen; Gg, groove for greater palatine nerve; If, incisive foramen; L, lesser palatine foramen; Lt, lateral pterygoid plate; Mb, maxillary bone: palatine process; Mp, median palatine suture; Mt, medial pterygoid; Nc, nasal conchae; Np, nasopalatine canal; Ns, nasal septum; Pb, palatine bone: horizontal plate; Pt, pterygoid process; Tp, pterygopalatine fossa; Ts, transverse suture. (Adapted with permission from Gray.²)

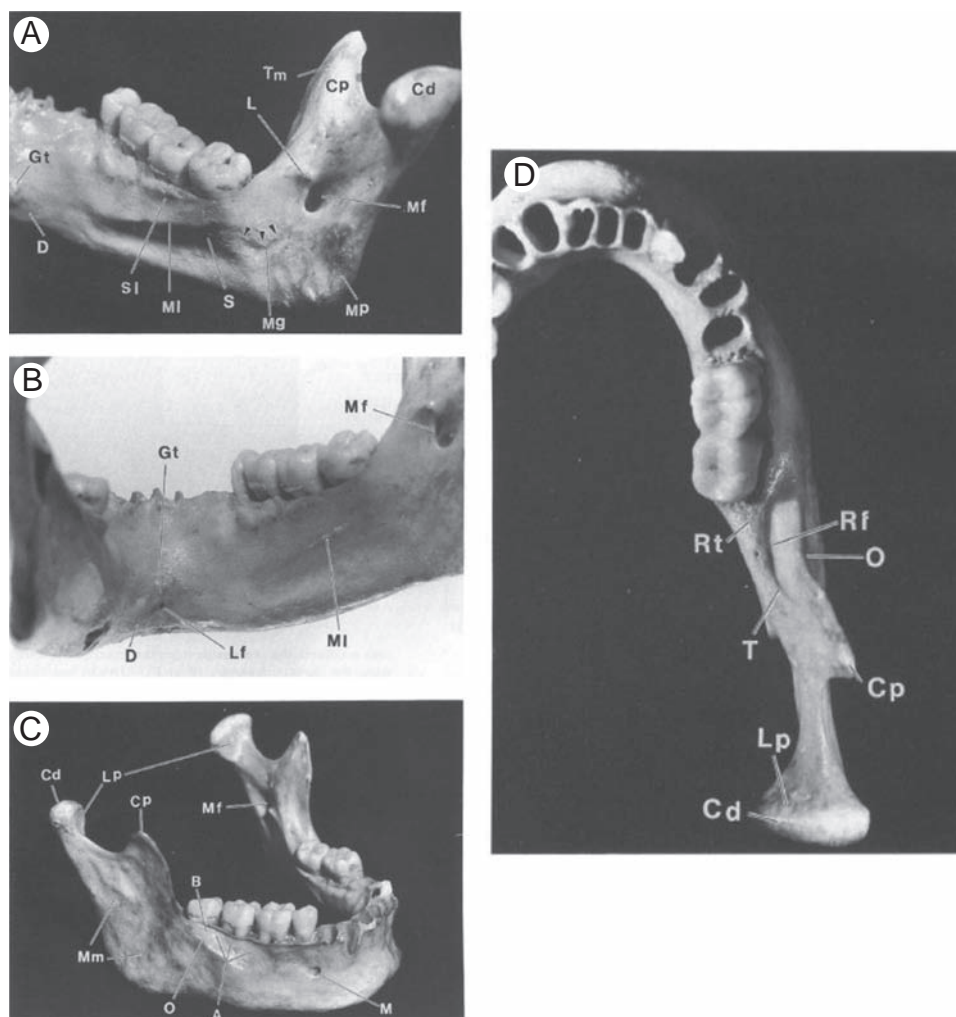


Figure 9 An anatomical specimen demonstrating the lingual (A and B), buccal (C), and superior (D) aspect of the mandible. A, alveolar process; B, buccinator muscle insertion; Cd, condyle; Cp, coronoid process; D, digastic fossa; Gt, genial tubercle; L, lingula; Lf, lingual foramen; Lp, lateral pterygoid muscle insertion; M, mental foramen; Mf, mandibular foramen; Mg, mylohyoid groove; MI, mylohyoid line; Mm, masseter muscle insertion; Mp, medial pterygoid insertion; O, oblique line; Rf, retromolar fossa; Rt, retromolar triangle; S, sublingual fossa; T, temporal crest; and Tm, temporalis muscle insertion; arrowheads, groove for mylohyoid nerve. (Adapted with permission from Gray.²)

they can also be referred to as medial or lateral for incisors and canines and anterior or posterior for premolars and molars. The biting surface is known as the occlusal surface, or that where the maxillary and mandibular teeth oppose each other (Fig. 6B). Direction can also be described using this terminology, such that toward the midline is labeled mesial or anterior, and toward the molars is labeled distal or posterior. Moving in the direction of the root apex is moving in an apical direction, and moving toward the crown of the tooth is moving in the coronal direction. For example, one can describe the impacted third molar in Figure 6A as follows: the crown of the third molar is oriented in a mesial direction and impacted in the distal surface of the second molar, and the root is oriented distally. In relation to the crown itself, occlusal is toward the occlusal surface and cervical is toward the cervical constriction. The roots of teeth may be labeled using this terminology, such that a mandibular molar has 3 roots: mesiobuccal, distobuccal, and lingual (Fig. 7).

Anatomy of the Maxilla

The bony anatomy of the maxilla^{8,11,12} is shown in Figure 8, and neurovascular anatomy¹³⁻¹⁵ is highlighted in Figure 11. In brief, the roof of the oral cavity anteriorly is formed by the bones of the hard palate, the maxilla, and the palatine bones, which are separated anteroposteriorly by the transverse suture. The hard palate is also divided into right and left halves by the median palatine suture, or palatine raphe. More posteriorly, the roof of the oral cavity is formed by the fibromuscular soft palate. The alveolar process forms the anterior and the lateral borders of the hard palate, and the pterygoid process of the sphenoid bone, as well as lateral and medial pterygoid plates, lie posterior to the alveolar process. The greater and lesser palatine foramina, containing the exiting greater and lesser palatine nerves, can be seen on the roof of the hard palate. The hard palate separates the oral cavity from the nasal cavity and paranasal sinuses superiorly. Most anteriorly, the nasal cavity,

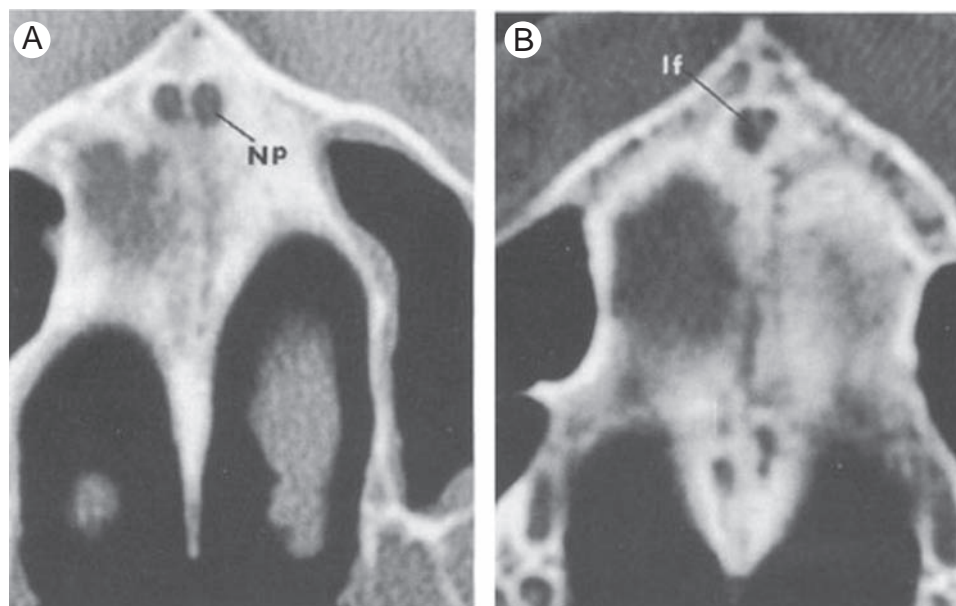


Figure 10 An axial CT image of the nasopalatine canals and incisive foramen. The more superior image (A) demonstrates the 2 nasopalatine canals (Np); the inferior slice (B) demonstrates their common opening, the incisive foramen (If). (Adapted with permission from Gray.²)

containing the nasal conchae, is separated in the midline by a nasal septum and a bony prominence on the anterior aspect of the maxilla, known as the anterior nasal spine. The nasopalatine nerves run anteroinferiorly on either side of the nasal septum and enter the hard palate through the nasopalatine canals on either side of the septum. The nasopalatine canals form a common opening on the inferior aspect of the palate, known as the incisive foramen. These structures are exceptionally demonstrated on axial CT images (Fig. 10). The maxillary sinuses are located posterior and lateral to the nasal cavity, and the pterygopalatine fossae lie posterior to them.

The maxillary division of the trigeminal nerve (V2) exits the foramen rotundum at the skull base and crosses the pterygopalatine fossa superiorly to enter the orbit through the inferior orbital fissure as the inferior orbital nerve (Fig. 11). The anterior branch of the superior alveolar nerve, arising from the inferior orbital nerve, supplies the canines and the incisors, as well as forms part of the superior dental plexus to supply the anterior part of the hard palate. The maxillary artery, via the posterior, middle, and anterior superior alveolar arteries, supplies the teeth of the maxilla. The nasopalatine nerve, a branch of the pterygopalatine ganglion, courses through the sphenopalatine foramen and enters the nasopalatine canal in the hard palate. The sphenopalatine artery follows the course of the nasopalatine nerve. In the pterygopalatine fossa, the maxillary nerve gives off 2 ganglionic branches that pass through the pterygopalatine ganglion without synapsing and form the lesser and greater palatine nerves. The greater palatine nerve supplies the molars and posterior two-thirds of the hard palate.

Anatomy of the Mandible

The bony anatomy of the mandible^{8,11,12} is shown in Figure 9 and the neurovascular anatomy¹³⁻¹⁵ in Figure 11. The mandible

consists of 2 vertical rami attached to a U-shaped body. The alveolar process, housing the teeth, is the most superior portion of the mandibular body, and the lower half is referred to as the basilar bone. Given that the alveolar process curves more sharply than the mandibular body does, it is positioned medially relating to the mandibular body. Posterior to the teeth, the alveolar process tapers into the retromolar triangle and joins the lingual aspect of the ramus to form the temporal crest. Buccal to the alveolar process, the anterior portion of the coronoid process joins the body of the mandible to form the oblique line. The retromolar fossa lies between the temporal crest and the oblique line.

The mylohyoid ridge is a prominent bony crest on the inner or lingual surface of the mandible, representing the point of origin of the mylohyoid muscle. Inferior to the mylohyoid ridge sits a concavity for the submandibular gland known as the submandibular fossa. Above the mylohyoid line sits a small concavity for the sublingual gland known as the sublingual fossa. In the midline on the lingual aspect of the mandible, there is a bony protuberance, the genial tubercle, for the insertion of the geniohyoid and genioglossus muscles. The mandibular foramen is situated on the lingual aspect of the mandibular ramus centrally approximately 1-2 cm posterior to the third molar at the levels of the crowns of the teeth. After the mandibular nerve (V3) exits the foramen ovale in the skull base and branches, the inferior alveolar nerve travels deep to the lateral pterygoid muscle to enter the mandibular foramen. Just before entering the foramen, a small branch, the mylohyoid nerve, does not enter the foramen and travels in a groove on the lingual surface of the mandible to supply the mylohyoid muscle. After entering the mandibular foramen, the inferior alveolar nerve travels through the mandibular canal (also called the inferior alveolar canal) to supply small dental and interdental branches that enter the apical foramina and travels

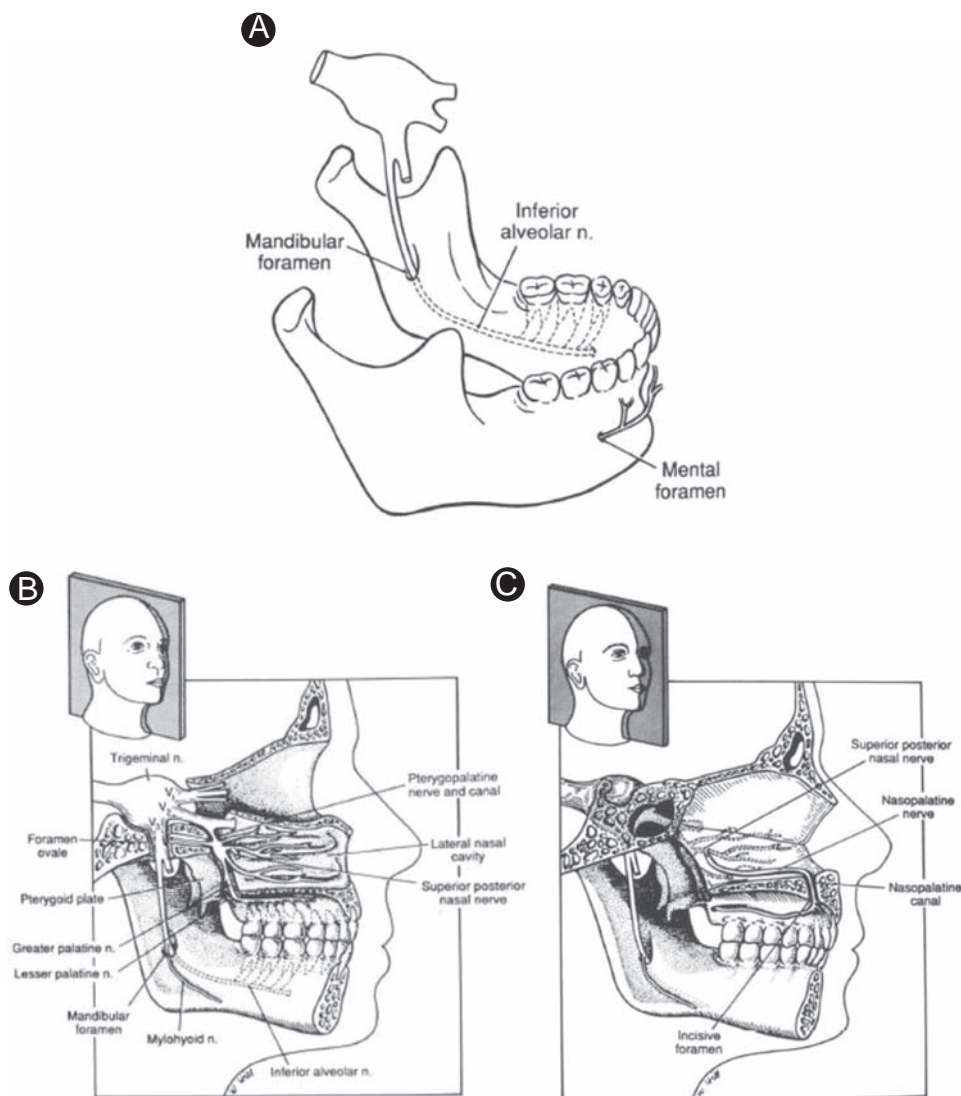


Figure 11 Neurovascular anatomy. (A) View of the mandible illustrating the mandibular foramen, the mental foramen, and the nutrient canals, which extend from the inferior alveolar canal toward the teeth. (B) Parasagittal view through the trigeminal nerve and the lateral nasal cavity. The mylohyoid nerve travels on the lingual surface of the mandible and does not enter the mandibular foramen. The greater palatine nerve arises from the pterygopalatine nerve, a branch of V2. (C) Midsagittal view through the incisive foramen and the nasal septum. The nasopalatine nerve, a branch of the superoposterior nasal nerve, travels along the nasal septum and through the incisive foramen. (Adapted with permission from Gray.²)

between teeth to supply the periodontal ligament. The inferior alveolar artery, a branch of the maxillary artery, accompanies the nerve in the mandibular canal. Between the first and the second premolars, the main terminal branch of the inferior alveolar nerve exits on the buccal surface of the mandible through the mental foramen as the mental nerve to supply sensation to the chin and the lower lip. A small terminal branch, the incisive nerve, travels anteriorly within the mandible toward the midline in the incisive canal to help innervate the canines and the lateral incisors. At the mental foramen, the inferior alveolar artery also branches into the mental and the incisive arteries, with the incisive artery exiting the mandible in the midline along its lingual aspect to travel through the lingual foramen and anastomose with branches of the lingual artery of the tongue.

Conclusions

Advancements in CT technology have provided radiologists the ability to assess pathology and anatomy of the teeth and jaws with detail that is not possible by conventional panoramic and intraoral radiography. Radiologists should possess a basic understanding of tooth development and anatomy to appropriately discriminate between normal, benign, and malignant processes, as well as to refer patients to dental specialists for further workup when indicated.

References

1. Abrahams JJ, Frisoli JK, Dembner J: Anatomy of the jaw, dentition, and related regions. *Semin Ultrasound CT MR* 16(6):453-467, 1995
2. Abrahams JJ: Anatomy of the jaw revisited with a dental CT software program. *Am J Neuroradiol* 14(4):979-990, 1993

3. Sperber GH: Craniofacial Embryology. London: Wright, 1989
4. Melfi RC: Permar's Oral Embryology and Microscopic Anatomy: A Textbook. Philadelphia: Lea & Febiger, 1994
5. Carlson BM: Human Embryology and Developmental Biology. St. Louis: Mosby, 1994
6. Moore KL, Persaud TVN: The Developing Human. Philadelphia: WB Saunders, 1988
7. Paulsen F, Waschke J: Head. Sobotta: Atlas of Human Anatomy. Munich, Elsevier GmbH 1-96, 2011
8. Gray H: Osteology, Anatomy of the Human Body. Philadelphia, Lea & Febiger 107-293, 1969
9. Nunez DW, Fehrenbach MJ, Emmons M: Mosby's Dental Dictionary. Philadelphia: Elsevier, 2004
10. Sicher H: The Viscera of the head and neck. St. Louis: Mosby, 1965
11. Meschan I: The skull, An Atlas of Anatomy Basic to Radiology. Philadelphia, Saunders 209-287, 1975
12. Sicher H: Oral Anatomy, The skull. St. Louis, Mosby 23-140, 1965
13. Gray H: The peripheral nervous system, Anatomy of the Human Body, (ed 28) Philadelphia, Lea & Febiger 907-1042, 1969
14. Sicher H: The Nerves of the Head and Neck. Oral Anatomy, (ed 4) St. Louis, Mosby 364-398, 1965
15. Gray H: Arteries of the head and neck, Anatomy of the Human Body, (ed 28) Philadelphia, Lea & Febiger 1161-1263, 1969

Imaging of the jaws



Lisa J. Koenig, BChD, DDS, MS*

Introduction

The mainstay of dental imaging has traditionally been the intraoral images called periapicals and bitewings, which for many years were made with film that was wrapped in a protective packet. Today these images are taken using small detectors or sensors that are placed inside the patient's mouth. The first digital intraoral solid-state detector, a charge-coupled device (CCD), was introduced in 1997.¹ These detectors are directly attached to the computer by a wire and give an almost instantaneous image on the computer monitor (Fig. 1). This provides huge savings in time compared with the traditional wet processing needed for films as well as for the ability to manipulate the image and change its brightness and contrast. In addition, because the images appear on a monitor within the operatory it allows for instant feedback to the operator and also the patient. Several manufacturers are now using complementary metal oxide semiconductor technology for their detectors, as it is less expensive to produce than CCD technology.² In dentistry these types of detectors are often referred to as "sensors" to differentiate them from an alternate digital intraoral detector, photo-stimulable phosphor (PSP) plates. PSP plates are thinner and more flexible than the solid-state sensors and are often tolerated better by the patient. They are the same size as traditional intraoral film packets and can be used with the same positioning devices without modification. Exposure to x-rays produces a latent image within the plate in the form of stored energy, which is released when the plates are "processed" by laser light in the manufacturer's scanning device or reader. The readers are often small enough that they can be placed in the dental operatory (Fig. 2). The image, therefore, like film is not instantaneous as this is a 2-step process. However, once placed in the reader the images can appear on the computer monitor in as little as 3 seconds. Some dental offices still use film-based imaging

but those dentists who have opted to go digital have a choice of using either solid-state sensors (CCD, complementary metal oxide semiconductor) or PSP detectors and some offices have a combination of both systems.

Pertinent Tooth Anatomy

A brief review of pertinent anatomy is helpful for a more complete understanding of the material that follows. Further detail of the anatomy can be obtained in Vahe et al.³ The adult dentition consists of 32 permanent teeth: 3 molars, 2 premolars (bicuspid), 1 canine (cuspid), and a lateral and a central incisor in each of the 4 quadrants. A tooth is made up of a crown and a root. The size and shape of the crown and the number of roots vary depending on the type of tooth. For instance, maxillary molars have 3 roots whereas a central incisor has only 1 root. Teeth have different functions. Molar crowns are larger with bigger surfaces for grinding. Incisor teeth have a thin "incisal" edge to their crowns for shearing.

The crown is covered by dense radiopaque enamel, which is approximately 96% mineralized and the hardest structure the body produces.⁴ It is designed to protect the tooth from occlusal forces and also from the potential hostile environment of the oral cavity. Under the enamel is the slightly less radiopaque dentin, which forms the bulk of the hard tissue of the tooth including crown and root. The dentin in the root is covered by a thin layer of cementum. This layer is less mineralized than enamel and susceptible to loss once the root of a tooth is exposed to the oral environment as in periodontal disease (loss of bone around the tooth root). It is not visible as a separate structure radiographically because it is so thin and also so similarly mineralized as dentin. Cementum is approximately 65% mineralized compared with dentin, which is approximately 70% mineralized.⁴

The enamel and dentin meet in the crown of the tooth at the dentinoenamel junction (DEJ) and this is an important landmark in caries (decay) detection (Fig. 3). Early or incipient interproximal (between teeth) caries is seen only in the enamel, which offers significant resistance due to its high mineralization. Once the caries reaches the DEJ and enters the dentin there is less resistance. The dentinal tubules offer a pathway for

*Professor and Program Director, Oral Medicine and Oral Radiology, Marquette University School of Dentistry, Milwaukee, WI 53233.

Address reprint requests to Lisa J. Koenig, BChD, DDS, MS, Oral Medicine and Oral Radiology, Marquette University School of Dentistry, PO Box 1881, Milwaukee, WI 53201-1881. E-mail: lisa.koenig@marquette.edu

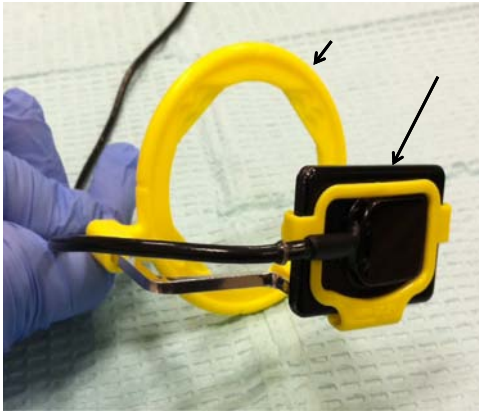


Figure 1 A typical intraoral sensor (long arrow) (Schick by Sirona, Long Island City, NY) is seen in its custom-positioning device (short arrow) (Dentsply Rinn, York, PA), which aids in placement in the mouth. (Color version of figure is available online.)

progression to the pulp chamber. The pulp chamber is located inside each tooth crown and provides nutrients to the tooth. It contains blood vessels and nerves, which enter the tooth through a foramen at the apex of the root. The nerves and vessels then course through the root in the root canal to the pulp chamber in the crown. The root canal and pulp chamber appear radiographically as a relative radiolucency compared with the radiopaque dentin (Fig. 3). The pulp can become inflamed if caries reaches the dentin (toothache).

The tooth root is supported in the bony socket by the periodontal ligament and this appears on the radiographs as a thin radiolucent line surrounding the entire root. The cortical lining of the socket is known as the lamina dura and appears in images as a thin radiopaque line peripheral to the radiolucent periodontal ligament. It surrounds the entire socket and also extends between the cervical portions of the teeth, where it is known as the crestal lamina dura or alveolar crest. The crestal lamina dura is an important landmark in determining loss of alveolar bone, which occurs in periodontal disease. The apical lamina dura, which surrounds the root apex, is an important landmark in determining the origin of lesions at the root apex (Figs. 4 and 5).



Figure 2 A PSP plate (arrow) is placed in the manufacturer's reader (Digora Optime, Soredex, Tuusula, Finland). The reader is compact enough that it can be placed chairside. (Color version of figure is available online.)

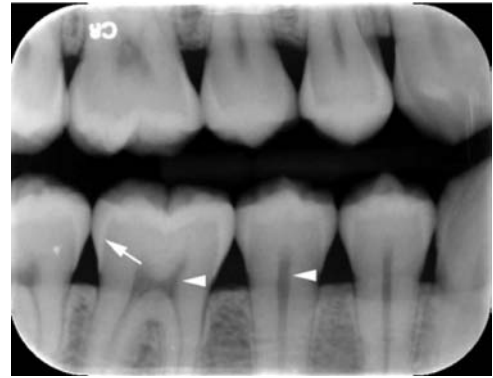


Figure 3 Well-positioned right premolar bitewing radiograph shows both maxillary and mandibular crowns and interproximal spaces between teeth to allow for early caries detection. Arrow shows the clear delineation between the more radiopaque enamel and less radiopaque dentin known as the dentinoenamel junction. The pulp chamber (left arrowhead) and root canal (right arrowhead) are seen as radiolucencies at the center of the teeth.

Intraoral Images

A full mouth series of intraoral radiographs consists of 4 bitewing views and periapical views of the maxilla and mandible, which can vary in number from 14-18 views.

Bitewing Views

Bitewing views, as the name infers, are taken with the teeth biting together or in occlusion as referred to in dentistry. Both a molar and a premolar bitewing are taken on the right and left (4 bitewings). Positioning devices or holders allow the detector to cover the maxillary and mandibular crowns of the teeth as well as the crestal alveolar bone between the teeth on each image. Correct positioning of these images is

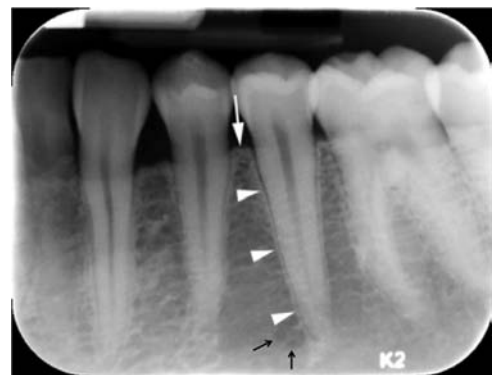


Figure 4 This periapical radiograph of the left mandibular premolar area shows the lamina dura as a thin white line that surrounds the tooth socket (arrowheads). Between the lamina dura and the tooth root is a thin radiolucent line known as the periodontal ligament space. The apical lamina dura (portion around root apex) can be seen intact through a radiolucency (black arrows) to the left of the root apex, confirming that this is not pulpal periapical inflammatory disease but in fact the normal mental foramen. The crestal lamina dura (white arrow) marks the normal height of the alveolar bone. In periodontal disease the crestal lamina dura is lost.



Figure 5 Right maxillary periapical radiograph shows anterior tooth-colored restorations (dental resin composite) on the canine and lateral incisor (arrowheads). The restorations are radiopaque but not as radiopaque as the amalgam restoration on the first molar (long arrow). Note the intact apical lamina dura on the lateral incisor, which appears as a continuous thin radiopaque line around the apex of the tooth (short arrows).

crucial to allow for visualization of the contacts between the teeth (Fig. 3). This is important because the outer edge of the enamel at the contact point is where decay, known as interproximal caries, begins. Because caries causes demineralization of the tooth it presents as a radiolucency within the radiopaque enamel. Interproximal caries begins just below or at the contact point between 2 teeth and in the early stages cannot be visualized clinically in posterior teeth. Hence bitewing views are necessary to detect early lesions known as incipient caries in the premolars and molars (Fig. 6). The use of bitewing images increases the detection of interproximal caries by 85%.⁵ Interproximal caries progresses through enamel in a triangular shape with its broad base at the outer edge of the enamel and its apex directed toward the DEJ. Caries that is still in the outer one-half of the enamel is known as incipient caries. Once the caries has reached the DEJ it spreads along the inner surface of the DEJ, creating a broad base at the outer edge of the dentin. The caries then progresses in a triangular pattern again toward the pulp chamber. Caries that has extended more than halfway between the DEJ and the pulp chamber is known as severe caries. Caries can occur on other surfaces of the teeth, including the biting surfaces, where it is known as occlusal caries. This type of caries can be detected clinically and can be seen only radiographically when it has already reached the dentin.

When a dentist detects caries within a tooth, and if the caries is extensive, an assessment has to be made as to whether the pulp has become involved. Several clinical tests may be performed, including vitality tests to determine if the tooth is still viable. Dentists use cold, heat, or an electric pulp tester to compare the response of the tooth in question to that of



Figure 6 This left premolar bitewing radiograph shows incipient caries on the distal (posterior) of tooth 20 (arrow) just below the contact point. A triangular radiolucency with its broad base at the outer edge of the enamel is seen within the enamel but does not extend to the DEJ. A lesion that has extended to the DEJ is seen on the mesial (anterior) of tooth 13 (arrowhead). Carious lesions in various stages are also present on several other teeth.

adjacent teeth. A negative vitality test informs the dentist that the pulp (neurovascular bundle) has been damaged irreversibly and hence before restoring the tooth the pulp needs to be removed. This procedure is known as endodontic therapy or a “root canal procedure.” After endodontic therapy, the normally radiolucent root canal appears radiopaque on images, because the treated root canal is filled with a radiopaque material (Fig. 7).

Restorations vary, but amalgam restorations have been historically the choice for posterior teeth as they offer resistance to biting forces and a good long-term prognosis. Amalgam-restorative materials, as the name implies, are a composite of mercury, silver, and tin and are sometimes called “silver fillings” because of their appearance. The metallic components of amalgam cause complete attenuation of the x-ray beam and amalgam restorations appear as an image void or complete radiopacity. Gold and high-noble replacement crowns also similarly attenuate the x-ray beam and appear completely

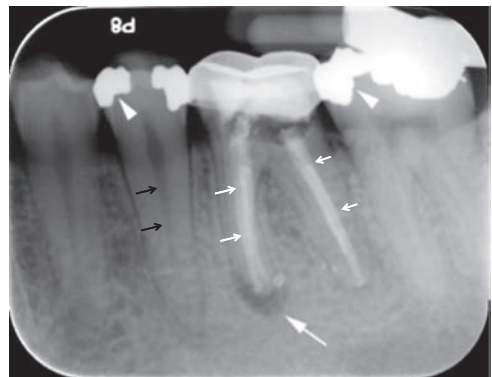


Figure 7 Periapical radiograph illustrating a periapical radiolucency (long arrow) involving a mandibular molar that has undergone root canal therapy. Note that the apical lamina dura is missing. The root canals are filled with gutta percha (short white arrows), which is radiopaque but not as radiopaque as amalgam restorations in crowns of adjacent teeth (arrowheads). Compare to adjacent tooth with normal radiolucent root canal (black arrows).



Figure 8 Periapical radiograph shows radiolucencies (arrowheads) at the apices of vital mandibular anterior teeth representing early lesions of periapical cemental dysplasia.

radiopaque. Metallic restorations cause significant streaking artifact on computed tomography (CT) scans and can confound interpretation. Tooth-colored restorative materials, known as dental resin composite, were historically used only in anterior teeth but are now frequently used also in posterior teeth. They usually contain a radiopaque filler, so they can be seen on the radiograph (Fig. 7). They are, however, less dense and so not as radiopaque as amalgams or gold crowns, and do not create the same artifact on CT scans.

Periapical Views

A periapical radiograph shows the view of the whole tooth including 2-3 mm of bone surrounding the apex of the root and is limited to teeth in 1 arch. This is in contrast with the bitewing view, which shows the crowns of both the maxillary and mandibular teeth together and does not show the root apices. A dentist may order from 14-18 periapical views depending on his/her preference and the patient's needs.

Periapical radiographs are taken to rule out lesions at the apex of the tooth, which may occur when the tooth has become nonvital. Death of the pulp results in degradation products that exit the tooth through the apex and set up an inflammatory response. This causes loss of apical bone and results in a periapical radiolucency (Fig. 7). The apical lamina dura, which normally appears as a thin radiopaque line, is also lost (compare Fig. 5 with Fig. 7). The presence of a radiolucency at the apex of a nonvital tooth automatically implies pulpal periapical inflammatory disease and only 2 options remain for the tooth: extraction or root canal therapy. The dentist determines which option is better for the tooth based primarily on restorability, that is, whether the tooth and root can be restored to optimal form and function. When a root canal therapy is performed the infected pulp is removed and

the canal or canals, depending on the tooth, are cleaned and debrided⁶ (Fig. 10). The canals are then filled with root-filling material, usually a rubber type material called gutta percha (Fig. 7). This appears radiographically as a radiopacity but is not as radiopaque as amalgam.

Vitality of the tooth is important as other lesions may appear as radiolucencies at the apex of teeth, most notably a condition called periapical cemental dysplasia (Fig. 8). This condition commonly occurs in middle-aged African American females and presents as a periapical radiolucency in the early stages of the disease. As the lesion matures, radiopacities representing dysplastic cementum are deposited within the radiolucency, making it less likely that it would be misdiagnosed as pulpal periapical inflammatory disease (Fig. 9). The teeth in periapical cemental dysplasia are vital and this condition is benign and requires no treatment.

Although periapical images are not adequate for preoperative implant planning, they are the image of choice for determining osseointegration of implants postoperatively (Fig. 10). Implants cause beam-hardening artifact on cone-beam CT (CBCT) scans, which precludes the use of this technology for postoperative implant evaluation. Periapical radiographs may also demonstrate other pathologies that occur in the alveolar bone, including common odontogenic lesions such as odontomas and dentigerous cysts. If the periapical image is not able to visualize the full extent of the lesion then the dentist may opt to take a panoramic radiograph, a CBCT scan, or a conventional medical CT scan.



Figure 9 Periapical radiograph shows a more mature stage of periapical cemental dysplasia. As the lesions mature, radiopacities are seen within radiolucencies (large arrow), which helps to distinguish this lesion from pulpal periapical inflammatory disease.

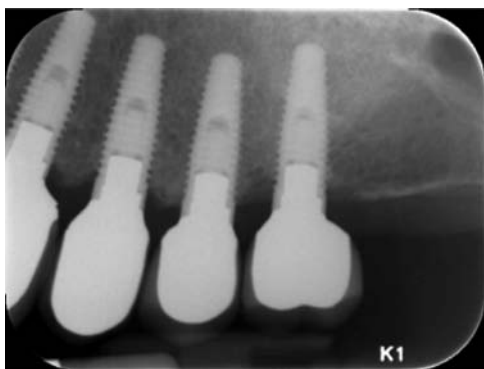


Figure 10 Periapical radiograph shows 4 implants in the left maxilla with osseointegration as evidenced by the bone engaging the threads of the implant and lack of any peri-implant radiolucency. The periapical radiograph is the imaging modality of choice for post-operative evaluation of implants.

Panoramic Radiographs

Panoramic radiographs allow visualization of both the maxilla and mandible and the surrounding oral and maxillofacial structures, including the temporomandibular joints (Fig. 11). Panoramic radiographs are extraoral images as the image receptor and x-ray source rotate synchronously around the patient's head. The machine uses a slit collimator and images are built up in thin slices. Receptors are larger versions of the intraoral digital sensors, being usually a CCD sensor or a PSP plate. Machines with CCD sensors display the image as acquired. PSP plates require "processing" in the manufacturer's reader, like intraoral plates. The patient either stands or sits within the machine and bites on a registration peg. Laser light or other positioning devices assist in placing the patient accurately within the machine's focal trough. This is the area between the image receptor and x-ray source where objects are imaged and in focus. A panoramic radiograph is commonly taken to evaluate third molars or extensive pathology that cannot be fully visualized on smaller intraoral periapical radiographs. The panoramic image also allows for visualization of teeth and pathology in relation to critical



Figure 11 A panoramic radiograph shows the maxilla and mandible and surrounding maxillofacial structures, including the temporomandibular joints. Note the impacted displaced right mandibular canine close to the inferior border of the mandible (arrows).

structures such as the mandibular canal and maxillary sinuses. However, owing to the 2-dimensional nature of the image the panoramic radiograph has significant limitations, including distortion, which precludes accurate measurements. Pathology cannot be evaluated in the buccal-lingual dimension (jaw thickness) and there is inherent magnification and overlapping of teeth in the technique, which varies depending on the machine. Many oral surgeons now prefer to take a CBCT image so that the pathology can be evaluated in 3 dimensions and the exact location of the lesion to vital structures such as the mandibular neurovascular bundle can be determined.

Cone-Beam Computed Tomography

The introduction of CBCT machines into the USA in the early 2000s revolutionized dental radiology. CBCT allows for 3-dimensional images of the oral and maxillofacial area, similar in appearance to images from conventional CT, but at a significant dose savings.^{7,8} In addition, the cost of the machine is significantly less than that of a conventional CT scanner and is therefore often affordable for dentists to place in their office. CBCT and medical CT images are acquired in different ways. There are 2 types of image receptor: flat panel and image intensifier. Most CBCT units currently use a flat panel detector comprising a large-area solid-state sensor. The units have a circular collimator; consequently the x-ray beam is cone shaped, hence the name cone beam.⁹ The x-ray source and image receptor rotate around the patient in a similar fashion to that of panoramic machines; however, the images acquired are similar to cephalometric images, which are large 2-dimensional lateral views of the head. The machine may rotate 360° around the patient in acquiring these images, called basis images. The x-ray beam is usually pulsed to reduce radiation exposure. The basis images are reconstructed into a volume and presented on a typical section screen as axial, sagittal, and coronal images. Most software programs also allow for viewing of 3D images without additional reformatting. Reconstruction time varies depending on the field of view and resolution selected.

There are a significant number of CBCT machines on the market targeted to the various dental specialties, each varying in the size and number of fields of view offered, and with options to have the patient sitting, standing, or supine. Smaller fields of view in the 5 cm × 5 cm range are usually used for endodontic applications as they generally provide a higher resolution, which is needed for visualization of additional root canals or fractures within the root of the tooth. Fields of view can vary from these very small volumes to extra-large volumes in the range of 24 cm × 17 cm, which are indicated for cephalometric analysis or cephalometric surgical planning. Images acquired with CBCT machines are similar to bone-window images in traditional medical CT imaging and therefore inadequate for evaluating soft tissue. Resolution is higher with isotropic voxel sizes in some of the newer machines as small as 0.05 mm. The radiologist is responsible for determining the optimal field of view and resolution using the principle

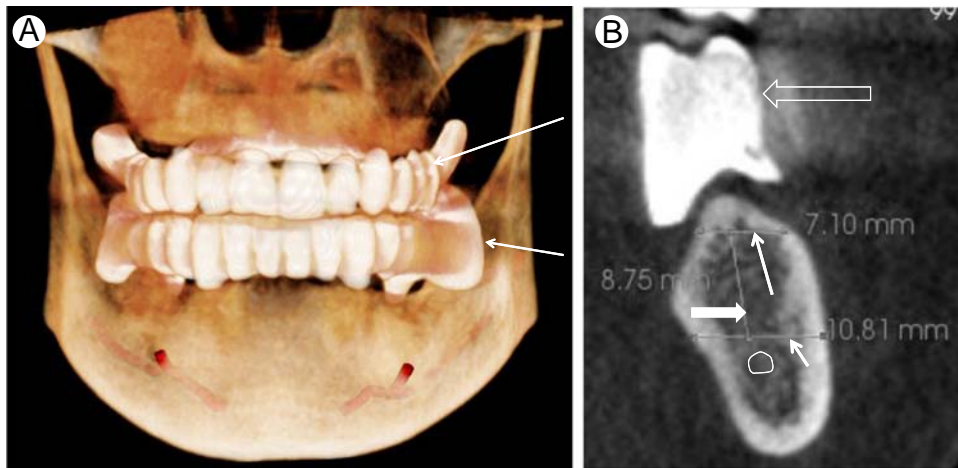


Figure 12 (A) 3D CBCT volume rendering. Patient is edentulous and wearing maxillary and mandibular radiopaque radiographic guides (arrows) made of temporary crown and bridge material (Integrity, Dentsply Caulk, Milford, DE). (B) Left mandibular cross-sectional CBCT image in the same patient shows the radiopaque guide (hollow bold arrow) at the first molar site straddling the mandibular ridge. Measurements of width are typically made at the superior border of the mandibular canal (short thin arrow) and the alveolar crest (long thin arrow). The bone height between these points (solid bold arrow) is also measured. Mandibular canal (white circle). (Color version of figure is available online.)

of As Low As Reasonably Achievable (ALARA), meaning radiation dose should be the minimum possible for the required diagnostic task.

The most common application of CBCT in dentistry is for implant planning. This is because it establishes the exact height, width, and contour of the alveolar ridge and the precise location of vital structures such as the maxillary sinuses and mandibular canal, all information necessary for safe implant placement.

Panoramic radiography is limited by its inability to generate cross-sectional images. Thus, when panoramic radiographs appear to demonstrate adequate bone for implant placement in the vertical dimension, the dentist usually obtains cross-sectional imaging with either conventional CT or CBCT to evaluate adequacy of bone in the buccal-lingual dimension and to obtain direct measurements of the prospective implant site(s).¹⁰

In 2012, the American Academy of Oral and Maxillofacial Radiology (AAOMR) published its position paper on the selection criteria for the use of radiology in dental implant planning.¹¹ The AAOMR concluded that panoramic radiography is considered unsuitable as a single imaging source for dental implant assessment. Furthermore, the AAOMR recommended that cross-sectional imaging be used for the assessment of all dental implant sites and that CBCT is the imaging method of choice for obtaining that information.

The radiologist determines the buccal-lingual width of the alveolar bone using the measuring tools in the CBCT imaging software. The distance of vital structures to the implant site is critical in determining whether sufficient bone is available for implant placement. Dentists often fabricate radiographic guides that help determine the ideal location and angulation for the implant. These guides, which are worn during the scan, may be full-coverage denture-like guides fabricated of radiopaque material (Fig. 12A) or localized guides that use radiopaque markers to indicate the ideal position of the implant.

The radiologist can then measure the height and width of the alveolar bone in the precisely desired location of the implant. Of consideration would be the proximity to vital structures such as the nasopalatine canal, floor of the nasal cavity, inferior alveolar neurovascular bundle, maxillary sinuses, etc. In the mandible, the width of the alveolar bone is typically measured both at the alveolar crest and at the superior border of the mandibular canal. Estimation of the available mandibular bone height for implant placement is then the measurement between these 2 points (Fig. 12B). Mesial to the mental foramen, where the mandibular canal ends, the height is measured from the alveolar crest to the bottom of the mandible. In the maxilla, the height is measured from the alveolar crest to the maxillary sinus. Dentists may also need to know the proximity of the adjacent teeth crowns and roots to determine whether sufficient space is available to restore the implant with the prosthesis once the implant is in place. If ample room is not available, orthodontics may be required to move teeth before implant surgery.

Surgical guides can be fabricated from the CBCT data and help the surgeon exactly place the implant in the desired location. This usually requires the CBCT data to be exported as DICOM files into third-party implant-planning software such as Simplant, NobelGuide, and Anatomage. The implant planning software merges 2 or 3 data sets depending on the program. In the Simplant program the patient is scanned wearing the radiographic guide and then the radiographic guide is scanned separately. In the Anatomage system the patient is scanned separately and then stone models derived from impressions of the patient are used by the dentist for prosthetic treatment planning. The models are scanned both before and after the treatment planning. Models are made by first taking an impression of the patient's arch, either maxilla or mandible, and then pouring up the impression with stone. The stone model, therefore, is a replica of the patient's maxilla or mandible including the soft tissue. By merging the scans, the



Figure 13 A typical maxillary surgical guide made with the Anatomage implant planning software. Pilot drill hole is seen on patient's right (arrowhead) and a master sleeve that allows insert tools is on the left (arrow). (Courtesy: T. Hart, DDS.) (Color version of figure is available online.)

implant planning software is able to accurately assess the ideal position of the implant relative to the available bone and the desired occlusion of the restored implant. Implant planning software programs have libraries of the various different types of implants and the desired shape, length, and width of the implant can be determined before surgery. This is accomplished by selecting a "virtual" implant from the library, superimposing it on the scan, and adjusting its size and shape to fit the patient¹². Once the correct virtual implant has been chosen and the exact angulation determined the data can then be exported for fabrication of the surgical guide. Surgical guides may contain just "pilot drill" holes, which allow for angulation of the initial pilot drill only and not subsequent drill sequences (Fig. 13). Alternatively, the guide may contain "master sleeves," which allow for guidance of every drill by the use of insert tools. The insert tools allow for guidance from the initial pilot drill through subsequent drills with gradually increasing diameters until the final desired diameter of the implant is reached.¹³ The use of surgical guides improves predictability of outcomes. If an

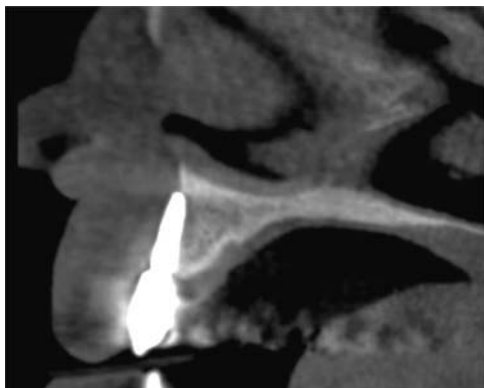


Figure 14 A sagittal CBCT view of the right anterior maxilla shows that the implant at the lateral incisor site has been placed too far facially and is out of the confines of the maxillary alveolar bone.

implant is placed by free hand there is a risk of violating critical structures or placing the implant outside the confines of the alveolar bone (Fig. 14).

In addition to CBCT there are several commercially available dental CT reformatting programs such as DentaScan (GE Medical System, Global Center, Milwaukee, WI) that are useful for imaging the teeth and jaw.

Conventional CT With Dental Reformatting Programs

Conventional medical CT imaging using reformatting software programs is also useful and frequently used for evaluating the teeth and jaws. The patient is placed supine in the CT gantry and may be secured using a head holder, chin strap, and sponges on either side of the head to prevent motion during the scan. A digital scout view is obtained to define the upper and lower boundaries of the scan and to ensure that the scan plane is parallel to the alveolar ridge.

Thin axial images are then acquired and the technologist selects one that ideally demonstrates the full contour of the mandible or maxilla and that is at the level of the roots of the teeth. Using this reference image, the technologist deposits the cursor in multiple positions along the curve of the mandible or maxilla. The CT software program then automatically connects these points, producing a smooth curved line, which defines the plane and location of a series of reformatted panoramic images produced buccal and lingual to the line. The program then places a series of numbered lines perpendicular to this curved line. The perpendicular lines are defined where multiple oblique sagittal (cross-sectional) images would be automatically reformatted. A 2-mm space is customarily used between reformatted cross-sectional images; however, this can be adjusted by the technologist. These reformatted images have the benefit of not being degraded by streak artifact as the artifact projects at the level of the crowns of the teeth and not over the area of interest, the bone and roots. When complete, 3 types of images are displayed: axial, oblique sagittal (cross-sectional), and panoramic. The DentaScan panoramic images are free from superimposition of other osseous structures, unlike standard panoramic radiographs. The oblique sagittal views are unique and allow clear identification of buccal and lingual cortical margins and buccolingual width, as well as normal anatomical structures such as the inferior alveolar canal, mental foramen, mandibular foramen, genial tubercle, greater and lesser palatine foramen, incisive canal, and maxillary sinus. In a typical study, 30-50 axial images, 40-100 cross-sectional images, and 5 panoramic images are generated.

Magnetic Resonance Imaging

Magnetic resonance imaging (MRI) is not typically used for implant planning. The primary indication for MRI is the evaluation of tumors and lesions of the jaw or for soft tissue lesions. It may also be used for evaluating the temporomandibular joint. T1 images are useful for determining marrow

replacement by tumor. Conventional medical CT may also be used. Cone-beam CT uses a bone setting and cannot characterize soft-tissue findings.

References

1. Sanderick GC, Miles DA: Intraoral detectors. CCD, CMOS, TFT, and other devices. *Dent Clin North Am* 44(2):249-255, 2000
2. Ludlow JB, Mol A: Digital imaging. In: White SC, Pharoah MJ (eds): *Oral Radiology: Principles and Interpretation*. ed 6. St. Louis, MO; Mosby 80, 2009
3. Zohrabian Vahe M, Poon Colin S, Abrahams James J: Embryology and anatomy of the jaw and dentition. *Semin Ultrasound CT MR* 36(5): 397-406, 2015
4. Bath-Balogh M, Fehrenbach MJ: *Dental Embryology, Histology and Anatomy*. ed 6. St Louis, MO; Elsevier Saunders, 2006
5. Hansen BF: Clinical and roentgenologic caries detection. *Dentomaxillofac Radiol* 9:34, 1980
6. Zohrabian Vahe M, Abrahams James J: Inflammatory diseases of the teeth and jaws. *Semin Ultrasound CT MR* 36(5):434-443, 2015
7. Mah J, Danforth R, Hatcher D: Radiation absorbed in maxillofacial imaging with a new dental computed tomography device. *Oral Surg Oral Med Oral Pathol Oral Radiol Endod* 96:508-513, 2003
8. Ludlow JB, Ivanovic M: Comparative dosimetry of dental CBCT devices and 64-slice CT for oral and maxillofacial radiology. *Oral Surg Oral Med Oral Pathol Oral Radiol Endod* 106:930-938, 2008
9. Scarfe WC, Farman AG: Cone-beam computed tomography. In: White SC, Pharoah MJ (eds): *Oral Radiology: Principles and Interpretation*. ed 6. St. Louis, MO; mosby 225, 2009
10. Wyatt CC, Pharoah MJ: Imaging techniques and image interpretation for dental implant treatment. *Int J Prosthodont* 11(5):442-452, 1998
11. Tyndall DA, Price JB, Tetradis S, et al: Position statement of the American Academy of Oral and Maxillofacial Radiology on selection criteria for the use of radiology in dental implantology with emphasis on cone-beam computed tomography. *Oral Surg Oral Med Oral Pathol Oral Radiol* 113:817-826, 2012
12. Zohrabian Vahe M, Sonick Michael, Hwang Debby, Abrahams James J: Dental implants. *Semin Ultrasound CT MR* 2015. [in this issue]
13. Chenin DL: Surgical guides. In: Tamimi DF (ed): *Specialty Imaging: Dental Implants*. Salt Lake City, UT: Amirsys 3:39, 2014

Dental Implants



Vahe M. Zohrabian, MD,^{*,†} Michael Sonick, DMD,^{*,†} Debby Hwang, DMD,^{*,†}
and James J. Abrahams, MD^{*,†}

Dental implants restore function to near normal in partially or completely edentulous patients. A root-form implant is the most frequently used type of dental implant today. The basis for dental implants is osseointegration, in which osteoblasts grow and directly integrate with the surface of titanium posts surgically embedded into the jaw. Radiologic assessment is critical in the preoperative evaluation of the dental implant patient, as the exact height, width, and contour of the alveolar ridge must be determined. Moreover, the precise locations of the maxillary sinuses and mandibular canals, as well as their relationships to the site of implant surgery must be ascertained. As such, radiologists must be familiar with implant design and surgical placement, as well as augmentation procedures utilized in those patients with insufficient bone in the maxilla and mandible to support dental implants.

Semin Ultrasound CT MRI 36:415-426 © 2015 Elsevier Inc. All rights reserved.

Introduction

A major cause of tooth loss in the United States is periodontitis, which in its mild to severe forms affects 46% of the population, with other tooth loss etiologies including, but not limited to caries, trauma, developmental defects, and genetic disorders, such as dentinogenesis imperfecta.¹ Before dental implants, dentures or bridges were used for cosmesis in edentulous patients. A removable denture (false teeth) is a prosthesis composed primarily of acrylic resin or porcelain seated in a plastic mount and supported by the surrounding hard and soft tissues of the oral cavity. A denture may be partial or complete depending on whether a patient is missing some or all of his or her teeth in a single arch. A bridge is a fixed (nonremovable) partial denture that is used to replace a missing tooth or several missing teeth. A bridge consists of an artificial or “dummy” tooth or teeth composed of gold, porcelain, or porcelain-fused-to-metal. A crown is used to anchor a bridge to the adjacent normal teeth (Fig. 1). An attractive alternative to standard dentures and bridges became available when dental implants were developed and refined. The basis for dental implants is osseointegration, in which osteoblasts grow and directly integrate with the surface of

titanium posts surgically embedded into the jaw.² Having become extremely popular over the last few decades, dental implants restore function to near normal in partially or completely edentulous patients.

Implant Design

Implants have become the state of the art in dentistry and are the most optimal substitute for missing teeth. As a single-tooth replacement, an implant is freestanding, not attached to adjacent teeth, and therefore, much easier to maintain. For patients who have lost multiple teeth, implants can provide support for a stable, healthy, and esthetic dentition that is not removable. Perhaps the most important aspect of implants is that they can restore quality of life and greatly boost a patient's self-esteem.

A root-form implant is the most frequently used type of dental implant today and consists of 3 main components: fixture, abutment, and prosthesis (Fig. 2). The fixture is a cylinder-shaped metal post that is surgically embedded into the osseous portion of the jaw, simulating the shape of the root of a tooth. After surgical insertion, the top of the fixture will be flush with the surface of the alveolar bone. The abutment is attached to the fixture using an abutment screw, which raises it from the bone surface to above the mucosal surface. The prosthesis is then either cemented to the implant or attached with a prosthesis screw. It is worth noting that a one-to-one ratio does not necessarily need to exist between the tooth and the implant. For example, a 5-tooth prosthesis might be

*Department of Diagnostic Radiology, Yale School of Medicine, New Haven, CT.

†Yale-New Haven Hospital, New Haven, CT.

Address reprint requests to Vahe M. Zohrabian, MD, Yale School of Medicine, 333 Cedar Street (Room CB-30), P.O. Box 208042, New Haven, CT 06520-8042. E-mail: vahe.zohrabian@yale.edu

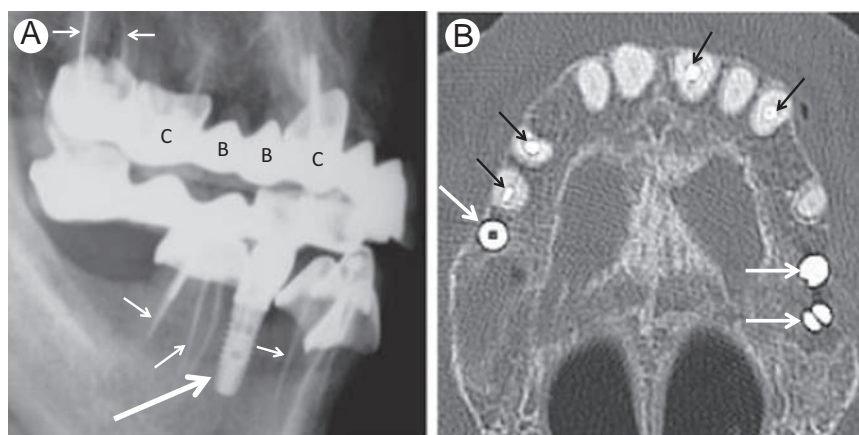


Figure 1 Imaging appearance of root-form implants in 2 different patients. (A) Lateral radiograph demonstrates a root-form dental implant with titanium-threaded fixture embedded in the mandibular alveolus (large arrow). Also, note maxillary bridge (B) supported by crowns (C) on adjacent teeth. Radiopaque gutta-percha (short arrows) is noted in the root canals from root canal procedures. (B) Axial CT with bone windows demonstrates 3 root-form implants in the right and left maxilla (white arrows). Prior root canal procedures are also depicted (black arrows).

supported by just 3 implants. Dental implants are readily seen on computed tomography (CT) scans using bone windows, as well as on plain radiographs (Fig. 1).

Before root-form implants, dentists used subperiosteal, blade, and transosseous implants.³ A subperiosteal implant consists of a metallic meshwork, which is implanted beneath the periosteum of the alveolar process (Fig. 3). Metallic posts extend from beneath the periosteum into the oral cavity to support the prosthesis. A blade implant is a type of endosseous implant that is rectangular shaped and consists of metallic posts that extend from the top of the osseous implant into the oral cavity (Fig. 4). Subperiosteal and blade implants have essentially been replaced by the more favorable root-form

implants, although they may still be occasionally encountered on imaging. For highly atrophic mandibles, a transosseous implant may be placed from underneath the chin, traversing the mandible from bottom to top until it is exposed in the mouth. However, transosseous implants are rarely used today secondary to the extensive surgery that is required to place them.

Dentists prefer to place the largest implant possible because it provides greater surface area, and thus, more effective osseointegration for a stronger anchorage. However, the maximum size of an implant is limited by the amount of alveolar bone available. At least 1-1.5 mm of bone on either side of the implant, as well as 1-2 mm of bone between the bottom of the implant and vital structures, such as the maxillary sinus or mandibular canal, should be present for dental implants to be successful.⁴ In addition to bone quantity, bone quality assessment is important in the workup of a dental implant patient. The density of the bone may be determined on cross-sectional reformatted CT images according to the Misch system that grades bone density from D-1 to D-4.⁵ The D-1 bone is characterized by thick, dense cortices surrounding densely calcified spongy bone with little or no porosity, whereas the D-2 bone is characterized by dense cortical plates and thick coarse trabeculae with small areolar spaces. The D-3 bone is thin cortical bone with thin trabeculae. Finally, the D-4 bone is thin or absent cortical plates with a paucity of mineralized trabeculae. The D-1 or D-2 bone offers the best chance of osseointegration.⁵

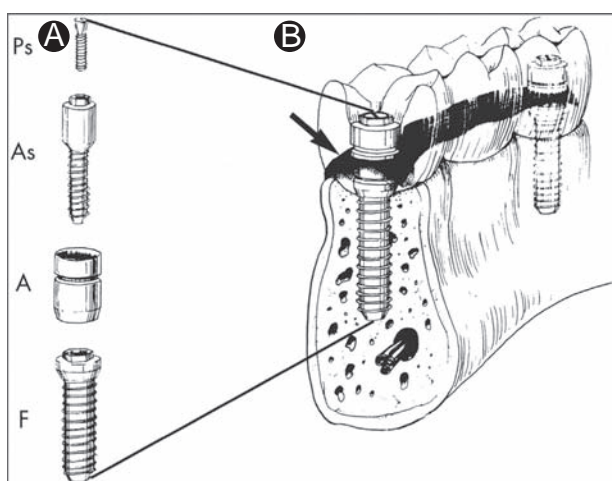


Figure 2 Illustration of 2 root-form implants supporting a 3-tooth prosthesis. (A) Root-form implant components: Prosthesis screw (Ps), abutment screw (As), abutment (A), fixture (F). (B) The threaded titanium fixture (F) is the portion embedded into the alveolar bone that undergoes osseointegration. The black portion running through the prosthesis (black arrow) represents a metal framework that supports the porcelain dental prosthesis. (Reprinted with permission from Abrahams and Kalyanpur.¹⁹)

Surgical Procedure

The implant surgical procedure is illustrated in Figure 5. Placement of the implant is typically achieved in 2 stages in a dentist's office using local anesthesia. During the first stage of surgery, the gingiva and periosteum are reflected back and an osteotomy site (hole) is drilled in the alveolar ridge in a predetermined desired location (Fig. 5A). A titanium fixture is

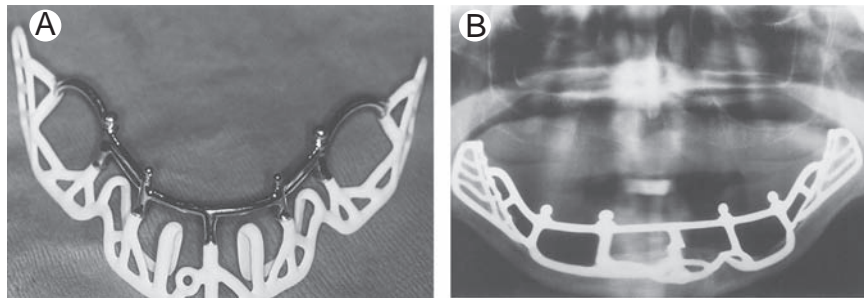


Figure 3 Subperiosteal implant. (A) Photograph of a subperiosteal implant. The white portion fits underneath the periosteum and on top of the alveolar process and may be coated with hydroxyapatite to stimulate bone growth. The metallic portion extends above the level of the gingiva to support the prosthesis. (B) Panoramic radiograph demonstrates the subperiosteal implant in a severely atrophic mandible. The prosthesis is not yet attached. (Courtesy of Wayne C. Jarvis, DDS, Dentofacial Surgery of Western New York, Williamsville, NY.)

then torqued or screwed into the prepared location in the osseous portion of the jaw. Fixtures range in size and are manufactured with threads, which are external ridges in the form of a helix to maximize initial contact, enhance surface area, and facilitate stresses at the bone-implant interface.⁶⁻⁸ Newer fixtures feature tapered, root-form silhouettes, decreased thread pitch (distance between ridges), as well as deeper thread projections—all characteristics that magnify surface area and curtail initial micromovement.^{9,10} Further implant stability occurs through implant body surface roughening, accomplished via titanium plasma-spraying, grit-blasting, acid-etching, anodization (oxide layer formation), or laser-sintering—texturing. Most of these topographic modifications are commercially available and correlate with long-term implant survival (95% rate), especially if they result in moderately roughed surfaces of 1-2 μm .^{11,12} Adding

biomimetic agents, such as bioceramics (calcium phosphate salts like hydroxyapatite), bioactive proteins (bone morphogenetic proteins), growth factors, type I collagen, Arg-Gly-Asp (peptide and chitosan), ions (fluoride), and other polymers to the tapered, threaded, and mechanically roughened fixture may amplify bone-to-implant contact and speed of osseointegration, though most of these agents either are not commercially available or have no long-term clinical evidence to advocate their standard use.¹³⁻¹⁷

After fixture insertion, either a healing abutment (Fig. 5D) is immediately screwed into the hollow exposed coronal portion of the implant fixture, or a cover screw (Fig. 5B) is first attached and followed by placement of a healing abutment, as seen in Figure 5. Cover screws are flush with the implant platform and bone surface, whereas healing abutments extend further and are flush with or slightly coronal to (above) the mucosal surface

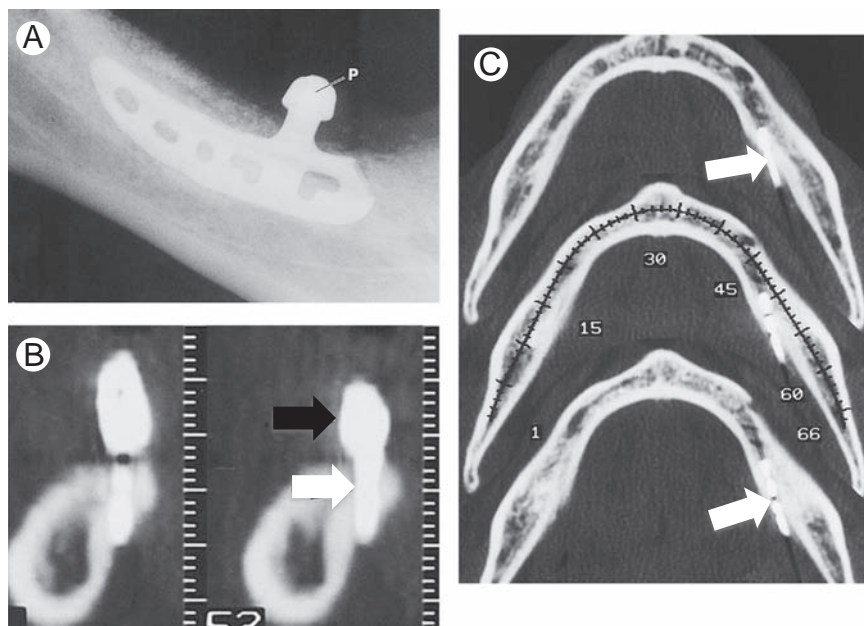


Figure 4 Blade implant. (A) Radiograph demonstrates a metallic blade implant inserted in the mandible after a linear osteotomy. A single post (P) extends above the level of the bone and gingiva to support a prosthesis. (B) Cross-sectional and (C) axial CT images demonstrate a blade implant in the mandible (white arrow) with a post extending into the oral cavity (black arrow). (Reprinted with permission from Abrahams and Kalyanpur.¹⁹)

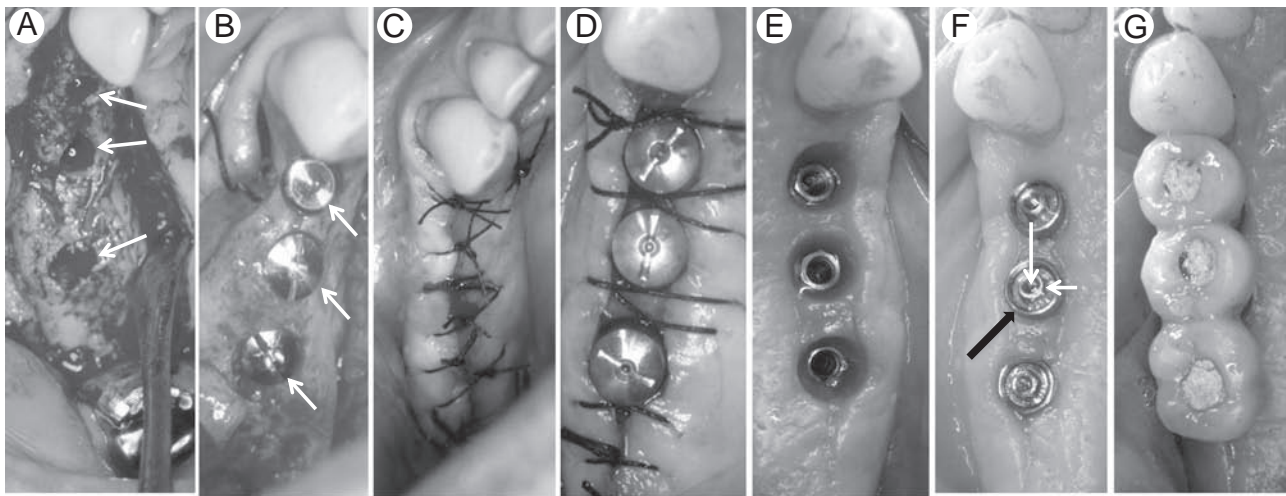


Figure 5 Dental implant surgery. (A) Incision is made and the soft tissue flap is reflected back, after which 3 holes are drilled (white arrows) for placement of implants. (B) Implant platforms flush with bone have openings occluded with cover screws (white arrows). (C) Incision is sutured, closed, and allowed to heal for 3-6 months. (D) Cover screws are surgically exposed for replacement with healing abutments. (E) Healing abutments are removed exposing the implant surface. (F) Permanent abutment (black arrow) is fixed to implant fixture with abutment screw (short white arrow). *Note:* hole in abutment screw (long white arrow) to accommodate screw for attaching prosthesis. (G) Prosthesis is screwed into abutments and access holes are filled with tooth-colored composite material. (Reprinted with permission from Abrahams.²¹)

and can actually be seen in the mouth extending slightly above the mucosal surface. In either case, the healing abutments and cover screws both prevent ingrowth of soft tissue or bone into the exposed hollow portion of the implant during the 3- to 6-month healing period that follows. Healing abutments allow for secondary intention healing. When cover screws are used, the soft tissue is sutured back over the fixture and cover screw, creating primary closure of the wound (Fig. 5C). Cover screws are typically reserved for more complicated scenarios that involve ridge augmentation or otherwise compromised implant placement.

During this first stage of surgery, where the fixture is placed in the bone, it is important to establish the proper angle of the implant with the alveolar ridge. Occlusal force vectors should be parallel to the vertical axis of the alveolar ridge, as any excess angulation of the implant may result in breakdown of the surrounding bone.⁴ The mean healing period to provide for osseointegration following this first phase of treatment is 3 months, though the wait time may range from 6 weeks (early prosthesis loading) to 6 months (more surgically complicated cases). During the 3- to 6-month healing phase, osteoblasts grow and “integrate” with the titanium fixture.

In the second stage of implant surgery, when healing is complete, the healing abutments are removed to expose the fixture platforms (Fig. 5E). The final abutments are next intimately connected to the fixture using abutment screws (Fig. 5F). The abutment screw, which is easily replaceable, is the structurally vulnerable component of the implant complex.¹⁸ In the event of unforeseen stress, it may loosen or even break, thus sparing the fixture itself from damage.⁴ Angled abutments may be used to correct for implants that are not parallel to the residual teeth.¹⁹

The final prosthesis, comprised of a single tooth crown or multiple teeth in a denture-type construction, is typically cemented onto the abutment. In lieu of cement retention, the prosthesis can be attached to the abutment using screws (Fig. 5G), which are used when there is limited interocclusal space or when easy retrievability is needed (long-span prostheses). A one-to-one implant-prosthesis ratio is not necessary, and a full 14-tooth prosthesis can be supported by only 6 root-form implants, though these implants must be strategically located to dissipate stress and distribute masticatory forces properly.

Radiologic Considerations

For a dentist to place an implant safely, the exact height, width, and contour of the alveolar ridge must be determined. Moreover, the precise locations of the maxillary sinuses and mandibular canals, as well as their relationships to the site of implant surgery must be ascertained. Inadvertent injury to the neurovascular bundle may result in permanent facial paresthesia, whereas violation of the maxillary sinuses may set the stage for oroantral fistula/infection and subsequent implant failure.

The radiologic assessment of the implant patient may begin with intraoral periapical radiographs to approximate the vertical height of the alveolar ridge. Although offering the best resolution (line pairs/mm) amongst all imaging modalities with minimal image distortion, periapical radiographs are limited by their small size and inability to precisely localize key anatomical structures. Moreover, the inability to visualize relevant anatomy in 3-dimensional (3-D) renders periapical radiographs inadequate in the accurate estimation of bone volume in the

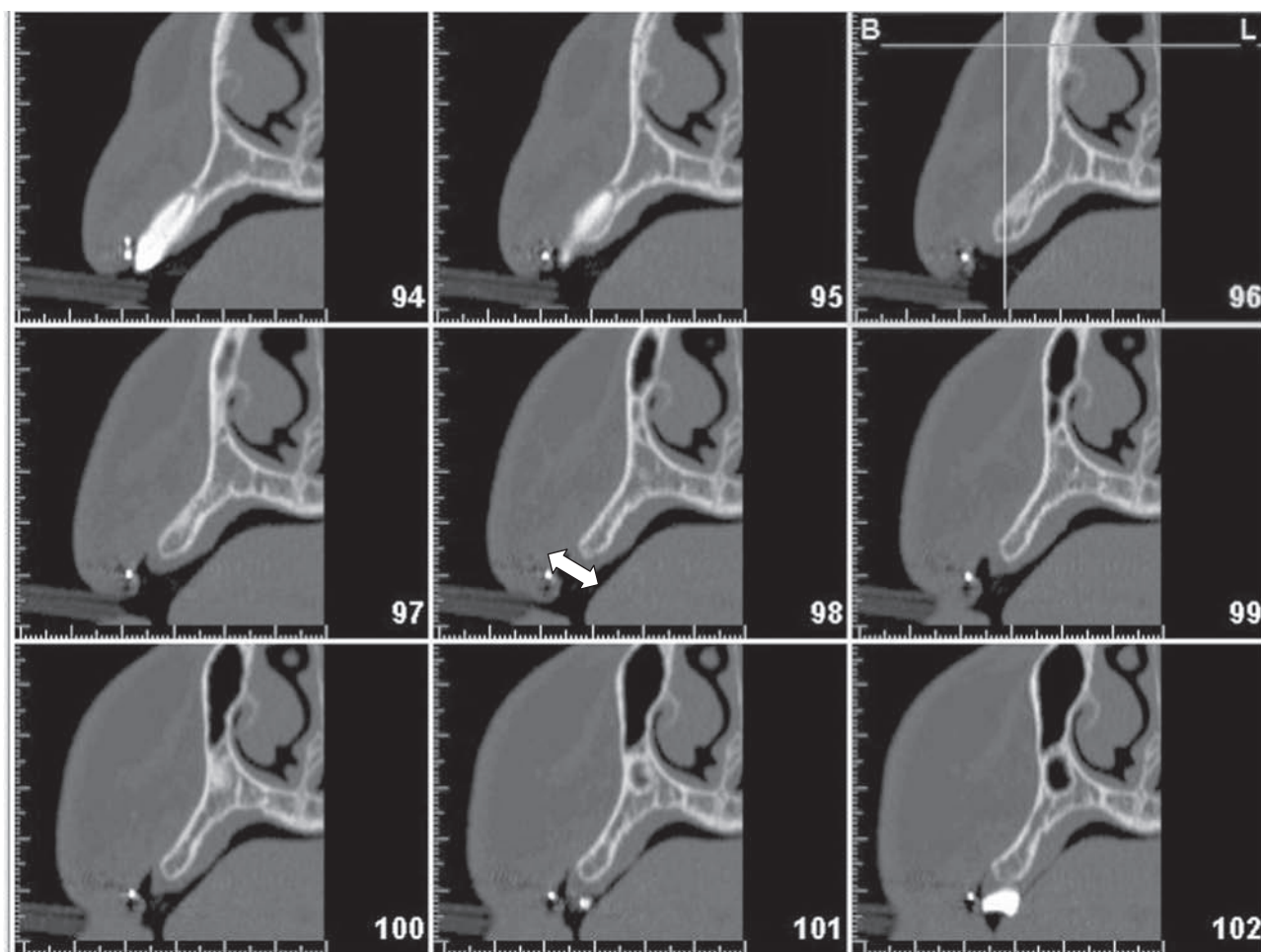


Figure 6 Cross-sectional CT images demonstrate atrophy particularly in buccolingual dimension (thickness), rendering inadequate bone for implant placement (center box and left-right white arrow).

edentulous site, especially in the buccolingual or horizontal dimension (thickness).

Panoramic radiography is the most widely used imaging study in the preoperative evaluation of the dental implant patient, although it too has its limitations. The magnification factor varies, and images may be distorted up to 25% secondary to a predetermined plane or focal trough incongruent with the patient's alveolar ridge. This makes accurate measurement of bone height and thickness unreliable. Panoramic radiographs may demonstrate adequate bone for implants in the vertical dimension (height), but will not provide information regarding the thickness of bone in the horizontal direction. Dentists may therefore obtain cross-sectional imaging with either conventional or cone beam CT (CBCT) to evaluate the adequacy of bone in the buccolingual dimension (thickness) (Fig. 6) and to obtain direct measurements of bone in the prospective implant site(s).²⁰ CBCT and conventional CT are the best modalities to evaluate patients for dental implants, although they are not needed in every patient and often reserved for more complex cases. A growing number of dental clinicians are acquiring in-suite CBCT scanners to accelerate diagnosis and preparation.

Multidetector thin-section CT and reformatting software programs have greatly facilitated dental implantology.^{21,22}

Commercially available interactive CT programs, such as SimPlant (Materialise, Leuven, Belgium), allow one to simulate implants on the CT image and permit preoperative planning that allow dentists to select the ideal location, trajectory, and size of the implant before surgery. Equally important is that they permit analysis of bone density, bone volume, distance to vital structures, and the location of areas that may require bone augmentation. These CT software packages also help the patient envision his or her own bone (or lack thereof), bolstering commitment to the treatment planning process. An educated patient takes on therapeutic responsibility along with the dental team, which makes for more reasonable goal expectations. Surgical guides that expedite accurate implant placement may also be created through the use of this imaging via 3-D printing technology. These surgical guides may be constructed simply using the images and virtual planning software. However, in challenging it is preferable for the patient to wear a customized, laboratory-manufactured scanning appliance that will show up on the images and demonstrate the ideal final tooth positioning. The appliance is made using impressions of the jaw and cast fabrication. In either case, final tooth positioning can be determined and a surgical guide made. Currently, only third-party providers offer 3-D printing; however, in-office fabrication of models and guides are very close to realization.

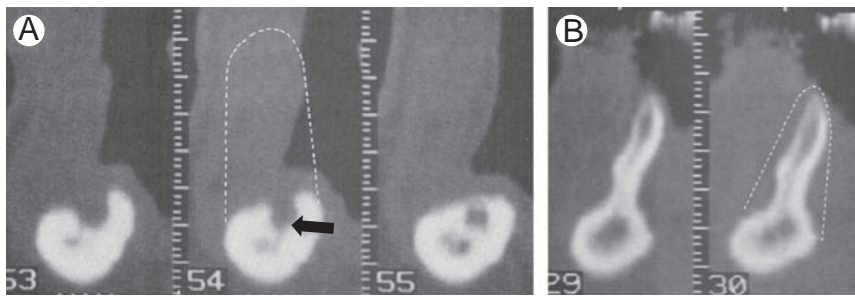


Figure 7 Bony resorption and atrophy. (A) Cross-sectional CT images of the mandible in this patient demonstrate atrophy of the height of the mandible, causing the mandibular canal (black arrow) to sit immediately beneath the gingival surface. The dotted white line in the center image shows how the bone contour should normally appear. (B) In a different patient, the width of the mandible is considerably diminished from atrophy. The dotted white line again shows how the bone should normally appear. (Reprinted with permission from Abrahams and Kalyanpur.¹⁹)

After surgery, periapical radiographs, panoramic radiographs, and CT images can be used to evaluate the adequacy of implants. Peri-implantitis refers to lack of osseointegration along the implant-bone interface, often due to infection around the fixture²³ or micromotion. This is apparent on periapical radiographs as a radiolucent rim around the implant fixture and loss of crestal bone at the implant site (saucerization), suggesting failure. The greatest degree of peri-implant vertical bone loss occurs within the first year after placement of the implants.²⁴ Severe bone loss may even result in complete rejection of the dental implant.

Augmentation Procedures of the Jaw

Patients must have sufficient bone in the maxilla or mandible to support implants. Most surgeons prefer to place implants in bone that measures at least 3 mm in width and 10 mm in height. The width criterion is based on the tooth to be replaced (smaller diameter for smaller teeth), and the length criterion is based on older investigations that showed improved longevity with at least 10-mm tall fixtures. Newer meta-analyses show that rough-surfaced short implants (no longer than 10 mm but

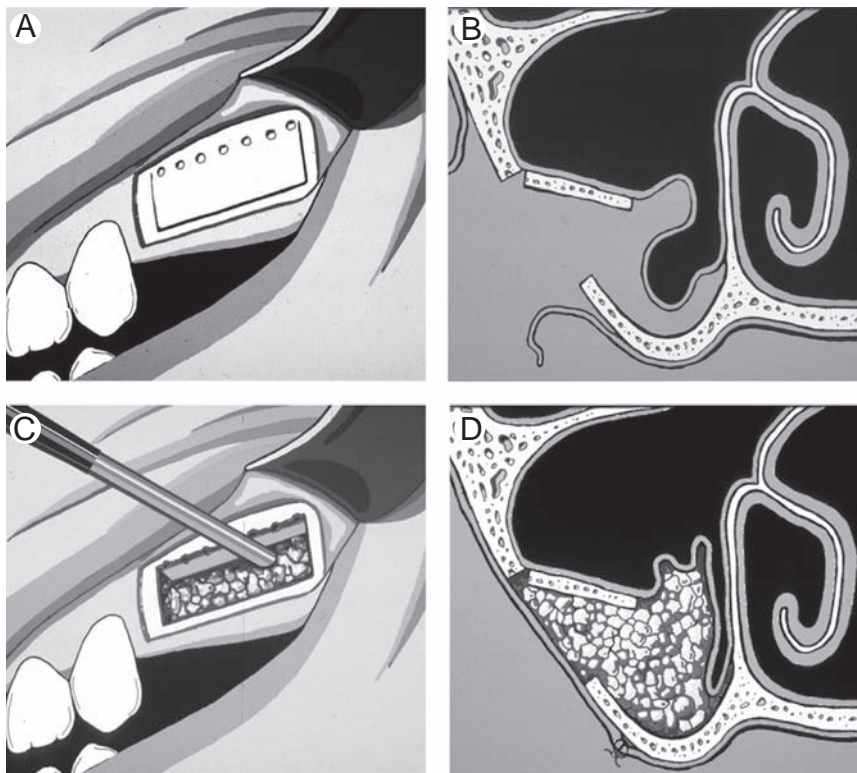


Figure 8 Illustration of sinus lift procedure. (A) A rectangular osteotomy is made in the lateral antral wall of the maxillary sinus. Closely positioned holes are drilled, which are then fractured inwards to create a trapdoor. (B) Cross-sectional (lateral) view of the maxillary sinus shows space that is created by pushing the trapdoor inward and maxillary sinus membrane. (C) The space is packed with bone graft material. (D) Cross-sectional (lateral) view shows bone graft material filling the space created by the osteotomy. (Reprinted with permission from Abrahams and Berger.²²)

at least 6 mm) may be as successful as their taller counterparts when applied in cases with missing single teeth.²⁵⁻³⁰ Unfortunately, after being edentulous for a long time, the bony alveolar ridge resorbs and becomes atrophic, often leaving insufficient bone to support metallic implants (Fig. 7). Fortunately, several surgical options have been developed to increase the amount of alveolar bone and render such patients suitable for dental implants.³¹

Sinus Lift Procedure

The lateral wall sinus elevation procedure (subantral augmentation or sinus lift), developed in the mid-1970s, involves placing bone-graft material in the maxillary sinus under the Schneiderian membrane to increase the height and width of the maxillary alveolus (Fig. 8).³²⁻³⁵ This common procedure, performed in the dentist's office, begins with the creation of a mucoperiosteal flap along the anterior wall of the maxillary sinus, similar to the Caldwell-Luc approach. A rectangular osteotomy is then made in the lateral antral wall of the maxillary sinus 3-4 mm above the floor of the sinus. Drilling closely positioned holes forms the superior horizontal segment

that is carefully fractured inwards to form a trapdoor. Special care is taken to prevent tears in the Schneiderian membrane. The membrane at the inferior aspect of the osteotomy is then dissected and elevated upwards to create a space for bone-graft material. Bone-graft material can be of several types,²³ including autogenous bone from the iliac crest or maxillary tuberosity, mineralized freeze-dried bone allograft (FDBA), demineralized FDBA (DFDBA), xenograft (bovine in particular), and alloplast such as hydroxyapatite. An absorbable membrane placed over the bony window prevents ingress of epithelium and helps contain the graft material, after which the mucoperiosteal flap is repositioned and sutured closed. At least 6 months is required for healing to take place before placing dental implants.

An alternative to lateral wall sinus lift is an osteotome-mediated sinus lift elevation.³⁶ In this technique, the site for the maxillary implant is drilled and stopped just short of the floor of the maxillary sinus. An osteotome, a mallet-like device, is then used to create an in-fracture of the osseous floor of the maxillary sinus. Bone graft is then pushed into the site, displacing the detached part of the sinus bony floor and overlying Schneiderian membrane. After the desired amount of

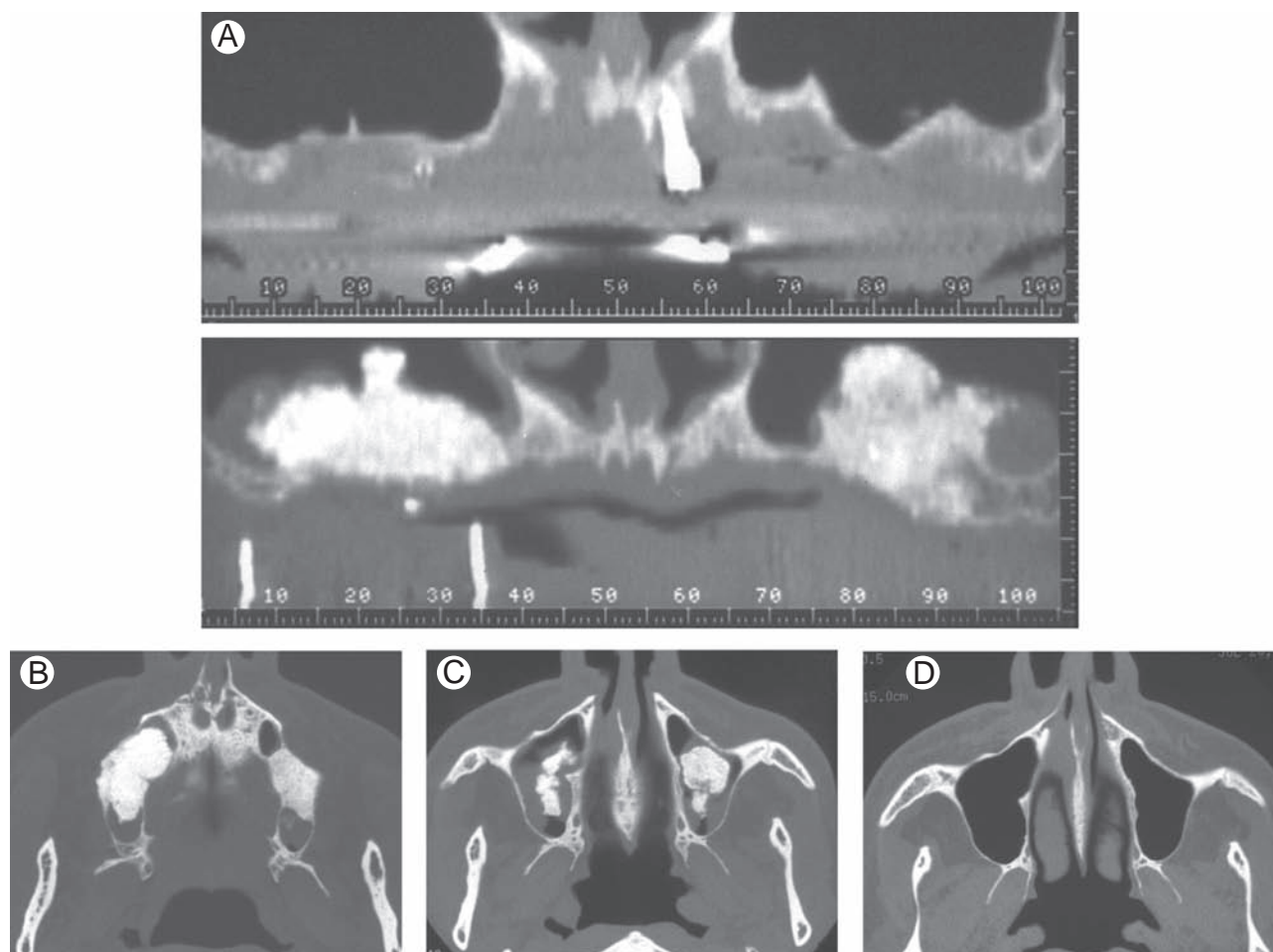


Figure 9 Radiographic appearance of sinus lift procedure. (A) Panoramic radiographs obtained before (top) and after (bottom) sinus lift procedure to treat alveolar atrophy. In the bottom image, note the position of the graft adjacent to the alveolar ridge in the caudal aspect of the maxillary sinus. (B-D) Axial CT images through the maxillary antrum demonstrate irregular dense masses in the center of the sinus, surrounded by soft tissue density between the graft and wall of the sinus in (B and C). Also note slight concavity at the osteotomy site in (B). (Reprinted with permission from Abrahams.³¹)

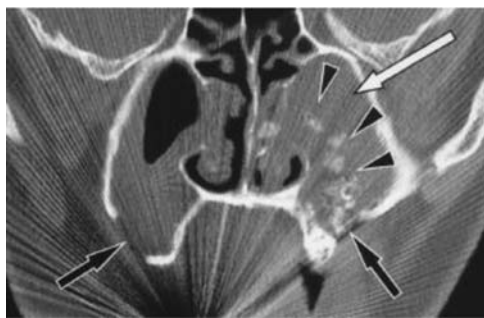


Figure 10 Sinus lift postoperative infection. Coronal CT scan demonstrates bilateral osteotomies (black arrows). There is complete opacification of the left maxillary sinus (white arrow). Note that bone graft material is diffusely dispersed on the left (black arrowheads) and absent on the right. (Reprinted with permission from Abrahams et al.³⁷)

elevation is achieved, as determined by periapical radiographs, the implant is torqued in. On axial CT images, the graft material from the lateral wall sinus lift procedure appears as irregular masses of high-density material similar to bone in the inferior half of the maxillary sinus, typically in the center of the sinus (Fig. 9). Zones of soft tissue and air density may surround high-density bone graft material. On panoramic and oblique sagittal CT images, the bone grafts are contiguous with and often indistinguishable from the floor of the sinus. The osteotomy may be seen on oblique sagittal views as a small area where bone graft material bulges slightly anteriorly through a defect in the wall of the sinus. Radiologists should be familiar with the appearance of the sinus lift procedure to avoid its confusion with pathologic entities such as osteomas, fibrous dysplasia, and odontomas. Although the outcome of the sinus lift procedure is generally good, failure may result from infection, which presents radiographically as markedly increased soft tissue density in the sinus and dissipation of the graft (Fig. 10). Failure may also result from lack of integration of the graft into the alveolar remnant.³⁷

Onlay Bone Grafting

Bone grafts harvested from the mandibular symphysis, mandibular ramus, maxillary tuberosity, or in extreme cases, iliac crest, may be used to augment severely atrophic alveolar bone.³⁸ Grafts are held in place with screws, or less often, wire sutures, and at times, may be supplemented with other graft materials, such as freeze-dried bone material. The radiographic appearance of these bone grafts varies according to the location of the graft and how closely they are apposed to the alveolar bone, although surgical wires or screws may outline the margins of the graft (Fig. 11). Cancellous instead of cortical bone makes distinguishing between the graft and alveolar ridge more difficult. Furthermore, considerable space between the graft and the alveolar ridge raises concern for poor apposition during surgery or migration after surgery.

Guided Bone Regeneration

When a tooth is lost, the normal pressure on the bone and surrounding tissues from the opposing tooth is also lost. As a result, the underlying alveolar bone or soft tissue atrophies and resorbs, creating a situation where there may be insufficient bone for implants. These and other patients may benefit from guided bone regeneration (GBR). Basically, GBR works by creating a potential space into which bone graft material is placed to encourage bony regeneration (Fig. 12). In cases with greater osseous deficits, the procedure is performed before the placement of implants and allowed to heal for approximately 6 months; in cases of minor bone loss, the implant can be placed at the time of the augmentation. This technique may also be used for the treatment of periodontal pockets (Chapter 5, Fig. 5). CT scan software with 3-D imaging helps the dental professional to identify alveolar morphology and determine the area where GBR is needed (Fig. 13 E and F).

GBR encourages regeneration in 2 ways: (1) by streamlining the migration of osteo-promotive cells into a clinically created

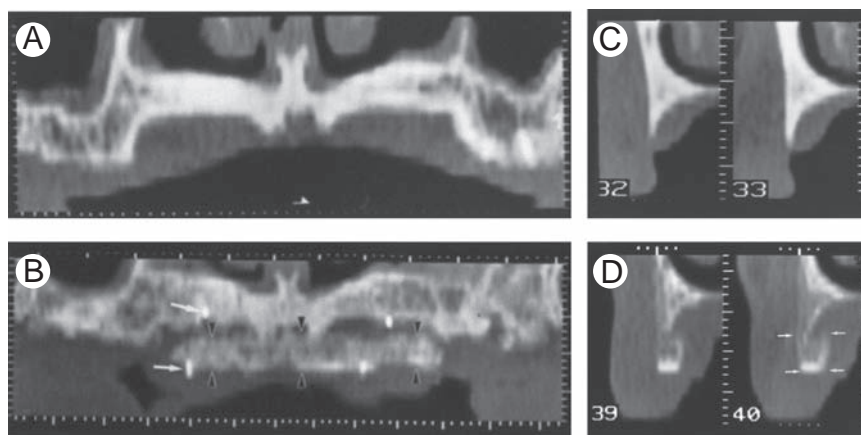


Figure 11 Onlay bone grafting. (A) Preoperative (panoramic) and (C) (cross-sectional) CT images in an edentulous patient demonstrate atrophy of the alveolar ridge, precluding placement of dental implants. (B) Postoperative panoramic CT image shows the atrophic alveolar ridge of the maxilla augmented by an iliac crest onlay bone graft (black arrowheads). Wire sutures are seen holding the graft in place (white arrows). (D) Postoperative cross-sectional CT image demonstrates that bone graft material has increased the height and width of the alveolus (white arrows). (Reprinted with permission from Abrahams.³¹)

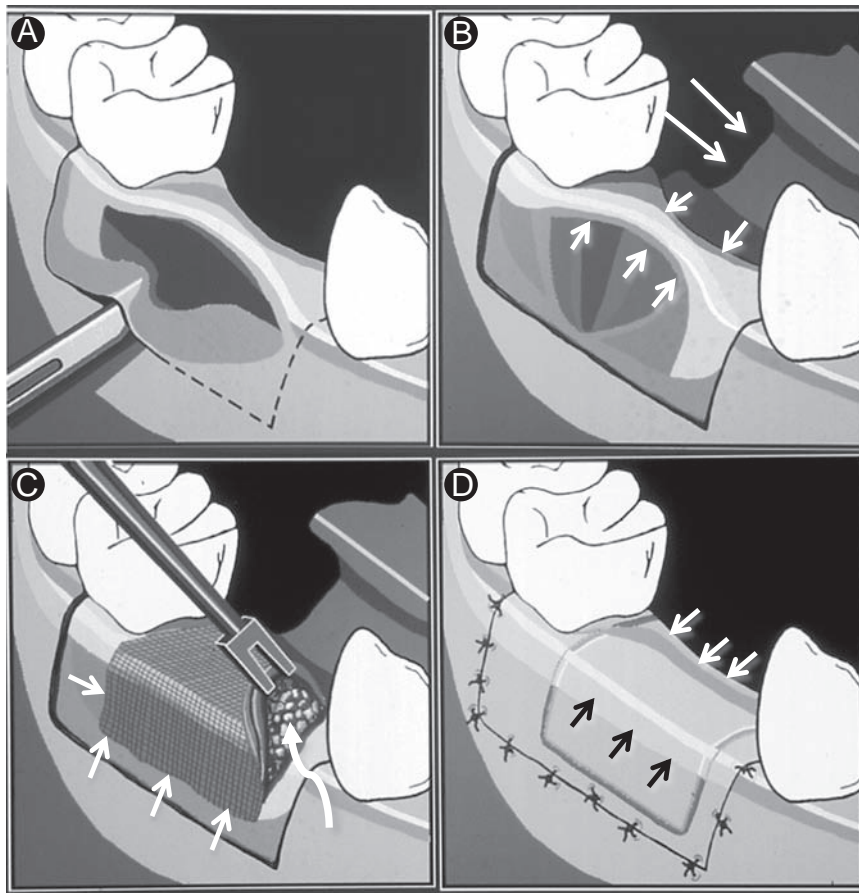


Figure 12 Illustration of guided regeneration using expanded polytetrafluoroethylene (ePTFE) membrane and bone graft material to augment an atrophic alveolar ridge. (A) Through an incision in the gingiva and periosteum, a soft tissue flap is created. (B) The soft tissue flap is reflected back (long arrows) to expose the atrophic alveolar ridge (short arrows). (C) Bone graft material is placed in the atrophic area (curved arrow) and is covered by a titanium-reinforced ePTFE membrane (short arrows). (D) The soft tissue flap is closed over the membrane and the graft is allowed to heal. The nonabsorbable ePTFE barrier will be removed during a separate surgery. Note that the width of the alveolus is restored (black and white arrows). (Reprinted with permission from Abrahams.³¹)

space during wound healing; the space eventually fills in with host bone and becomes the anticipated expanded ridge and (2) by creating a bone-stimulating milieu within the constructed space.³⁹ An exclusionary membrane acts as a barrier to undesired cell types, such as fast-migrating epithelium, thus enabling bone progenitors to thrive within the created space. These membranes may be nonabsorbable (eg, expanded polytetrafluoroethylene) or bioabsorbable (eg, natural materials, including collagen, acellular dermal matrix, pericardium, laminar bone, fascia lata, dura mater, or synthetic substances such as polymers and calcium sulfate). Bioabsorbable membranes require no retrieval after healing, which is attractive in situations that do not normally warrant a second surgery, and hence, are most frequently used in straightforward GBR cases. The most prevalent and well-studied absorbable barriers are made from either bovine or porcine cross-linked collagen.⁴⁰ To prompt the development of bone, the potential space bounded by the barrier is filled with exogenous bone graft material, either alone, or in conjunction with bioactive agents that encourage bone growth, such as growth hormone. Adjunctive use of bioactive agents (bone morphogenetic

protein-2, platelet-derived growth factor, plasma rich in growth factors that contains higher concentrations of platelet-derived growth factor, and transforming growth factor-beta), in theory, fuels osteogenesis or angiogenesis and shows promise in hastening initial healing, although lacks supporting long-term clinical evidence.^{41,42}

Particulate allograft is osteo-inductive, readily obtainable, and, in the FDA, slower-resorbing, and thus, better at maintaining the constructed space, which is appealing in the correction of larger deficiencies.⁴³ For these reasons, allograft and xenograft (osteo-conductive and typically bovine) are the most commonly employed and thoroughly investigated materials in GBR.

The general surgical steps of GBR are shown in Figure 13; a patient who required implants owing to congenitally missing tooth #7 (maxillary right lateral incisor) and tooth #12 (maxillary first left premolar). As a result, he first required orthodontics to create space for the implants and then GBR to augment the atrophic alveolar ridge. The GBR portion of his treatment starts by reflecting back a full-thickness flap (mucosa and periosteum) to expose the area of concern (Fig. 13G).

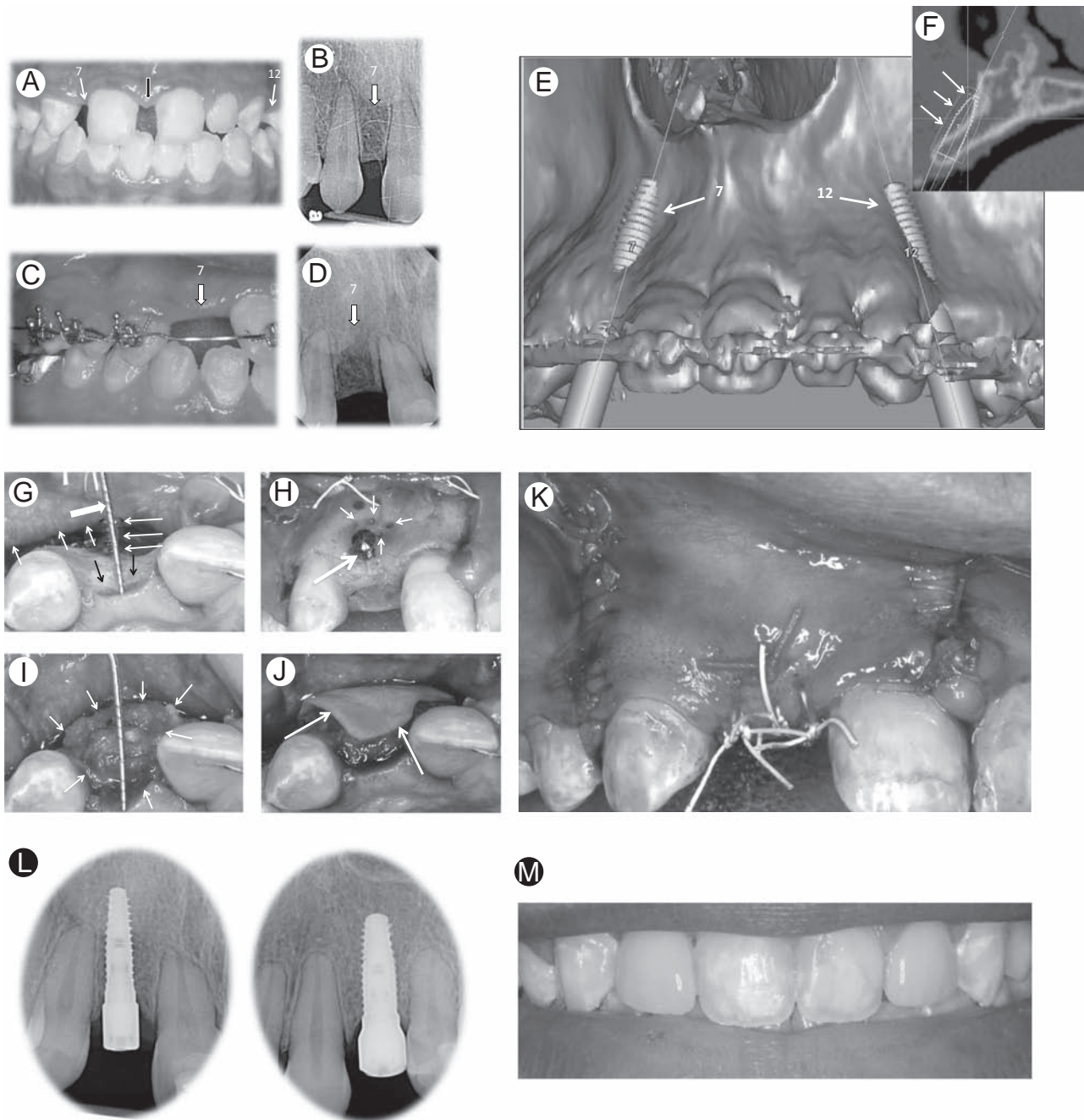


Figure 13 A male patient presented with congenitally absent teeth #7 and #12, requiring orthodontics, bone augmentation, and implants. (A) Photograph shows congenitally absent teeth #7 and #12 (7, 12). Remaining teeth migrated toward missing teeth to fill gaps, creating additional space between central incisors (black arrow). (B) Radiograph on right at tooth #7 demonstrates insufficient room between teeth for implant placement (7) secondary to migration of teeth. Tooth #12 was similar but is not shown. (C and D) Photograph and radiograph after orthodontic treatment now demonstrate sufficient space between teeth for implants (white arrow). Compare with (A) and (B) above. (E) A 3-D reconstruction image from CT-based interactive presurgical planning system (SimPlant) demonstrates inadequate bony coverage of simulated dental implants in tooth locations #7 and #12 (white arrows). (F) Cross-sectional view with simulated implant demonstrates inadequate thickness of maxillary bone to support implant at tooth #7 and identifies region on buccal aspect for potential bone grafting (white arrows). Ridge augmentation to increase bone in facial aspect of maxillary alveolar ridge. (G) Mucosal and periosteal flap is reflected back (short white arrows) to expose bone and identify site for augmentation in facial aspect of alveolar ridge (black arrows). Tenting screw (long white arrows). Note the metal probe measuring depth of bone defect (bold arrow). (H) Holes are drilled to create bleeding bone (small arrows). Tenting screw (large arrow). (I) Bone graft material (arrows) covering defect and tenting screw. (J) Pericardial membrane (white arrows) placed over bone graft and tenting screw. (K) Soft tissue flap is pulled over membrane and sutured closed. (L) Final postoperative radiographs demonstrate placement of implants (without prosthesis). (M) Prostheses attached to implants, resulting in restoration of cosmesis.

Fixation devices (nonabsorbable or absorbable screws or pins) may be inserted into the bone to prop up the membrane and fortify creation of the regenerative space. Note that in this patient there is a concavity or defect in the facial aspect of the alveolar ridge (Fig. 13G). A screw is thus placed into the fundus of the concavity with a portion of the screw sticking out of the bone (Fig. 13G and H). A membrane is then placed over this region, with the screw keeping the membrane away from the bone, and therefore, creating a potential space (Fig. 13J). The screw is thus referred to as a “tenting” screw. Indeed, the dental implant itself may act as a fixation device in cases of vertical deficiency. After debridement, if the bone does not automatically bleed, holes are drilled through the cortex to produce bleeding bone (Fig. 13H). This is felt to expose the area to growth factors from the cancellous bone that can facilitate bone regeneration and trigger a regional acceleratory phenomenon.^{44,45} Before the placement of the membrane, particulate bone material (typically either allograft or xenograft, but possibly autograft, or combination thereof) is contoured to fill the defect (Fig. 13I). A bioactive agent may be mixed into the bone graft material before placement. Larger defects may call for a stiffer, self-bracing nonabsorbable membrane, or alternately, an absorbable membrane in conjunction with fixation screws or pins. Tacks may be used at the edges of the membrane to prevent drifting and to help contain the particulate bone matter. The incision (gingival and periosteal flap) is then closed over the membrane, tenting screw, and bone graft (Fig. 13K) and allowed to heal for a period of at least 3 months for minor regenerative cases and for at least 6 months for larger grafts. After the healing period, surgery for implant placement commences. Radiographically, it is often not possible to distinguish fully healed bone constructed through GBR from the native alveolar arch.

Some patients will require multiple different procedures to eventually be restored with dental implants. This was true of the patient in Figure 13. Because of the congenitally missing teeth, the other teeth migrated toward the gaps created by the missing teeth, resulting in an additional, less-cosmetically pleasing space between the central incisors (Fig. 13A). Furthermore, because the spaces in the location of the congenitally absent teeth were diminished, there was not enough room to accommodate implants (Fig. 13B). Therefore, orthodontics was first required for 18 months to close the gap between the central incisors and create adequate space for implant placement (Fig. 13C and D). Next, a CT scan was performed to accurately determine adequacy of alveolar bone for implants. Using SimPlant (Materialise, Leuven, Belgium), simulated implants were superimposed on the images to determine the ideal implant angulation and highlight areas where bone augmentation would be required (Fig. 13E and F). One can determine from the images that the long-term absence of teeth in these locations resulted in bone atrophy and resorption, thus significantly diminishing the amount of bone in the buccolingual dimension (thickness). After successful GBR, root-form implants were inserted in a separate surgery (Fig. 13L) and eventually restored with dental prostheses. One can appreciate the marked improvement by comparing Figure 13A with M.

Conclusions

Dental implants restore function and cosmesis to edentulous patients, and as such, are the standard of care in tooth replacement in most cases today, with dentures and bridges used less frequently. Imaging is a key component in the evaluation of a patient for dental implants, and advances in CT technology and software have increased the success of dental implant surgery. Radiologists should be familiar with the practical considerations in the workup of a dental implant patient, including the varied radiographic appearances of dental implants, findings related to implant failure, as well as augmentation procedures used to increase alveolar bone in the maxilla and mandible.

References

1. Eke PI, Dye BA, Wei L, et al: Update on prevalence of periodontitis in adults in the United States: NHANES 2009 to 2012. *J Periodontol* 86(5):611-622, 2015
2. Per-Ingvar B: Introduction to osseointegration in. In: Branemark Per-Ingvar, Zarb G, Albrektsson T (eds): *Tissue-Integrated Prosthesis: Osseointegration in Clinical Dentistry*. Chicago and Berlin: Quintessence, 1985
3. Shetty VBB: *Orofacial implants*. In: White SP MJ (ed): *Oral Radiology: Principles and Interpretation*. St. Louis, Mosby 622-635, 2000
4. DelBalso AM, Greiner FG, Licata M: Role of diagnostic imaging in evaluation of the dental implant patient. *Radiographics* 14(4):699-719, 1994
5. Misch CE: Density of bone: Effect on treatment plans, surgical approach, healing, and progressive bone loading. *Int J Med Robot* 6(2):23-31, 1990
6. Steigenga JT, al-Shammari KF, Nociti FH, et al: Dental implant design and its relationship to long-term implant success. *Implant Dent* 12(4):306-317, 2003
7. Sahiwal IG, Woody RD, Benson BW, et al: Radiographic identification of threaded endosseous dental implants. *J Prosthet Dent* 87(5):563-577, 2002
8. Sahiwal IG, Woody RD, Benson BW, et al: Radiographic identification of nonthreaded endosseous dental implants. *J Prosthet Dent* 87(5):552-562, 2002
9. Abuhussein H, Pagni G, Rebaudi A, et al: The effect of thread pattern upon implant osseointegration. *Clin Oral Implants Res* 21(2):129-136, 2010
10. Vandeweghe S, Cosyn J, Thevissen E, et al: The influence of implant design on bone remodeling around surface-modified Southern Implants (R). *Clin Implant Dent Relat Res* 14(5):655-662, 2012
11. Glauser R, Ruhstaller P, Windisch S, et al: Immediate occlusal loading of Branemark System TiUnite implants placed predominantly in soft bone: 4-year results of a prospective clinical study. *Clin Implant Dent Relat Res* 7(suppl 1):S52-S59, 2005
12. Wennerberg A, Albrektsson T: Effects of titanium surface topography on bone integration: A systematic review. *Clin Oral Implants Res* 20(suppl 4):172-184, 2009
13. Krauser JT: Hydroxylapatite-coated dental implants. Biologic rationale and surgical technique. *Dent Clin North Am* 33(4):879-903, 1989
14. Cook SD, Kay JF, Thomas KA, et al: Interface mechanics and histology of titanium and hydroxylapatite-coated titanium for dental implant applications. *Int J Oral Maxillofac Implants* 2(1):15-22, 1987
15. de Lange GL, Donath K: Interface between bone tissue and implants of solid hydroxyapatite or hydroxyapatite-coated titanium implants. *Biomaterials* 10(2):121-125, 1989
16. Avila G, Misch K, Galindo-Moreno P, et al: Implant surface treatment using biomimetic agents. *Implant Dent* 18(1):17-26, 2009
17. Junker R, Dimakis A, Thoneick M, et al: Effects of implant surface coatings and composition on bone integration: A systematic review. *Clin Oral Implants Res* 20(suppl 4):185-206, 2009
18. Jung RE, Pjetursson BE, Glauser R, et al: A systematic review of the 5-year survival and complication rates of implant-supported single crowns. *Clin Oral Implants Res* 19(2):119-130, 2008

19. Abrahams JJ, Kalyanpur A: Dental implants and dental CT software programs. *Semin Ultrasound CT MR* 16(6):468-486, 1995
20. Wyatt CC, Pharoah MJ: Imaging techniques and image interpretation for dental implant treatment. *Int J Prosthodont* 11(5):442-452, 1998
21. Abrahams JJ: The role of diagnostic imaging in dental implantology. *Radiol Clin North Am* 31(1):163-180, 1993
22. Abrahams JJ, Berger SB: Inflammatory disease of the jaw: Appearance on reformatted CT scans. *Am J Roentgenol* 170(4):1085-1091, 1998
23. Reiskin AB: Implant imaging. Status, controversies, and new developments. *Dent Clin North Am* 42(1):47-56, 1998
24. Manz MC: Factors associated with radiographic vertical bone loss around implants placed in a clinical study. *Ann Periodontol* 5(1):137-151, 2000
25. Pommer B, Frantal S, Willer J, et al: Impact of dental implant length on early failure rates: A meta-analysis of observational studies. *J Clin Periodontol* 38(9):856-863, 2011
26. Monje A, Fu JH, Chan HL, et al: Do implant length and width matter for short dental implants (< 10 mm)? A meta-analysis of prospective studies. *J Periodontol* 84(12):1783-1791, 2013
27. Mezzomo LA, Miller R, Triches D, et al: Meta-analysis of single crowns supported by short (< 10 mm) implants in the posterior region. *J Clin Periodontol* 41(2):191-213, 2014
28. Srinivasan M, Vazquez L, Rieder P, et al: Survival rates of short (6 mm) micro-rough surface implants: A review of literature and meta-analysis. *Clin Oral Implants Res* 25(5):539-545, 2014
29. Lee SA, Lee CT, Fu MM, et al: Systematic review and meta-analysis of randomized controlled trials for the management of limited vertical height in the posterior region: Short implants (5 to 8 mm) vs longer implants (> 8 mm) in vertically augmented sites. *Int J Oral Maxillofac Implants* 29(5):1085-1097, 2014
30. Al-Ansari A: Short implants supporting single crowns in atrophic jaws. *Evid Based Dent* 15(3):85-86, 2014
31. Abrahams JJ: Augmentation procedures of the jaw in patients with inadequate bone for dental implants: Radiographic appearance. *J Comput Assist Tomogr* 24(1):152-158, 2000
32. Wheeler SL, Holmes RE, Calhoun CJ: Six-year clinical and histologic study of sinus-lift grafts. *Int J Oral Maxillofac Implants* 11(1):26-34, 1996
33. Lazzara RJ: The sinus elevation procedure in endosseous implant therapy. *Curr Opin Periodontol* 3:178-183, 1996
34. Raghoebar GM, Brouwer TJ, Reintsema H, et al: Augmentation of the maxillary sinus floor with autogenous bone for the placement of endosseous implants: A preliminary report. *Int J Oral Maxillofac Surg* 51(11):1198-1203, 1993. [discussion 203-5]
35. Smiler DG, Johnson PW, Lozada JL, et al: Sinus lift grafts and endosseous implants. Treatment of the atrophic posterior maxilla. *Dent Clin North Am* 36(1):151-186, 1992. [discussion 87-8]
36. Summers RB: A new concept in maxillary implant surgery: The osteotome technique 152. *Compendium* 15(2):4-6, 1994. [8 passim; quiz 62]
37. Abrahams JJ, Hayt MW, Rock R: Sinus lift procedure of the maxilla in patients with inadequate bone for dental implants: Radiographic appearance. *Am J Roentgenol* 174(5):1289-1292, 2000
38. Smiler DG: Surgical solutions to prosthetic problems. *J Dent Symp* 1:44-49, 1993
39. Sonick MK, Hwang D, et al: Implant site development. Ames, IA: Wiley, 2012
40. Kim TS, Holle R, Hausmann E, et al: Long-term results of guided tissue regeneration therapy with non-resorbable and bioabsorbable barriers. II. A case series of infrabony defects. *J Periodontol* 73(4):450-459, 2002
41. Wikesjo UM, Qahash M, Huang YH, et al: Bone morphogenetic proteins for periodontal and alveolar indications; biological observations—Clinical implications. *Orthod Craniofac Res* 12(3):263-270, 2009
42. Kaigler D, Avila G, Wisner-Lynch L, et al: Platelet-derived growth factor applications in periodontal and peri-implant bone regeneration. *Expert Opin Biol Ther* 11(3):375-385, 2011
43. McAllister BS, Haghghat K: Bone augmentation techniques. *J Periodontol* 78(3):377-396, 2007
44. Frost HM: The regional acceleratory phenomenon: A review. *Henry Ford Hosp Med J* 31(1):3-9, 1983
45. Deguchi T, Takano-Yamamoto T, Yabuuchi T, et al: Histomorphometric evaluation of alveolar bone turnover between the maxilla and the mandible during experimental tooth movement in dogs. *Am J Orthod Dentofacial Orthop* 133(6):889-897, 2008

Dental Implant Complications



Kevin Liaw, MD,* Ronald H. Delfini, DDS,[†] and James J. Abrahams, MD*

Dental implants have increased in the last few decades thus increasing the number of complications. Since many of these complications are easily diagnosed on postsurgical images, it is important for radiologists to be familiar with them and to be able to recognize and diagnose them. Radiologists should also have a basic understanding of their treatment. In a pictorial fashion, this article will present the basic complications of dental implants which we have divided into three general categories: biomechanical overload, infection or inflammation, and other causes. Examples of implant fracture, loosening, infection, inflammation from subgingival cement, failure of bone and soft tissue preservation, injury to surround structures, and other complications will be discussed as well as their common imaging appearances and treatment. Lastly, we will review pertinent dental anatomy and important structures that are vital for radiologists to evaluate in postoperative oral cavity imaging.

Semin Ultrasound CT MRI 36:427-433 © 2015 Elsevier Inc. All rights reserved.

The dental implant procedure often requires the involvement of several different dental professionals. For example, the general dentist may refer the patient to a periodontist for implant evaluation and placement. In some cases, this could result in a determination that orthodontics would first be required to create sufficient space for the implant and prosthesis and that a bone augmentation procedure or bone grafting procedure would also first be required to establish sufficient bone for the implant. Of course, there may also be teeth that need to be extracted. Thus, an oral surgeon could also become involved. At the end, a restorative dentist who deals with the actual prosthesis is typically involved. Therefore, for a successful outcome, a close-knit dental team that communicates and works well together is vital. For example, what if a patient uses his friend, “the oral surgeon” to have the teeth extracted? The oral surgeon, who is not working with the implant team, may simply extract the teeth without any concern to preserving the surrounding bone and tissue. When the patient later presents for implant placement, it may be determined that the failure to preserve tissue at the time of tooth extraction resulted in insufficient bone for implants, thus requiring the patient to

undergo additional augmentation surgery before implantation. Having a close-knit implant team that works well together is therefore the first step in avoiding additional surgery and complications. Even in the best of hands, however, complications do occur and it is important for radiologists to be familiar with these complications. We have divided them into those caused by “Biomechanical Overload,” those caused by “Infection or Inflammation,” and those from “Other Causes.”

Biomechanical Overload

Biomechanical overloading may result from poor implant angulation or position, inadequate posterior support (ie, missing posterior teeth), inadequate surrounding bone, or parafunctional habits like bruxism (teeth grinding).¹

Overloading manifests either by *loosening* or by *fracture* of an implant component. Loosening can occur (1) if the cement holding the prosthesis to the abutment fails, (2) if the prosthesis screw or abutment screw loosens, or (3) if there is actual osseointegration failure of the implant fixture itself. Implant fractures can involve (1) the actual implant fixture itself, (2) the abutment screw, or (3) the prosthesis screw (for illustration of implant components see Fig. 2, by Zohrabian et al²).

Mobility of the implant fixture itself most often results from fracture of the implant, lack of osseointegration, or even infection or inflammation causing loss of bone support.³⁻⁵

Many of these complications such as loosening of screws or cement are simply diagnosed in the dentist's office; however,

*Department of Diagnostic Radiology, Section of Neuroradiology, Yale Medical Center, New Haven, CT.

[†]Yale School of Medicine, Yale Medical Center, New Haven, CT.

Address reprint requests to James J. Abrahams, MD, Department of Diagnostic Radiology, Section of Neuroradiology, Yale Medical Center, New Haven, CT. E-mail: james.abrahams@yale.edu

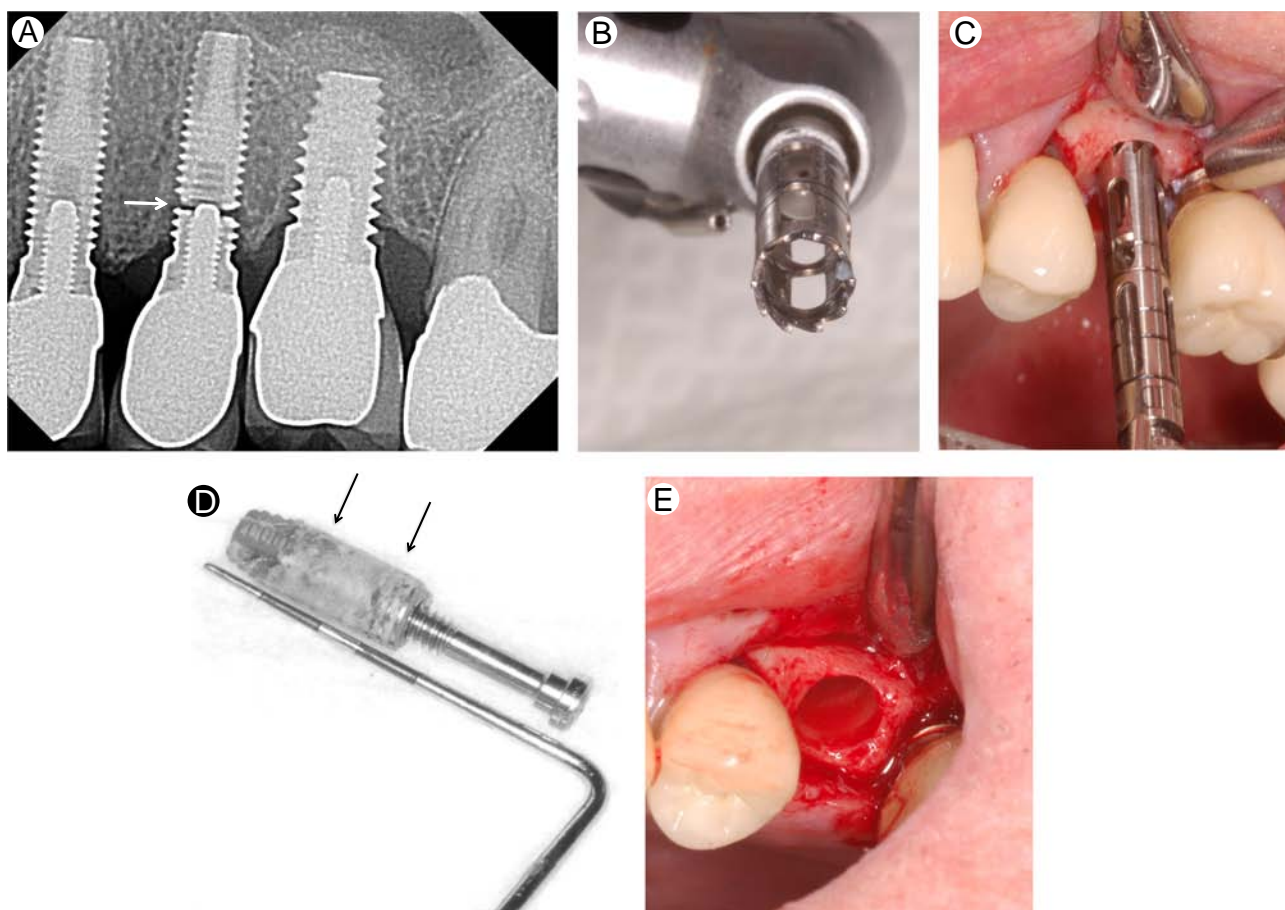


Figure 1 Radiograph of a patient with 3 implants. (A) Note the transverse fracture through middle implant (arrow). (B) Drill with trephine used to remove remaining portion of fractured implant. (C) Trephine over retained implant fragment. (D) Removed implant fragment (arrows). (E) Hole in bone after removal of implant fragment. (Color version of figure is available online.)

radiologists can play an important role related to diagnosing fractures, infection or inflammation, osseointegration failure, injury to surrounding structures, etc.

Implant Fracture

Fractures are a common occurrence secondary to biomechanical overloading. Bone resorption around an implant may contribute to implant fracture by decreasing the amount of supporting bone surrounding the implant and thus placing undue stress on the implant itself. Often the fracture line is detected on radiographs or computed tomography (CT) as a radiolucent line through the dense implant (Fig. 1A).³ The treatment of a fractured implant first requires complete removal of the implant. How does one, however, remove the portion of the fractured implant that remains imbedded in the bone? A special surgical microdrill that has a trephine attached to it is used (Fig. 1B). The trephine, which is hollow, fits over the retained implant fragment and drills around the periphery, allowing its removal (Fig. 1C-E). Once the implant is removed, it may simply be replaced with another wider and longer one; however, if there is significant bone loss or resorption of

bone, a bone graft or augmentation procedure may first be required.

Loosening Osseointegration Failure

In addition to implant fracture, poor osseointegration (failure of bone cells to grow and integrate with the implant) can also lead to movement of the implant fixture itself.⁴ Radiographically, there is often a radiolucent area surrounding the implant (Fig. 2). These cases would need to be clinically evaluated for underlying issues such as infection; however, the cause of the osseointegration failure is often not determined.

A natural tooth root is attached to the bone via the periodontal ligament, allowing for slight mobility of the tooth, but a successful implant is fused to the bone and has no mobility. Successful implants are also stable and totally asymptomatic. In fact, patients are often unaware of where their implant is. The predictability of implant success is very high and most (>90%) implants successfully integrate with the bone. The true test for successful integration is when a measured force, or a torque test, is applied to the implant and results in no mobility.

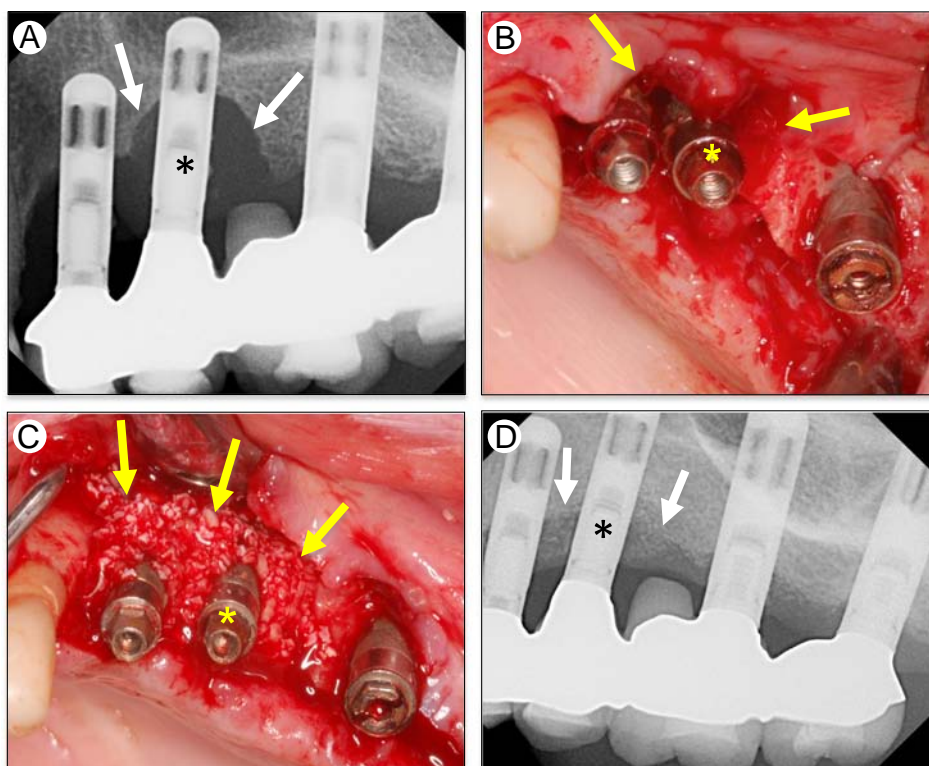


Figure 2 Patient with implant failure and bone resorption. * Identifies the same implant in (A)-(D). (A) Radiograph demonstrates bone resorption (arrows). (B) At surgery, note bone resorption around implant (arrows). (C) Defect has been packed with bone graft material (arrows). Periosteum and mucosa would next be sutured and closed over bone graft. (D) After the period of healing this radiograph demonstrates that bone has regenerated around the implant (arrows) and has filled the defect that was noted in (A). Compare (A) and (D). (Color version of figure is available online.)

An implant that presents with even the slightest mobility is considered a failed implant and complication even if not symptomatic. The cause of this osseointegration failure is often not known, but some believe it is related to micromotion during the healing phase. The process of osseointegration (bone fusing with the implant) is an “all or nothing” phenomenon.⁴ This may be analogous to fixation of a long bone fracture where the pieces are held immobile with a cast and the bone fuses. If the pieces of healing bone have a micromotion, it allows a layer of scar tissue to form, causing a nonunion. Micromotion of the healing implant produces the same non-integration and leads to a failed implant. As a result, implants are frequently allowed to heal for up to 12 weeks before placement of the actual prosthesis.⁶ Despite this, implants at times are placed and immediately restored with a crown and without a healing phase, often referred to as “teeth in a day.” Some initial force on the implant can actually increase the bone to implant contact, although too much leads to a failed implant. When considering immediate restoration, the patient population must be carefully selected.

Treatment of implant failure may vary. Generally, if there is implant fixture loosening, the implant requires removal followed by replacement with a larger implant (if sufficient bone remains) or by packing the defect with bone graft material followed by reimplantation. When failing implants are owing to infection or other causes, attempts can be made to save the implant by treating with antibiotics and surgically packing any bone defects with bone graft material or freeze-dried bone

(Fig. 2B and C). This would often fill the bony defect, recover the bone loss, and allow adequate fixation of the implant. Radiographically, the regenerated bone appears as normal bone where a radiographic lucency previously existed (Fig. 2D).

Cement Failure and Abutment Screw Loosening

Cement failure and abutment screw loosening commonly affect the prosthesis attachment and this is relatively easily remedied by recementing the prosthesis to the implant or by tightening or replacing the abutment screw. Occasionally the abutment screw may actually fracture and require replacement.

Infection or Inflammation

Infection

Good dental hygiene is important for preservation of the implant. Failure to do so can lead to microbial buildup and an infection around the implant.⁵ Patients present with redness, induration, and painful inflammation of the gingiva surrounding the implant. When an infection occurs, it frequently causes erosion and resorption of the bone surrounding the implant. Radiographically, this complication appears as perihardware radiolucency (Fig. 3). It is important to relay this finding to the referring clinician because early intervention can often save the implant. Treatment depends on the degree and extent of the infection. If advanced, the implant may have to be surgically

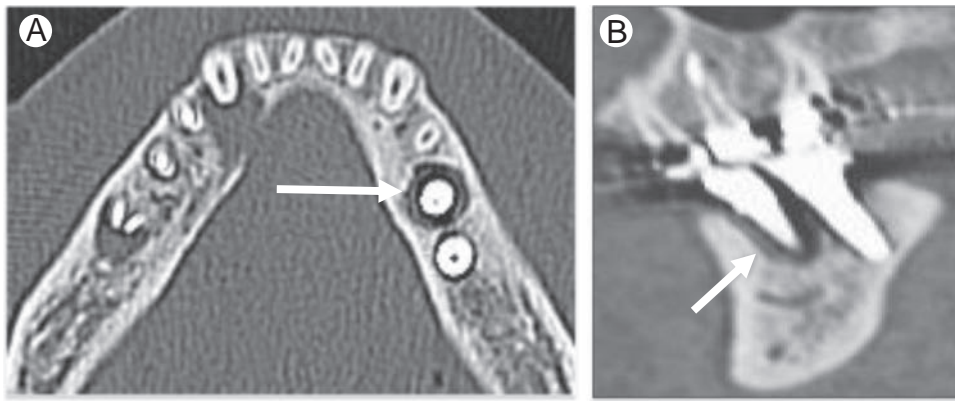


Figure 3 Axial (A) and oblique sagittal CT (B) shows infection resulting in bone resorption and perihardware radiolucency (arrows).

removed and the defect curettaged and packed with bone graft material with anticipation of replacing the implant when healed. Antibiotics are often required. If the infection is less advanced, the patient is placed on antibiotics to get the infection under control. The defect created by the bone resorption can then be surgically packed with bone graft material with the hope of regenerating the lost bone and saving the implant. Bone regenerating procedures are discussed in greater detail by Zohrabian et al.²

Subgingival Cement

Once the implant has successfully integrated into the bone, it is restored by placing a prosthesis (crown) on it. This is typically cemented to the implant but occasionally screwed to it. When cemented, excess cement can be forced subgingivally. Cement is toxic to the tissue and elicits a foreign body reaction. This reaction can be immediate or more delayed and presents with focal gingival inflammation, erythema, and some discomfort (Fig. 4A).⁷ Most, but not all, cements are radiopaque. Radiographs can reveal excess cement on the mesial and distal aspects of the implant (Fig. 4B). However, if the excess cement is on the buccal or lingual aspects, it is often obscured by the overlying dense metallic implant. There have been reports of symptoms occurring from subgingival cement not manifesting themselves for years after the initial cementation. Initial treatment requires removal of the excess cement. It may simply be

removed with a curette (Fig. 4C), but often a soft tissue flap is required to visualize the damage and more thoroughly remove the cement. The reaction to the excess cement can also cause resorption of bone around the implant. In this case, a flap is necessary to debride the inflamed tissue and attempt to regenerate the bone around the implant. Regeneration of bone vertically is not predictable with the implant in place. An implant can survive with some loss of bone. However, excessive loss would require removal of the implant, grafting the site with freeze-dried bone or other grafting material, and often placing a membrane under the soft tissues and over the bone graft to contain it during a 4-6-month healing period. Once the bone has regenerated, a new implant can be placed.⁷

Other Causes

Bone and Soft Tissue Preservation

The loss of a tooth or teeth is tragic but not uncommon. When this occurs, it triggers a cascade of events that can further compound the tragedy. First, following an extraction or loss of a tooth the alveolar bone and soft tissue would predictably undergo atrophy and shrink both in height and width from disuse.⁶ Edentulous areas no longer have the normal vertical pressure on the underlying bone and tissue from apposing teeth. As a result, the bone undergoes atrophy and resorption, contributing to diminished height and thickness of the alveolar

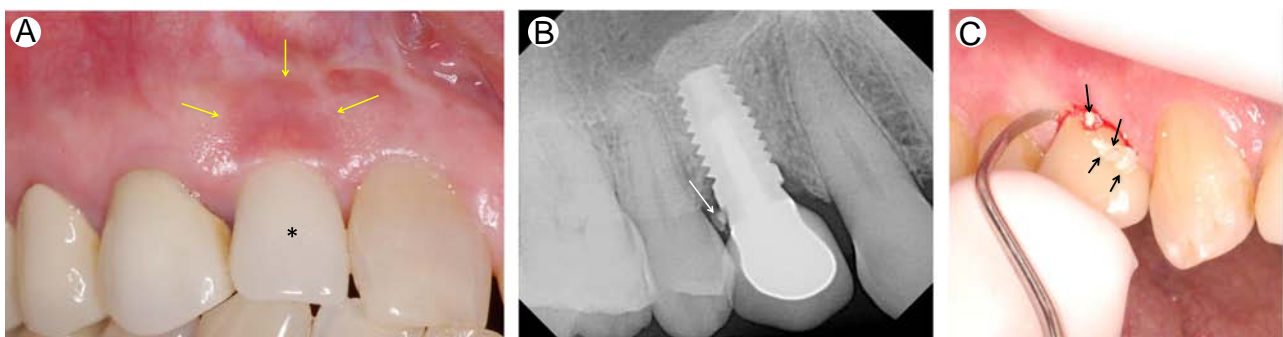


Figure 4 (A) Photo of a patient with subgingival cement causing inflammation (arrows) in area of restored implant (*). (B) Radiograph reveals radiopaque cement on distal aspect of implant (arrow). (C) Photograph demonstrates removal of the cement (arrows). (Color version of figure is available online.)

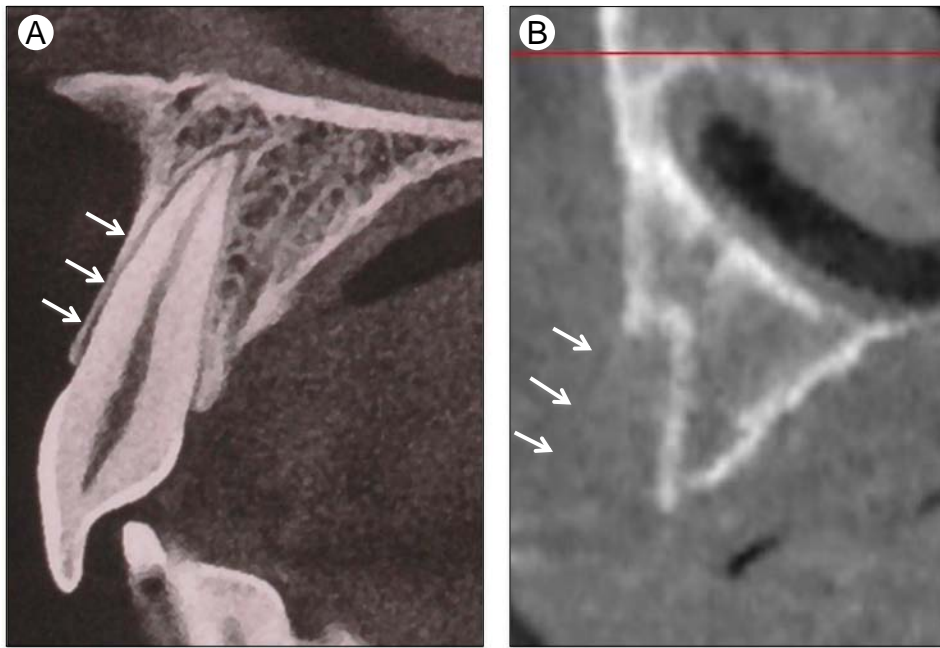


Figure 5 (A) Radiograph demonstrates normal thin anterior cortical plate (arrows), which should be preserved to allow healing socket to be filled with bone. (B) Sagittal CT demonstrates failure to preserve anterior cortical plate at the time of tooth extraction (arrows), limiting available bone for implant. (Color version of figure is available online.)

bone over time. The amount of bone in the alveolar ridge is therefore variable and preoperative imaging may be important to determine whether sufficient bone exists for implants. If it is not, a number of augmentation procedures are available that can increase the amount of bone and make implantation possible. These include procedures such as the sinus lift procedure, guided bone regeneration, hydroxyapatite augmentation, bone grafts, etc.⁶ which are discussed further by Zohrabian et al.²⁰ Patients who are completely edentulous

undergo a significant amount of bone resorption over their lifetime. This can be so severe that they can no longer wear dentures, especially in the mandibular arch. Also, the facial (anterior) bone around teeth is thin, especially in the maxillary anterior region, and that bone can often be lost, leading to increased shrinkage (Fig. 5A).

The use of dental implants, however, has addressed these problems by helping arrest tissue loss by restoring the normal stresses on the bone and by restoring the esthetic look and

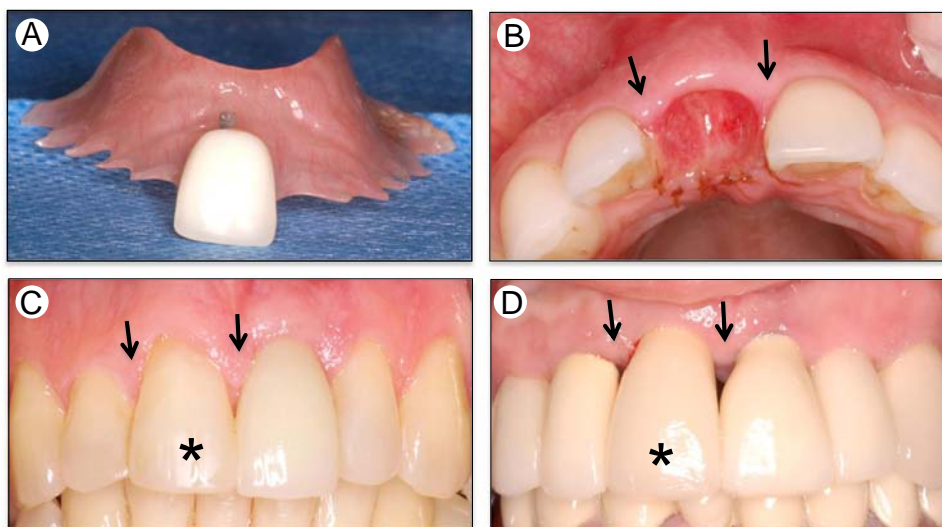


Figure 6 (A) Temporary flapper worn during implant healing and before restoration with prosthesis. (B) Note that the flapper has preserved normal papilla (arrows). (C) Flapper has been removed and implant restored with right central incisor prosthesis (*). Note normal preservation of papilla (arrows). (D) A different patient with restored right central incisor implant (*) and atrophy of papilla (arrows) secondary to poor-fitting flapper and lack of continual use. (Color version of figure is available online.)

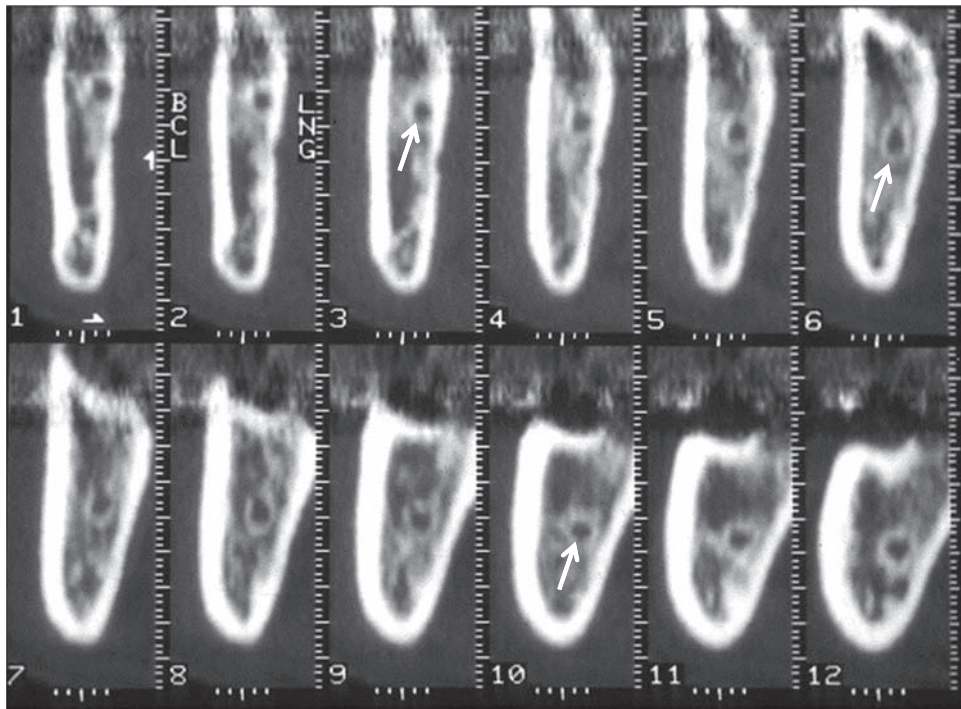


Figure 7 Sagittal cross-sectional CT reformatted images demonstrate normal mandibular canal (arrows), which appears as a round radiolucency with a denser peripheral cortical margin.

function of the missing tooth. Implants are thus the best replacement for missing teeth.⁸ As a single tooth replacement, an implant is free standing, not attached to adjacent teeth, and much easier to maintain by the patient. For patients who have lost multiple teeth or all their teeth, implants can provide support for a stable, healthy, and esthetic dentition that is not removable. Perhaps the most important aspect of implants is that they can restore a quality of life.

In preparation for dental implants, failing teeth have to be extracted first. In doing so, it is paramount that the surgeon preserves any residual bone and soft tissue to help ensure successful implantation and cosmetics. In addition, at the time of extraction some patients may benefit from grafting the site of the extracted tooth with freeze-dried bone or other grafting material to help maintain and assure preservation of bone. This should be followed by implant placement in a timely manner, 4-6 months after extraction.⁶ If the tooth is not timely replaced with an implant, the bone resorption continues until it is replaced. Lastly, if the tooth is not replaced, the adjacent teeth gradually drifts into the void or space created by the extracted or lost tooth, thus diminishing the space, often to the point where an implant and prosthesis would no longer fit. When this occurs, orthodontics may then first be required to regain sufficient room for an implant.

As the “front” teeth in the maxillary anterior region are exposed during one’s smile, they must be esthetic as well as functional. Loss of 1 mm of tissue in height or width can result in a cosmetically unacceptable result. During tooth extraction, if there is traumatic loss of bone in this region, the alveolar ridge may not have adequate underlying bone to accept the implant. This is often seen in the maxilla, where the facial cortical plate can be destroyed during the tooth

extractions (Fig. 5). Preservation of bone and soft tissue at the time of extraction is preferable to attempts for resurrection afterward. Once resorption of bone and tissue occurs, it can require multiple reconstructive surgeries to attain favorable esthetics.

Similarly, soft tissue preservation is another important factor that is necessary for good cosmetic results. Specifically, during

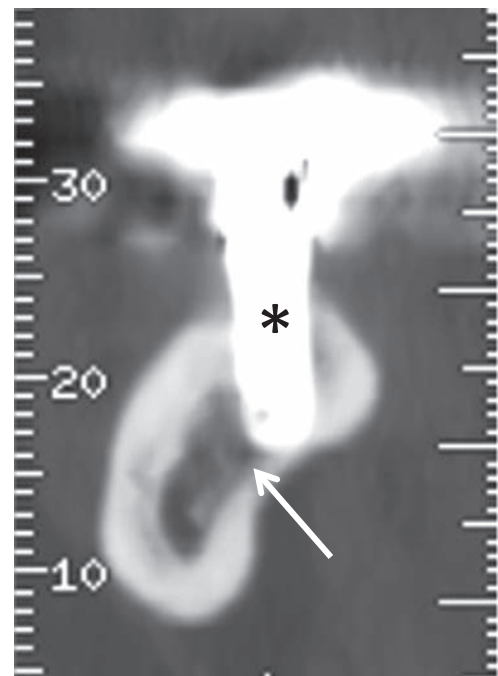


Figure 8 Sagittal reformatted CT image demonstrates mandibular canal violated (arrow) by poorly placed implant (*).

the fixture healing phase, the gingival papilla or the triangular soft tissue that extends between each tooth at the gum line needs to be maintained so a space does not appear between the teeth (Fig. 6). This soft tissue can undergo atrophy after tooth extraction.⁹ Therefore, a flipper, which is a specially designed artificial tooth, can be used to maintain the confines of the removed tooth. The patient typically wears this temporary removable prosthesis until the implants have integrated with the bone and the final prosthesis is complete. This can take several months. The flipper can be designed to preserve the papilla but one that is poorly designed or not continually used can cause the papilla to shrink, or be lost entirely, resulting in poor cosmetics (Fig. 6).

Injury to Surrounding Structures

There are surrounding vital structures including the mandibular canal (neurovascular bundle), maxillary sinus, nasal cavity, and incisive foramen that can be injured during dental implant surgery. The radiologist must be cognizant of these areas on pre- and postoperative images and this anatomy is further detailed by Zohrabian et al.¹⁰

The neurovascular bundle enters the mandibular canal (also called inferior alveolar canal) from the lingual surface of the ramus via the mandibular foramen.⁸ From here it travels through the mandible to exit the body of the mandible slightly distal to the midline on the buccal surface via the mental foramen (Fig. 1A, by Zohrabian et al.¹⁰). Before surgical placement of an implant, the mandibular canal must be localized. This way, during surgery, care is taken to carefully preserve the canal and underlying neurovascular bundle and make sure that there is no direct damage to the canal. On sagittal cross-sectional CT reformatted images, the canal appears as a round radiolucency with a denser peripheral cortical margin (Fig. 7). If care is not taken, the canal can be violated during implant surgery, resulting in facial paresthesias or other neurosensory disturbances such as pain (Fig. 8).¹¹

CT DentaScans or similar reformatting programs and cone-beam CT provide accurate preoperative measurements from the top of the alveolar ridge to the top of the mandibular canal as well as the thickness of the alveolar ridge and can thus determine if sufficient bone exists above the mandibular canal to safely accommodate implants. The imaging report should include measurements from the top of the canal to the top of the alveolar ridge in the edentulous regions as well as

measurements of the width of the bone. Imaging can also help the dentist select the appropriate length and width of the implant preoperatively. Panorax images provide a rough estimate of the amount of bone above the mandibular canal, but they do not provide accurate measurements and any information regarding the thickness of the alveolar ridge.⁸

The maxillary sinus and nasal cavity can also be violated during the surgical placement of implants. Violation of the maxillary sinus can lead to infection or oroantral fistulas (abnormal communication between oral cavity and maxillary sinus) and increase the risk of implant failure. If there is inadvertent implant loss into the maxillary sinus, then trans-antral endoscopic surgery is performed to remove the foreign body.

Other Complications

Other complications related to implant surgery include mandibular fracture, aspiration or ingestion of the implant, hemorrhage, and devitalization of adjacent teeth.¹¹

References

1. Abrahams JJ: Dental CT imaging: A look at the jaw. *Radiology* 219:334-345, 2001
2. Zohrabian Vahe M, Sonick Michael, Hwang Debby, Abrahams James J: Dental implants. *Semin Ultrasound CT MRI* 2015 (in this issue)
3. Marcelo CG, Filié Haddad M, Gennari Filho H, et al: Dental implant fractures—etiology, treatment and case report. *J Clin Diagn Res* 8(3): 300-304, 2014
4. Sakka S, Baroudi K, Nassani MZ: Factors associated with early and late failure of dental implants. *J Investig Clin Dent* 3(4):258-261, 2012
5. Tanner A, Maiden MF, Lee K, et al: Dental implant infections. *Clin Infect Dis* 25(suppl 2):S213-S217, 1997
6. Abrahams JJ: The role of diagnostic imaging in dental implantology. *Radiol Clin North Am* 31(1):163-180, 1993
7. Pualetto NI, Lahiffe BJ, Walton JN: Complications associated with excess cement around crowns on osseointegrated implants: A clinical report. *Int J Oral Maxillofac Implants* 14(6):865-868, 1999
8. Abrahams JJ: CT assessment of dental implant planning. *Oral Maxillofac Surg Clin North Am* 4:1-18, 1992
9. Mi-Si Si, Long-Fei Zhuang, Xin Huang, et al: Papillae alterations around single-implant restorations in the anterior maxillae: Thick versus thin mucosa. *Int J Oral Sci* 4:94-100, 2012
10. Zohrabian Vahe M, Poon Colin S, Abrahams James J: Embryology and anatomy of jaw and dentition. *Semin Ultrasound CT MRI* 2015 (in this issue)
11. Misch K, Wang HL: Implant surgery complications: Etiology and treatment. *Implant Dent* 17(2):159-168, 2008

Inflammatory Diseases of the Teeth and Jaws



Vahe M. Zohrabian, MD, and James J. Abrahams, MD

The teeth are unique in that they provide a direct pathway for spread of infection into surrounding osseous and soft tissue structures. Periodontal disease is the most common cause of tooth loss worldwide, referring to infection of the supporting structures of the tooth, principally the gingiva, periodontal ligament, cementum, and alveolar bone. Periapical disease refers to an infectious or inflammatory process centered at the root apex of the tooth, usually occurring when deep caries infect the pulp chamber and root canals. We review the pathogenesis, clinical features, and radiographic findings (emphasis on computed tomography) in periodontal and periapical disease.

Semin Ultrasound CT MRI 36:434-443 © 2015 Elsevier Inc. All rights reserved.

Relevant Anatomy

A brief review of tooth anatomy, as described in detail in this issue's chapter by Zohrabian et al.¹ (and as depicted in Figures 4 and 5 of that chapter), is necessary to understand periodontal and periapical disease. A tooth is divided into 2 parts: an *anatomical crown* projecting into the oral cavity, and a *root* embedded in alveolar bone and projecting below the gingival margin (gum line). The number of roots varies between different teeth. A tooth is composed primarily of *dentin*, a bonelike substance of intermediate radiodensity. Dentin lies deep to hard, protective *enamel* overlying the crown, which is the most radiopaque substance in the human body, and *cementum* covering the root(s), which is of nearly the same radiodensity as that of dentin. Dentin surrounds the radiolucent *pulp chamber* and radiolucent *root canal(s)*. The neurovascular bundle enters the radiolucent *apical foramen* at the root apex of a tooth and travels through the root canal(s) to enter the pulp chamber at the center of a tooth. The *lamina dura* is the thin cortical lining of the bony tooth socket. The *periodontal ligament* holds a tooth in its socket by attaching to both the lamina dura of the socket and the cementum of the root.

Periodontal Disease

Periodontal disease affects the supporting structures of the tooth (periodontium) and is the most common cause of tooth

loss worldwide.² In the setting of poor oral hygiene, chronic accumulation of anaerobic bacteria—laden plaque around the gingival margin of the tooth results in inflammation of the gums, termed gingivitis. If the infection persists, it can travel along the periodontal ligament, termed marginal periodontitis. This results in resorption of bone adjacent to the sides of the root and the formation of a periodontal pocket (Fig. 1). An even larger abscess may form if a foreign body becomes lodged in a periodontal pocket or if a pocket becomes occluded. Marginal periodontitis may be localized or generalized, depending on whether, respectively, less or more than 30% of residual teeth in the oral cavity are affected. Conditions that negatively affect host immunity and predispose to periodontal disease include, but are not limited to, smoking, diabetes, and human immunodeficiency virus. Moreover, mechanical pressure on gingival tissues resulting from misaligned teeth, suboptimal (ie, overhanging) restorations, dental anomalies such as enamel pearls (ectopic enamel formation on the root surface), or habitual tooth picking may also predispose to periodontal disease.

Patients with gingivitis have easily bleeding gums because of the hyperemia caused by the inflammatory process. Clinical features of periodontal disease include gingival redness, swelling, gingival recession, suppuration, and tooth hypermobility. Clinically, a dentist or dental hygienist examines for periodontal disease using a thin blunt-tipped, metallic periodontal probe called a Michigan-O probe with Williams markings at 3, 6, and 8 mm. If the periodontal ligament is intact, the probe should not advance significantly when inserted between the gingiva and tooth (Fig. 2A). However, with periodontal disease, the probe advances to the depth of the periodontal pocket (Fig. 2B). The measurement of the pocket is made from the cemento-enamel junction, or the

Department of Radiology, Yale School of Medicine, New Haven, CT.

Address reprint requests to Vahe M. Zohrabian, MD, Department of Radiology, Yale School of Medicine, 333 Cedar St (Room CB-30), P.O. Box 208042, New Haven, CT 06520-8042. E-mail: vahe.zohrabian@yale.edu

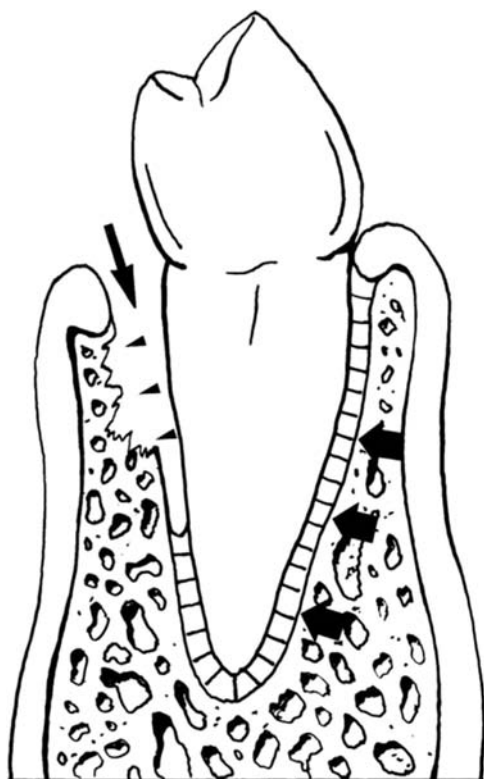


Figure 1 Illustration of periodontal disease. The normal periodontal ligament space is thin and has a constant width along the surface of the root (short black arrows). In periodontal disease, infection of the ligament causes erosion of adjacent alveolar bone (black arrowheads), resulting in focal widening of the periodontal ligament space and formation of a periodontal pocket (longer black arrow). (Adapted with permission from Abrahams and Kalyanpur.³¹) (Color version of figure is available online.)

junction between anatomical crown and root of a tooth, to the base of a periodontal pocket. The cemento-enamel junction demarcates where the gingiva attaches to a healthy tooth and is normally located 1-2 mm above the bony alveolar crest. Thus, a probe can normally insert to a depth of approximately 1-3 mm, with anything beyond 3-4 mm diagnostic of a periodontal pocket.

The radiographic evaluation of periodontal disease provides useful information on bone levels, patterns of bone loss, root lengths, and most importantly, length of root surrounded by remaining alveolar bone. Radiographs may also be useful in revealing predisposing factors, such as overhanging restorations and root anomalies or malformations. The examination typically begins with intraoral radiographs, specifically vertical bitewings and periapical radiographs. No radiographic abnormality is typically demonstrated in the early stages of gingivitis as the inflammatory response is limited to the gums without periodontal ligament involvement and alveolar bone loss. Early radiographs may show loss of cortical density, blunting or rounding of the normally sharp angle between the alveolar crest and the lamina dura, as well as a slight loss of alveolar crest height. The imaging hallmark of marginal periodontitis is widening of the normally thin, radiolucent periodontal ligament space adjacent to the surface of the root (Fig. 3). Chronic

periodontitis may result in reactive sclerosis of the adjacent bone, termed condensing osteitis (Fig. 4). Widening of the periodontal ligament space most commonly results from periodontal infection; however, this finding is nonspecific, and may also be seen in apical periodontitis, orthodontic treatment, trauma, and malignancy (ie, leukemia, metastases, and osteosarcoma). Malignancy should be considered whenever radiolucency is ill defined and localized to only 1 or 2 teeth, with relative preservation of the periodontal ligament space surrounding the remainder of the dentition.

Treatment of Periodontal Disease

Regular brushing and flossing help in eliminating bacterial buildup and plaque adherent to the tooth surfaces, and therefore, are critical in the prevention of dental caries and periodontal disease. When oral hygiene is insufficient, plaque mineralizes into calculus, also known as “tartar,” and as such, routine cleaning is no longer effective in removing these hardened deposits. A professional cleaning by a dentist or dental hygienist is needed to remove tartar through the use of special tools, such as curettes.

The treatment of periodontal disease typically begins with nonsurgical scaling and root planning, also known as periodontal cleaning or “deep cleaning,” to remove bacteria-laden plaque from deep periodontal pockets. Scaling involves removing plaque from tooth surfaces, whereas root planning refers to smoothing the root surfaces and removing any infected tooth structures, although both are done at the same time. As offending bacteria are mostly anaerobic, patients may afterward be instructed to brush with dilute hydrogen peroxide to prevent the deposition of dental calculus. Dilute hydrogen peroxide can also be delivered mechanically to deep periodontal pockets by patients using a water pick. Moreover, germicidal mouthwashes and site-specific antibiotics may be prescribed to promote further disinfection and healing.

More severe cases of periodontal disease may necessitate gingival flap surgery to clean and reduce the size of deep periodontal pockets. Bone grafts, soft tissue grafts, or guided tissue regeneration, in which tissue-stimulating proteins are used to enhance bone growth, may also be required (Fig. 5). Minimally invasive laser-based therapy, PerioLase MVP-7, has revolutionized gum surgery by using a 6-W, free-running Nd:YAG laser to remove bacteria and regenerate soft tissues.

Dental Caries

Colloquially referred to as a “cavity,” dental caries is caused by demineralization of enamel and dentin by lactic acid produced by bacterial fermentation of carbohydrates.³ Remineralization of enamel may cause a carious lesion to regress, especially in the presence of fluoride and acid-neutralizing saliva.³ Caries are typically diagnosed using dental radiographs, as further discussed in this issue's chapter by Koenig⁴; however, they can also be seen on computed tomography (CT), appearing as a focal radiolucency in the opaque enamel or dentin extending from the surface of the tooth.⁵ Caries commonly occur at

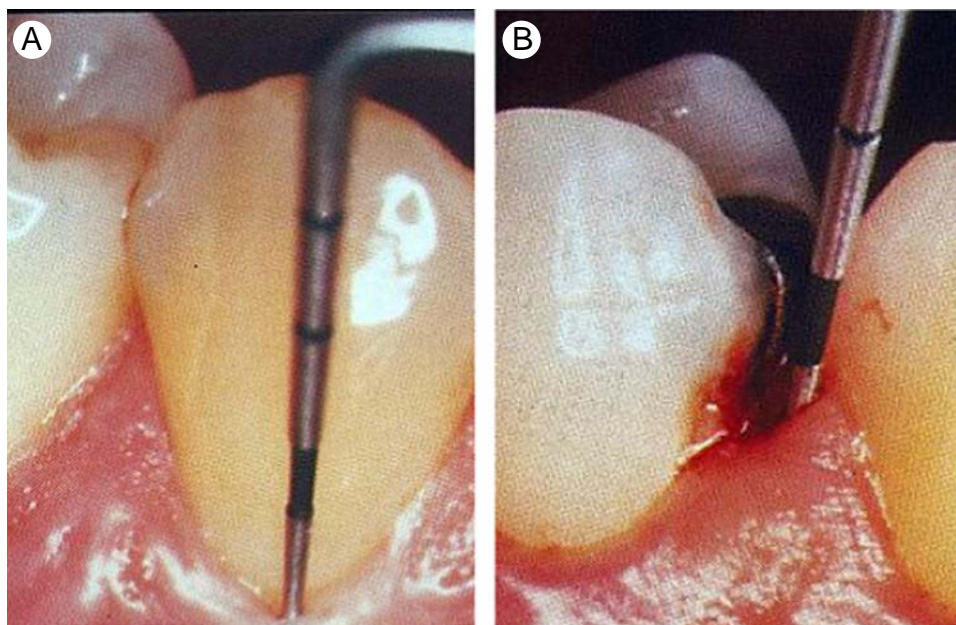


Figure 2 Periodontal disease. (A) Probe with millimeter markings does not advance significantly with normal intact periodontal ligament. (B) In periodontitis, probe advances to depth of periodontal pocket. Note gingival bleeding, commonly associated with gingivitis. (Color version of figure is available online.)

contact points between teeth, which are areas not amenable to direct visual inspection, and therefore, they require radiographs for diagnosis. They typically have a mushroom shape, with the “stalk” representing a narrow channel through the more peripheral enamel and the “head” representing a larger area of demineralization within the more central dentin⁶ (Fig. 6). Caries can be single or multiple, and when severe, may extend into the radiolucent pulp chamber. When this occurs, it often renders the tooth nonvital and results in formation of an abscess or granuloma at the tooth apex. This is further discussed in the “Periapical Disease” section. Lesions in the anterior teeth and advanced lesions in the posterior teeth are often more ovoid.⁶ Carious lesions deep to dental restorations, such as fillings or crowns, are difficult to visualize on CT

due to metallic streak artifact, but they can be seen in radiographs. As cone-beam CT is able to achieve submillimeter isotropic spatial resolution, it is more sensitive than conventional multidetector CT in the detection of small caries. Sagittal cone-beam CT images are particularly useful for visualizing caries on occlusal surfaces.⁷

Periapical Disease

Severe or prolonged caries may extend through the dentin and into the deeper pulp chamber, which contains the neurovascular components of the tooth. This results in pulpal inflammation, termed pulpitis, which can be reversible or

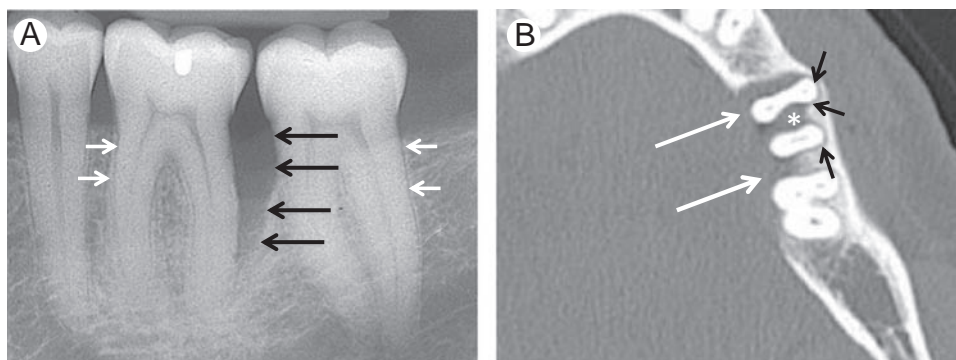


Figure 3 Marginal periodontitis. (A) Radiograph of mandible demonstrates vertical alveolar bone loss with widening of periodontal ligament space adjacent to distal root of left first mandibular molar (black arrows). Compare this with the normally thin, radiolucent periodontal ligament space (white arrows). (B) Axial CT image in the same patient demonstrates widening of periodontal ligament space adjacent to left first mandibular molar roots (white arrows). This is in contrast with the normal periodontal ligament space along the buccal aspect of the root (black arrows). Also demonstrated is involvement of the furcation, or space between roots (white asterisk).

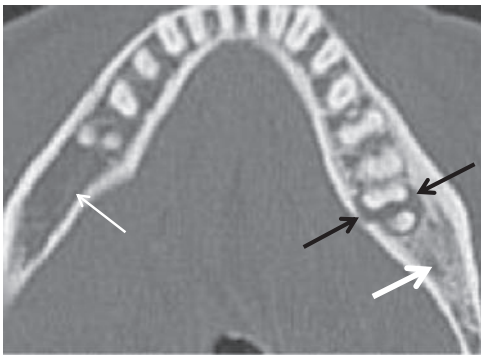


Figure 4 Chronic periodontitis. Axial CT image demonstrates lucency and periodontal pocket surrounding roots of left mandibular molar (black arrows). Note cortical thickening and sclerosis in surrounding bone (thick white arrow), compatible with reactive sclerosis (condensing osteitis). Compare this with normal bone on the opposite side (thin white arrow).

irreversible. Without treatment, the ongoing inflammatory response increases pressure within the tooth, eventually resulting in pulp necrosis and death of the tooth (devitalization), as well as subsequent infection of the pulp chamber and root canals. Bacteria can then travel down the tooth root via the root canals and exit the apical foramen at the root apex to release toxic metabolites. This establishes a localized, periapical inflammatory infiltrate composed of neutrophils, lymphocytes, and macrophages, termed apical periodontitis (Fig. 7). In the chronic state, this periapical lesion, composed of

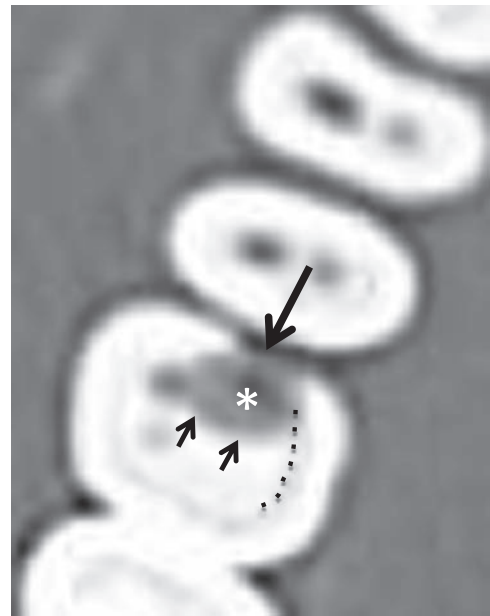


Figure 6 Caries. Axial CT image demonstrates focal mushroom-shaped lucency (white asterisk) representing demineralization or destruction in enamel at the contact point between teeth (long arrow) and dentin (short arrows) along the mesial surface of right first molar. Note the normal demarcation between peripheral enamel and central dentin (dotted curved line). Narrow “stalk” extends through enamel, whereas “head” is seen as larger area of demineralization in dentin.

granulation tissue and inflammatory cells, represents a balance between bacteria and host immune factors and serves to contain the spread of infection.

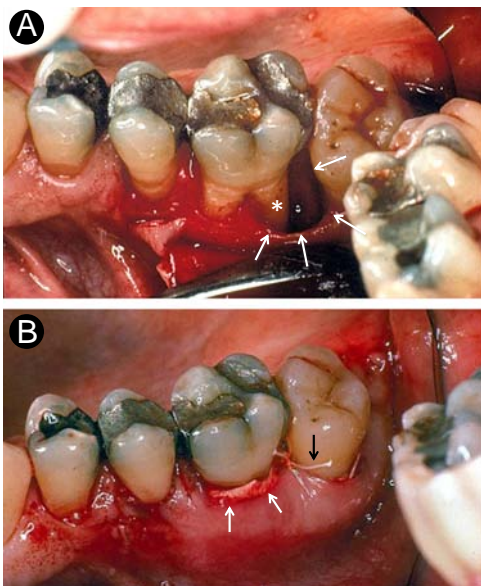


Figure 5 Photographs illustrating treatment of first molar periodontal pocket. (A) Soft tissue flap reflected back to expose bone and periodontal pocket (arrows). Note resorption of bone around the distobuccal root (white asterisk). (B) The periodontal pocket has been curettaged, packed with bone graft material, and a Gortex membrane (white arrows) placed between the bone graft and soft tissues to prevent ingrowth of undesirable tissue. After 6 weeks of healing, the suture retaining the membrane (black arrow) is clipped to allow easy membrane removal. (Color version of figure is available online.)

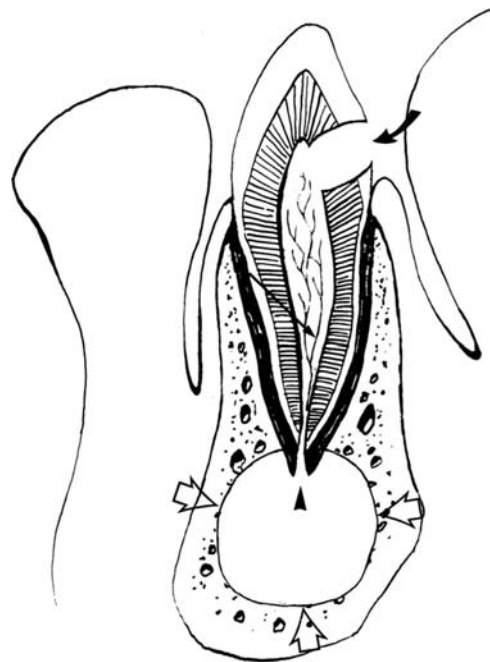


Figure 7 Illustration of periapical inflammatory disease. Dental caries (curved black arrow) permit bacteria to enter the pulp chamber and travel down the root canals (long black arrow) to the apical foramen (black arrowhead), resulting in a periapical lucency (white open arrows). (Adapted with permission from Abrahams et al.⁶)

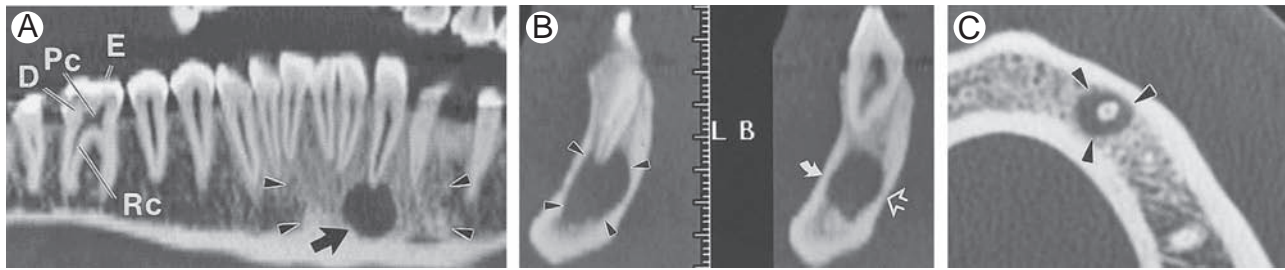


Figure 8 CT of periapical disease. (A) Reformatted panoramic image demonstrates rounded, focal lucency centered at root apex of left lateral incisor (black arrow). Note subtle, increased zone of sclerosis (black arrowheads) compatible with condensing osteitis from chronic infection. E, enamel; D, dentin; Pc, pulp chamber; Rc (root canal). (B) Cross-sectional views in the same patient demonstrate relationship of periapical lucency (black arrowheads) to the buccal cortex (curved white arrow) and lingual cortex (open white arrow). (Adapted with permission from Abrahams et al.⁶). (C) Axial CT in a different patient demonstrates “target sign,” with central focus of high attenuation representing root and surrounding lucency (black arrowheads) representing periapical inflammatory disease. Note relative sclerosis of surrounding bone compared with other areas of mandible, consistent with condensing osteitis. (Adapted with permission from Abrahams and Berger.³²)

Patients with periapical inflammatory disease may be asymptomatic or may experience tooth pain, sensitivity, or swelling. A periapical abscess presents with severe tooth pain, possible elevation of the affected tooth, and sometimes, systemic symptoms such as fever and lymphadenopathy. The clinical examination of a patient presenting with such symptoms involves tooth percussion, mobility, and palpation, combined with tests of pulp vitality. Dentists use thermal or electric pulp testing to assess the integrity of nerve fibers in the dentine-pulp complex. A cold test involves application of a cold stimulus to a tooth, usually in the form of ice, dry ice, or ethyl chloride sprayed onto a cotton pledget. In electric testing, a pulp tester is connected to a probe and delivers a pulsating electrical stimulus to the tooth in question. Healthy, vital pulp responds by producing a painful sensation that is not pronounced or exaggerated, and which does not linger after removal of the stimulus. Irreversible pulpitis and acute apical periodontitis demonstrate a severe and prolonged painful response, whereas chronic apical periodontitis has no response to thermal or electric testing given that the pulp is already necrotic.

A periapical abscess may erode through the facial or lingual cortical plate of the mandible or maxilla to extend into the adjacent soft tissues. These patients often present with facial swelling, facial mass, pain, and signs of infection. The true source of the infection often eludes radiologists, who may not take the time to thoroughly review images in bone windows and to carefully examine the teeth for possible periapical radiolucencies. This is discussed in greater depth in the “[Extra-Dental Manifestations](#)” section.

There are 3 basic types of periapical inflammatory lesions: granuloma, cyst, and abscess. Radiographically distinguishing among these lesions is difficult, as all of them similarly demonstrate lucency surrounding the root apex⁸ (Fig. 8A and B). On axial CT, lesions demonstrate a “target” appearance, with a central focus of high attenuation representing the root surrounded by lucency representing resorbed bone (Fig. 8C). The size of a periapical lesion cannot be used to predict its histology: granulomata may be large and cysts may be small. As periapical cysts enlarge, they displace adjacent structures and result in progressive resorption of root and alveolar bone. The internal attenuation of granulomata and cysts on CT can also

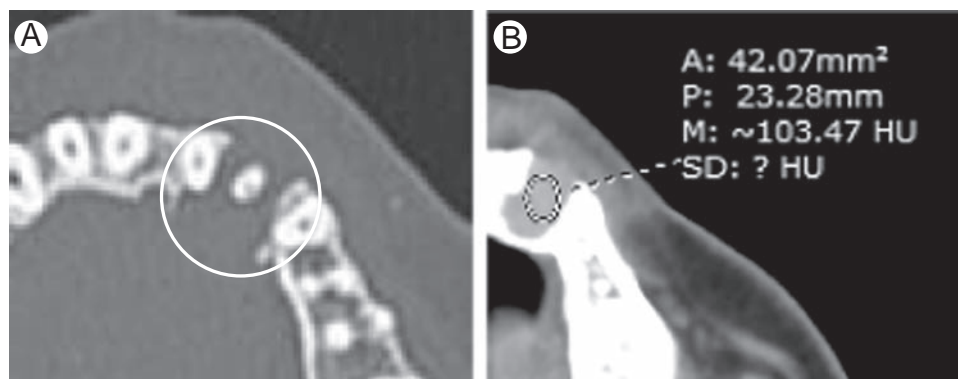


Figure 9 Periapical cyst. (A) Axial CT image in bone window demonstrates an ovoid, expansile lucency in association with the root apex of the left maxillary cuspid (white circle). There is cortical breakthrough along the buccal and lingual surfaces of the left maxillary alveolus. (B) Axial CT of the same section in soft tissue window demonstrates that CT Hounsfield units of the cyst measure soft tissue attenuation, although histopathology was consistent with a benign inflammatory cyst.

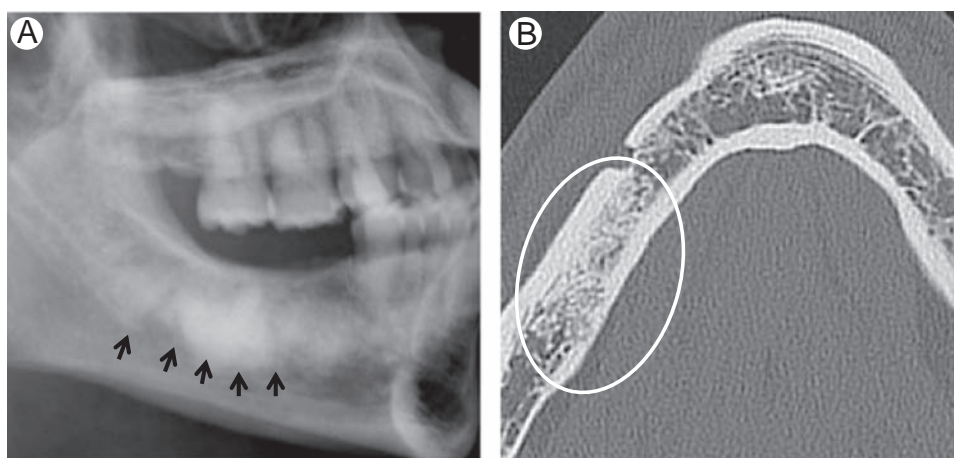


Figure 10 Condensing osteitis. (A) Lateral radiograph demonstrates foci of sclerosis in the mandibular body (black arrows) in the expected location of the root apices in this partially edentulous patient, compatible with condensing osteitis. (B) Axial CT image in a different patient reveals a nonexpansile zone of increased density in the right mandible, with trabecular preservation and without destruction of the adjacent cortex (white circle). The increased density gradually fades into normal bone in the periphery, typical of condensing osteitis.

vary considerably (Fig. 9). Furthermore, it is no longer believed that granulomata must demonstrate ill-defined borders whereas cysts must have sharp borders.¹⁰ Rather, a lesion with well-defined, sharp borders only indicates one that is long standing.¹⁰ Long-standing periapical cysts may occasionally demonstrate dystrophic wall calcifications. Chronic periapical lesions are associated with condensing osteitis (reactive sclerosis of the adjacent bone).¹¹ Although the sclerosis from condensing osteitis may be extensive and very dense, it typically gradually blends into normal bone in the periphery (Fig. 10). Condensing osteitis can also be seen with periodontal disease (Fig. 4). A periapical abscess develops when a granuloma or cyst becomes reinfected and bacteria travel through the necrotic pulp and out of the apical foramen.

Although lucency surrounding the tooth root apex is quite classical for apical periodontitis, odontogenic and nonodontogenic lesions, including, but not limited to, keratocystic odontogenic tumor, cemento-osseous dysplasia, osteomyelitis, osteonecrosis, leukemia, lymphoma, myeloma, and metastasis, may rarely mimic the periapical disease.¹²⁻¹⁶

Treatment of Periapical Disease

After confirming the diagnosis with tests of pulp vitality, the treatment of periapical inflammatory disease involves root canal therapy, surgery, or tooth extraction.^{3,12} After treatment, the periapical radiolucency often begins to fill with bone or scar tissue over the course of several months.^{17,18} However, it is not unusual to see persistence of the periapical radiolucency even after root canal therapy. For small periapical lesions and nonvital teeth, a root canal therapy usually suffices (Fig. 11).¹⁹ Here, the dentist drills a hole in the enamel to access the pulp chamber, after which special endodontic files are used to remove the infection and shape the root canals. The root canals are then sealed with a compound composed of zinc

oxide and gutta percha, a radioopaque latex material with antimicrobial properties. Radiographically, the root canals of treated teeth appear radiopaque rather than normally radiolucent. Sometimes, a metal rod (post) may be inserted into a devitalized root canal and covered by a filling (core) for increased support. Eventually, nonvital teeth discolor and become brittle, necessitating placement of a prosthetic crown as the final stage of the root canal procedure. The crown improves cosmesis and reinforces the underlying tooth. In order for a prosthetic crown to fit, the patient's existing crown is filed down, or if necessary, built up using amalgam or composite resin. Impressions of the teeth are then taken in a material such as polyvinyl siloxane and sent to a laboratory. Impressions are used to form an imprint, or negative mold, of the patient's dentition so that a cast may be constructed, which serves as a model for creation of a crown. There are many different types of materials that may be used to fabricate crowns, which may be metal, porcelain, or porcelain fused to metal.

Perio-Endo Lesions

Inflammatory lesions affecting both the periodontium and pulpal (neurovascular) tissues in varying degrees are termed "perio-endo" lesions. They occur when severe periodontal disease extends to involve the apical foramen at the root apex, representing the most common and direct route of communication between the periodontium and pulp chamber. Furthermore, periodontal pockets can communicate with the neurovascular bundle-containing pulp chamber by way of accessory or lateral canals in the sides of the roots. It is important to note that communications between the periodontal ligament and nerve canals are bidirectional, such that periapical lesions may also travel retrograde toward the gingival margin to result in periodontal disease. Rarely, true combined perio-endo lesions result from concomitant primary periodontal and primary endodontic pathology that join together.

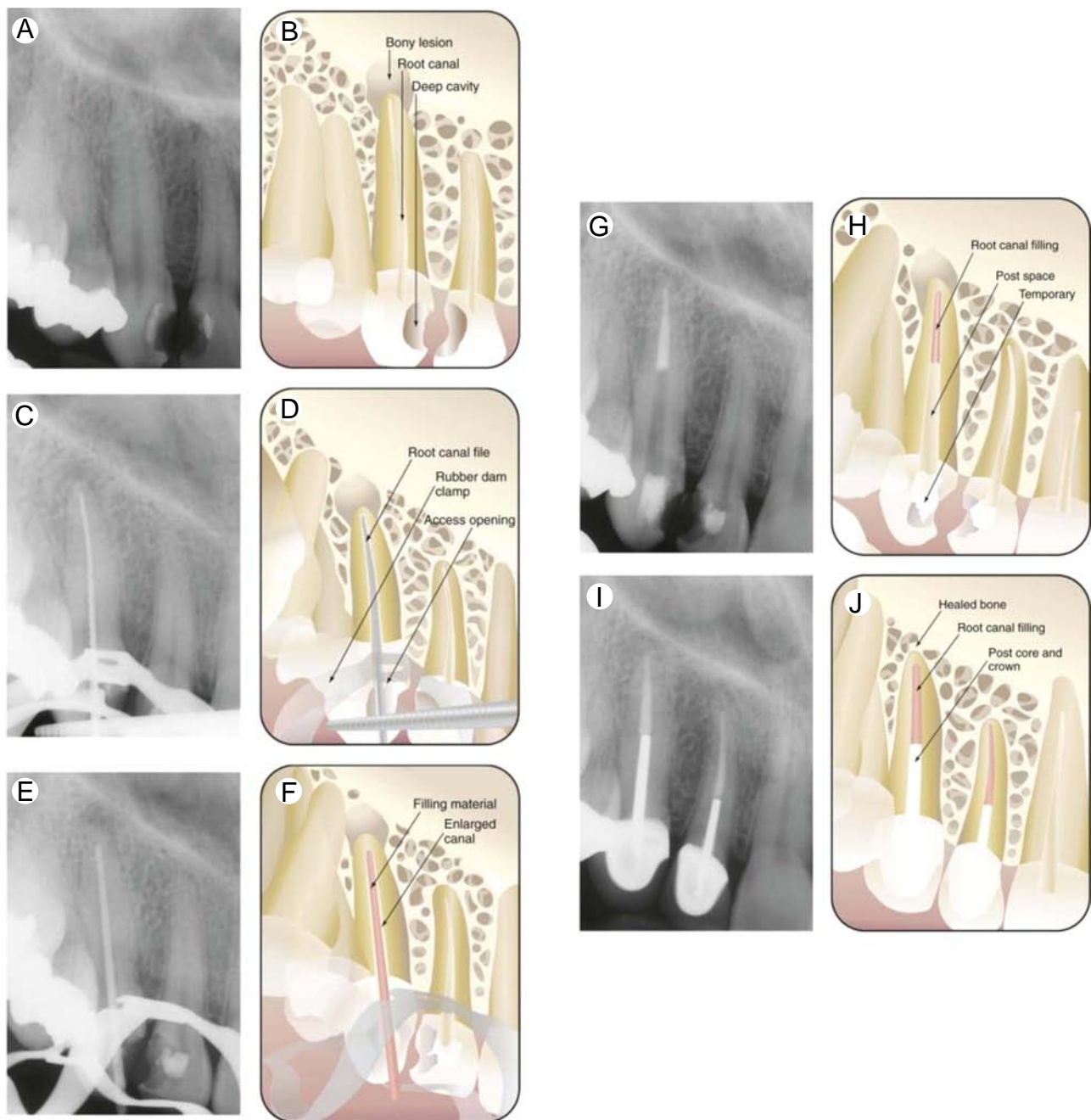


Figure 11 Root canal therapy. Series of radiographs and illustrations demonstrating root canal treatment of a maxillary canine. (A and B) Maxillary canine with a deep carious lesion and periapical lucency. (C and D) Endodontic file corresponding to length of canal used to clean and shape canal. (E and F) Endodontic filling material placed after cleaning and shaping of canal. (G and H) Canal system filled and post space made. (I and J) Follow-up of 1 year shows completed restoration and healed periapical bone. (Adapted with permission from Hargreaves.¹⁶) (Color version of figure is available online.)

On imaging, perio-endo lesions can result in a “floating in air” appearance of the affected tooth (Fig. 12). However, primary malignancies, such as osteosarcoma and Langerhans histiocytosis, may also present with teeth floating in space.^{20,21} The treatment of perio-endo lesions depends on whether the primary pathology is periodontal or endodontic. With an advanced perio-endo lesion, extraction of the affected tooth is often required. True combined lesions should first be treated endodontically, with reevaluation after several months to determine the need for periodontal therapy.

Pericoronitis

Pericoronitis refers to inflammation of the soft tissues surrounding the crown of a partially erupted tooth, typically affecting impacted mandibular third molars in young adults. The partially erupted tooth is covered by soft tissue known as an operculum. Bacteria and debris, either in the setting of poor oral hygiene or trauma, may be deposited beneath an operculum, resulting in inflammation. Patients with pericoronitis clinically present with severe pain and trismus.

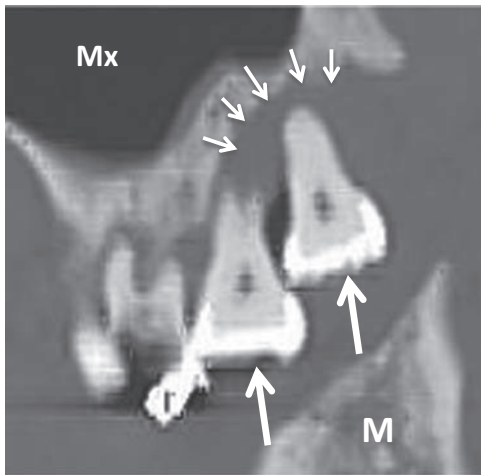


Figure 12 Perio-endo lesion. Sagittal CT image demonstrates combined periodontal and periapical disease with marked resorption of maxillary alveolar bone (short white arrows) that normally surrounds roots. This creates a “floating-in-air” appearance of left first and second maxillary molars (longer white arrows). Mx, maxillary sinus; M, mandible.

Radiographically, pericoronitis presents as bone loss or radiolucency adjacent to the crown, along with localized sclerosis in the surrounding bone. The infection may spread into the deep neck to involve the masticator, submandibular, parapharyngeal, or sublingual spaces.²² The management of acute pericoronitis involves pain relief and antibiotics, as needed. Definitive treatments include operculectomy and tooth extraction. In some cases, optimizing oral hygiene is all that is needed to treat and prevent pericoronitis.

Extra-Dental Manifestations

The roots of maxillary teeth may normally protrude into the adjacent maxillary sinuses. As such, a periapical abscess may perforate through the floor of the maxillary sinus and disrupt the mucoperiosteum (Schneiderian membrane), permitting

access of infection into the sinus and resulting in “odontogenic” sinusitis.^{23,24} Patients with odontogenic sinusitis may complain of purulent nasal discharge, cheek pain, or facial pressure, which do not improve after antibiotic therapy. The organisms isolated from the sinus have been shown to differ from those isolated from odontogenic sinusitis.²⁴ Sagittal and coronal CT images demonstrate focal ballooning or dehiscence of the floor of the maxillary sinus above a periapical lesion associated with unilateral mucosal thickening or sinus opacification (Fig. 13).⁶ Treatment involves periodontal or root canal therapy, as well as administration of antibiotics.²⁵ Less severe periapical disease can appear radiographically as soft tissue mounds of inflammatory tissue surrounding the root apex and protruding into the floor of the maxillary sinus. On axial CT images, these may have the appearance of polyps or retention cysts, and are often misdiagnosed.²³

An oroantral fistula, or abnormal communication between the maxillary sinus and oral cavity, may arise from infection or when an extraction socket fails to heal properly. The connection between the tooth socket and maxillary sinus is lined by epithelium, and patients may experience symptoms similar to sinusitis. On CT, an oroantral fistula appears as a small defect in the cortical floor of the maxillary sinus overlying an extraction socket.^{26–30} The ipsilateral maxillary sinus also demonstrates fluid and mucosal thickening. The defect may be closed using hydroxyapatite, bone graft material, or a surgical flap.

Periodontal and periapical disease may extend into the soft tissues of the head and neck, with involvement of the parapharyngeal, submandibular, anterior visceral, masticator, and sublingual spaces.^{9,31–34} Although dental infection is one of the most common sources of such infections, it is often unnoticed by radiologists, partially because of their unfamiliarity with this region. In all cases of facial swelling, it is essential to view CT images in bone windows so as to identify any offending periapical or periodontal lesions. Periapical infections often break through the facial or lingual cortical plates to involve the surrounding soft tissues (Fig. 14). Periapical disease of the mandibular molars typically involves

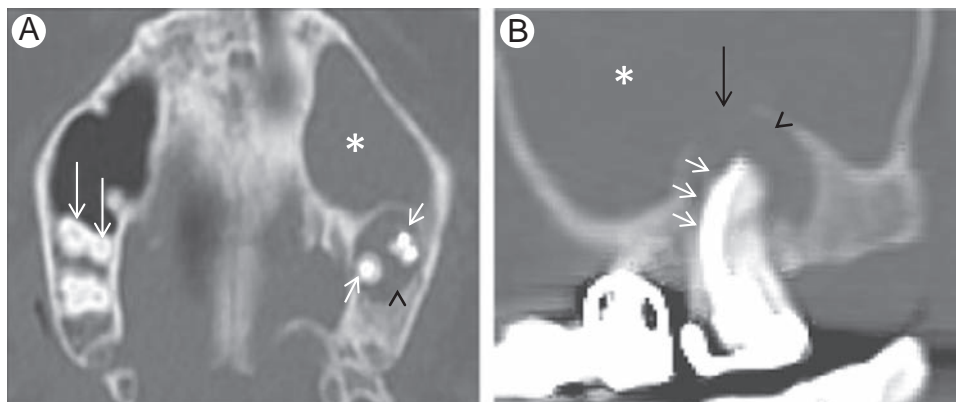


Figure 13 Odontogenic sinusitis. (A) Axial and (B) sagittal CT images demonstrate prior root canal therapy for left maxillary molar. Note very-high-density gutta percha filling the root canals (short white arrows), compared with normal radiolucent root canals on the right (longer white arrows). Periapical radiolucency (black arrowhead) causes focal ballooning and dehiscence (black arrow) of the floor of the left maxillary sinus, as well as complete opacification of left maxillary antrum (white asterisks).

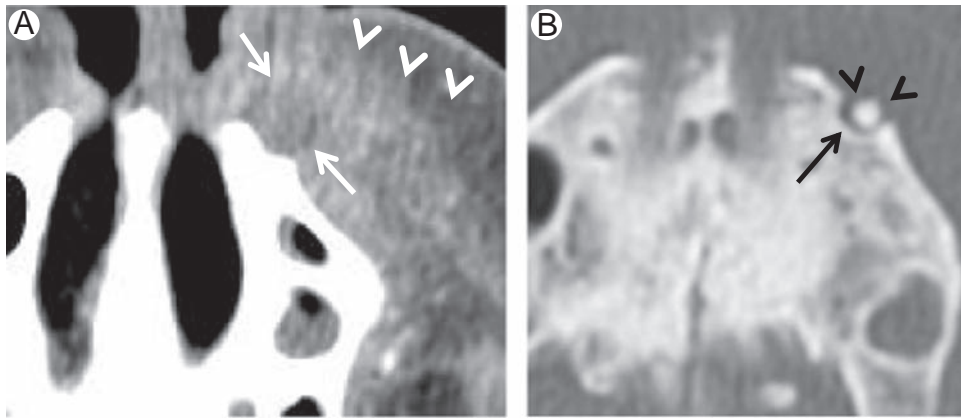


Figure 14 CT of cortical breakthrough. (A) Axial contrast enhanced in soft tissue window demonstrates left-sided swelling with stranding of underlying subcutaneous fat (white arrowheads). There is also a small abscess adjacent to the left maxillary alveolus (white arrows). (B) Axial contrast-enhanced CT in bone window reveals the source of abscess and swelling to be periapical infection and lucency (black arrow), which has broken through the facial cortical plate (black arrowheads) to involve the surrounding soft tissues.

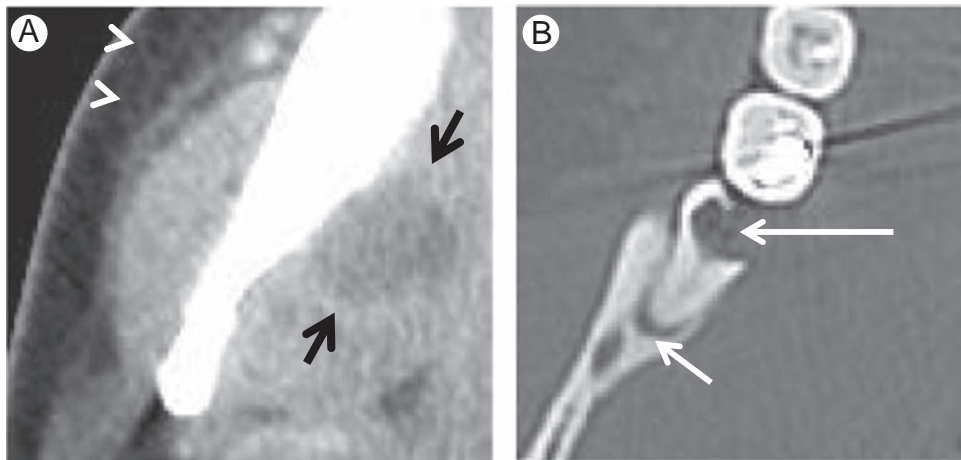


Figure 15 CT of abscess secondary to dental infection. (A) Axial contrast-enhanced CT in soft tissue window demonstrates a fluid collection with rim enhancement (black arrows) in the right masticator space involving medial pterygoid muscle. Note loss of fat planes in the region of the medial pterygoid muscle and minimal stranding (white arrowheads) in the overlying subcutaneous fat. (B) Axial contrast-enhanced CT in bone window (more cephalad section) demonstrates a large carious lesion in the adjacent right third molar (long white arrow), with infection resulting in small periapical lucency (short white arrow), the source of the masticator space abscess in this patient.

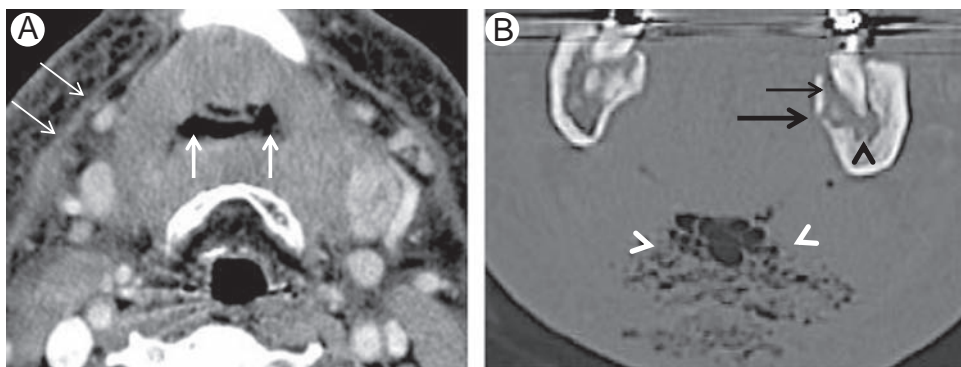


Figure 16 CT of Ludwig's angina. (A) Axial contrast-enhanced CT in soft tissue window shows bilateral facial swelling with edema and stranding of subcutaneous fat, as well as mild thickening of the right platysma muscle (thin white arrows). Note soft tissue gas (thicker white arrows). (B) Coronal bone window reveals the source of infection to be from periodontal (thin black arrow) and periapical disease (black arrowhead) involving left second mandibular molar with lingual cortical breakthrough (thick black arrow). Note the soft tissue gas (white arrowheads).

the submandibular space first, whereas periapical disease of the remaining teeth in the mandible initially extends into the sublingual space.³² On CT, subtle clues to odontogenic deep neck infection include adjacent fat stranding and thickening of the platysma muscle. Contrast-enhanced CT images are useful in demonstrating rim-enhancing subperiosteal or extraosseous abscesses (Fig. 15). Ludwig's angina is a serious, progressive soft tissue infection of the floor of the mouth associated with high morbidity and mortality, as well as the potential for airway compromise^{35,36} (Fig. 16). Patients typically present with fever, neck swelling, and difficulty swallowing or speaking, and are treated aggressively with antibiotics, drainage, and airway management, as needed.^{36,37} Again, CT to evaluate swelling in the face or neck should always be thoroughly reviewed in both bone and soft tissue windows in multiple planes to rule out an odontogenic source of infection.

Conclusions

Inflammatory diseases of the teeth and jaws are commonly encountered in routine radiology practices, and radiologists should be familiar with the varied manifestations of periodontal and periapical disease. Advancements in CT have allowed for remarkable delineation of internal tooth anatomy. Furthermore, dental CT reformatting programs have addressed problems of streak artifact caused by dental restorations, improving the visualization of cortical margins and roots. Even with enhanced imaging algorithms, periodontal and periapical disease continues to be underappreciated by radiologists as an important cause of head and neck pathology. Accurate recognition of inflammatory dental lesions streamlines patient care and allows for prompt, appropriate referral to a dentist for clinical evaluation and treatment.

References

- Zohrabian VM, Poon CS, Abrahams JJ: Embryology and anatomy of the jaw and dentition. *Semin Ultrasound CT MRI* 36(5):397-406, 2015
- Molloy S: Microbiome: Tipping the balance. *Nat Rev Microbiol* 10(1):3, 2012
- Mitchell L, Mitchell DA: *Oxford Handbook of Clinical Dentistry*. USA, Oxford University Press, 29, 2005
- Koenig LJ: Imaging of the jaws. *Semin Ultrasound CT MRI* 36(5):407-414, 2015
- Tyndall DA, Rathore S: Cone-beam CT diagnostic applications: Caries, periodontal bone assessment, and endodontic applications. *Dent Clin North Am* 52(4):825-841, 2008. [vii]
- Scheinfeld MH, Shifteh K, Avery LL, et al: Teeth: What radiologists should know. *Radiographics* 32(7):1927-1944, 2012
- Miracle AC, Mukherji SK: Conebeam CT of the head and neck, part 1: Physical principles. *Am J Neuroradiol* 30(6):1088-1095, 2009
- Abrahams JJ, Frisoli JK, Dembner J: Anatomy of the jaw, dentition, and related regions. *Semin Ultrasound CT MR* 16(6):453-467, 1995
- Abrahams JJ, Berger SB: Inflammatory disease of the jaw: Appearance on reformatted CT scans. *Am J Roentgenol* 170(4):1085-1091, 1998
- Abbott PV, Yu C: A clinical classification of the status of the pulp and the root canal system. *Aust Dent J* 52(suppl 1):S17-S31, 2007
- Holly D, Jurkovic R, Mracna J: Condensing osteitis in oral region. *Bratisl Lek Listy* 110(11):713-715, 2009
- Scholl RJ, Kellett HM, Neumann DP, et al: Cysts and cystic lesions of the mandible: Clinical and radiologic-histopathologic review. *Radiographics* 19(5):1107-1124, 1999
- Pace R, Cairo F, Giuliani V, et al: A diagnostic dilemma: Endodontic lesion or odontogenic keratocyst? A case presentation. *Int Endod J* 41(9):800-806, 2008
- Manfredi M, Vescovi P, Bonanini M, et al: Nevroid basal cell carcinoma syndrome: A review of the literature. *Int J Oral Maxillofac Surg* 33(2):117-124, 2004
- Horner K, Forman GH: Atypical simple bone cysts of the jaws. II: A possible association with benign fibro-osseous (cemental) lesions of the jaws. *Clin Radiol* 39(1):59-63, 1988
- Morag Y, Morag-Hezroni M, Jamadar DA, et al: Bisphosphonate-related osteonecrosis of the jaw: A pictorial review. *Radiographics* 29(7):1971-1984, 2009
- Huumonen S, Orstavik D: Radiographic follow-up of periapical status after endodontic treatment of teeth with and without apical periodontitis. *Clin Oral Investig* 17(9):2099-2104, 2013
- Orstavik D: Time-course and risk analyses of the development and healing of chronic apical periodontitis in man. *Int Endod J* 29(3):150-155, 1996
- Hargreaves KM, Berman LH: *Cohen's Pathways of the Pulp*, (ed 10). St. Louis: Mosby, 2010
- Underhill TE, Katz JO, Pope TL, et al: Radiologic findings of diseases involving the maxilla and mandible. *Am J Roentgenol* 159(2):345-350, 1992
- Keusch KD, Poole CA, King DR: The significance of floating teeth in children. *Radiology* 86(2):215-219, 1966
- Ohshima A, Arijji Y, Goto M, et al: Anatomical considerations for the spread of odontogenic infection originating from the pericoronitis of impacted mandibular third molar: Computed tomographic analyses. *Oral Surg Oral Med Oral Pathol Oral Radiol Endod* 98(5):589-597, 2004
- Abrahams JJ, Glassberg RM: Dental disease: A frequently unrecognized cause of maxillary sinus abnormalities? *Am J Roentgenol* 166(5):1219-1223, 1996
- Brook I: Microbiology of acute and chronic maxillary sinusitis associated with an odontogenic origin. *Laryngoscope* 115(5):823-825, 2005
- Brook I: Sinusitis of odontogenic origin. *Otolaryngol Head Neck Surg* 135(3):349-355, 2006
- Kurien M, Anandi V, Raman R: Maxillary sinus fusariosis in immunocompetent hosts. *J Laryngol Otol* 106(8):733-736, 1992
- Spoor TC, Harding SA: Orbital tuberculosis. *Am J Ophthalmol* 91(5):644-647, 1981
- Felix DH, Wray D, Smith GL, et al: Oro-antral fistula: An unusual complication of HIV-associated periodontal disease. *Br Dent J* 171(2):61-62, 1991
- Abrahams JJ, Berger SB: Oral-maxillary sinus fistula (oroantral fistula): Clinical features and findings on multiplanar CT. *Am J Roentgenol* 165(5):1273-1276, 1995
- Abrahams JJ: Dental CT imaging: A look at the jaw. *Radiology* 219(2):334-345, 2001
- Yonetsu K, Izumi M, Nakamura T: Deep facial infections of odontogenic origin: CT assessment of pathways of space involvement. *Am J Neuroradiol* 19(1):123-128, 1998
- Kim HJ, Park ED, Kim JH, et al: Odontogenic versus nonodontogenic deep neck space infections: CT manifestations. *J Comput Assist Tomogr* 21(2):202-208, 1997
- Obayashi N, Arijji Y, Goto M, et al: Spread of odontogenic infection originating in the maxillary teeth: Computerized tomographic assessment. *Oral Surg Oral Med Oral Pathol Oral Radiol Endod* 98(2):223-231, 2004
- Abrahams JJ, Kalyanpur A: Dental implants and dental CT software programs. *Semin Ultrasound CT MR* 16(6):468-486, 1995
- Nguyen VD, Potter JL, Hersh-Schick MR: Ludwig angina: An uncommon and potentially lethal neck infection. *Am J Neuroradiol* 13(1):215-219, 1992
- Rana RS, Moonis G: Head and neck infection and inflammation. *Radiol Clin North Am* 49(1):165-182, 2011
- Osborn TM, Assael LA, Bell RB: Deep space neck infection: Principles of surgical management. *Oral Maxillofac Surg Clin North Am* 20(3):353-365, 2008

Lesions of the Jaw



Kristine M. Mosier, DMD, PhD

Imaging of lesions within the maxilla and mandible is often fraught with difficulty owing to the similarity in the imaging appearance of a diverse array of pathological processes. Principally, lesions arise from either odontogenic sources or from primary bone lesions. The response of the cancellous and cortical bone to pathologic insult can be expressed either through an osteolytic or an osteoblastic response; thus the majority of lesions within the jaws can be classified as cystic or lytic appearing, sclerotic, or a mixture of the two. This article will review the imaging features of the most common cysts, fibro-osseous lesions, benign and malignant neoplasms, and highlight those features key to the differential diagnosis.
Semin Ultrasound CT MRI 36:444-450 © 2015 Elsevier Inc. All rights reserved.

Introduction

Imaging of lesions within the maxilla and mandible is often fraught with difficulty owing to the similarity in the imaging appearance of a diverse array of pathologic processes. Principally, lesions arise from either odontogenic sources (lesions arising from tooth forming epithelium) or primarily from bone. The response of the cancellous and cortical bone to pathologic insult can be expressed either through an osteolytic or an osteoblastic response; thus, most lesions within the jaws can be classified as cystic or lytic appearing, sclerotic, or a mixture of the two. This article will review the imaging features of the most common cysts, fibro-osseous lesions, benign and malignant neoplasms, and highlight those features key to the differential diagnosis.

Cystic Lesions: Cysts and Benign Tumors

Most lesions arising within the jaws present with some form of osseous demineralization, rarefaction, or remodeling rendering them lytic or cystic appearing on imaging. The degree of osseous rarefaction and remodeling will differ among inflammatory, benign, and malignant lesions, and it is this feature, along with location of the lesion, which allows for differentiation.

The most common odontogenic cyst is the radicular cyst, which arises secondary to pulpal necrosis of a tooth following endodontal infection or periodontitis. The resultant necrotic cavity surrounding the root apex will undergo subsequent epithelialization by odontogenic epithelium, the rests of Malassez.¹ These lesions are thus intimately associated with the root apex of a tooth and the computed tomographic appearance will essentially be identical to that of apical periodontitis in endodontal disease, except that in the radicular cyst, the lytic area is bounded by a thin sclerotic rim (Fig. 1). A key feature to distinguish this lesion from other noninflammatory cysts is the inflammatory effect on the tooth root, resulting in resorption of the root apex.

The most common noninflammatory cyst in the jaws is the dentigerous cyst or follicular cyst. The dentigerous cyst is a developmental cyst that occurs as a result of cystic degeneration of the reduced enamel epithelium with subsequent fluid accumulation between this epithelial layer and the crown of the developing tooth.¹ Hence dentigerous cysts arise from around the crown of unerupted or impacted teeth, most frequently in the posterior quadrants of the alveolus. The cystic fluid tends to concentrically expand the alveolus with well-defined sharp margins. Morphologically, the distinguishing feature of these lesions, aside from the pericoronal presentation (around the crown), is their tendency to displace the tooth in the opposite direction of the cyst (Fig. 2A). On magnetic resonance imaging (MRI) these lesions are classically T1 hypointense and T2 hyperintense with an enhancing rim; however, the cyst may contain cholesterol crystals or proteinaceous material, rendering the lesions T1 hyperintense (Fig. 2B).

The association of dentigerous cysts with the dentition complicates the differential diagnosis, as the 2 most common benign odontogenic tumors, the keratocystic odontogenic

Department of Radiology and Imaging Sciences, Indiana University School of Medicine, Indianapolis, IN.

Address reprint requests to Kristine M. Mosier, DMD, PhD, Department of Radiology and Imaging Sciences, Indiana University School of Medicine, 355 W 16th St, Suite 4100, Indianapolis, IN 46202.
E-mail: kmosier@iupui.edu

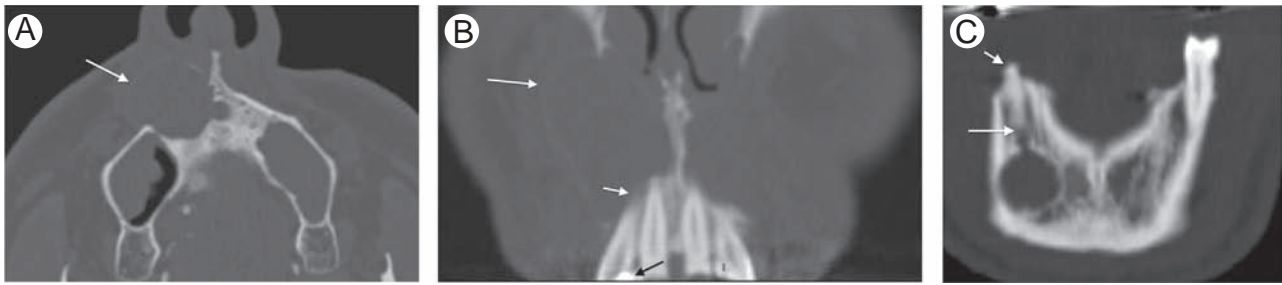


Figure 1 Radicular cyst. (A) Axial computed tomographic (CT) image with bone algorithm shows an expansile cystic mass in the right maxillary alveolus. Note the thin, corticated rim (arrow). (B) Coronal bone CT from the same patient in (A) shows that the cystic mass (long white arrow) is intimately associated with resorption of the root apex (short white arrow). Endodontal infection from the restoration (black arrow) was the culprit in this case. (C) Coronal bone CT shows a well margined and thinly corticated cystic mass in the right mandible. Note the communication with the root apex (long arrow) and the loss of the crown of the tooth (short arrow).

tumor (KCOT) and the Ameloblastoma, will likewise appear cystic.

Indeed, the most common benign odontogenic tumors involving the maxilla and mandible all share a tendency to appear as a cystic expansile mass; importantly they all demonstrate locally aggressive behavior and relatively high recurrence rate if incompletely treated. The surgical management is different depending on the tumor and therefore a finely honed differential diagnosis is important to ensure adequate treatment. The KCOT was formerly known as the odontogenic keratocyst (OKC); the change in terminology reflects more recent molecular phenotyping demonstrating overlapping molecular profiles with other benign and malignant odontogenic and nonodontogenic tumors.^{2,3} KCOTs may arise anywhere within the jaws, but more frequently arise in the posterior quadrants and have a predilection for the posterior body, angle, and ramus of the mandible.⁴ These lesions originate from odontogenic epithelium (remnants of the dental lamina) and as such will be centered within the tooth bearing areas of the alveolus, and are often associated with unerupted or impacted teeth. In contrast to the dentigerous cyst, however, these lesions when larger will envelop the entire tooth. Larger lesions will be mildly expansile, however, those in the mandible have a tendency to enlarge along the long axis of

the body of the mandible before expanding medial laterally (Fig. 3A). On MRI, KCOTs generally appear as a cystic mass with a homogenous T2-hyperintense signal of the central contents and a thin to moderately thick enhancing rim. KCOTs may contain perakeratin or orthokeratin that will shorten the T1, thus these lesions will appear hypointense to mildly hyperintense on T1-weighted images. This latter feature helps to distinguish them from other benign odontogenic tumors, whereas the tendency to envelop the entire tooth would distinguish it from a dentigerous cyst. KCOTs are typically single lesions; however, there is a subset of multiple KCOTs that occur in association with nevoid basal cell syndrome (Gorlin-Goltz) syndrome (Fig. 3B and C). The odontogenic lesions in nevoid basal cell syndrome often present as either multiple KCOTs within the maxilla and or the mandible, however, more uncommonly, there may be multiple dentigerous cysts or mixed combinations with KCOTs.⁵ Extra-alveolar extension, and in particular, extension into the orbit from maxillary lesions or extension into the masticator space or pterygopalatine fissure from maxillary or mandibular lesions is important to recognize as soft tissue spillage of the viscous contents of these lesions is notoriously difficult to extirpate surgically. Owing to breach of the alveolus and contamination by oral cavity flora, extra-alveolar extension of KCOTs or any

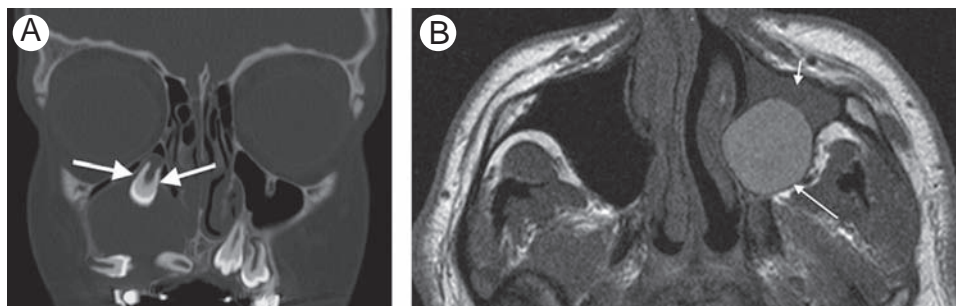


Figure 2 Dentigerous cyst. (A) Coronal bone CT shows a large cystic mass extending from around the crown and cemental-enamel junction (CEJ, arrows) of an unerupted tooth. The tooth is displaced superiorly, whereas the leading edge of the cyst has displaced surrounding unerupted teeth inferiorly. (B) Axial T1-weighted magnetic resonance (MR) image of a dentigerous cyst shows a sharply margined hyperintense cystic mass (long arrow). Compare the hyperintensity of the cyst with the isointense (cf. muscle) signal of the associated mucosal thickening in the maxillary sinus (short arrow). CT, computed tomographic.

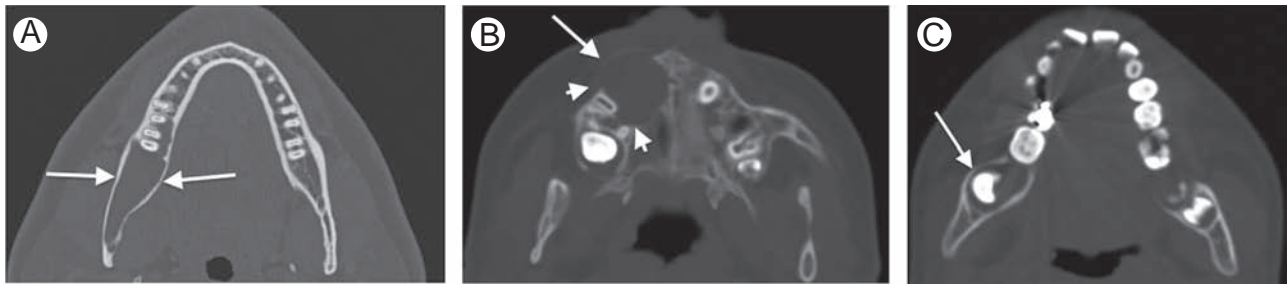


Figure 3 Keratocystic odontogenic tumor. (A) Axial bone CT shows a classic appearance of keratocystic odontogenic tumor (KCOT). The cystic mass in the right mandible demonstrates uniform expansion along the long axis. Note the smoothly margined thinning of the buccal and lingual cortex (arrows) reflecting the benign but locally aggressive character of the mass. (B) Axial bone CT of a different patient with nevoid basal cell carcinoma syndrome (NBCCS). The cystic mass appears similar to the radicular cyst in [Figure 1](#) (arrow); however, the expansion along the buccal cortex and in between the roots of adjacent teeth (arrowheads) suggests a benign but more aggressive mass. (C) Axial bone CT in the same patient as (B). The cystic expansile mass enveloping the developing molar is classic KCOT; this lesion combined with the maxillary lesion should prompt consideration of NBCCS. CT, computed tomographic.

other intra-alveolar neoplasm may involve a superimposed inflammatory component, mimicking osteomyelitis and cellulitis; the presence of an expansile cystic mass, however, should reveal the neoplastic etiology. Controversy remains over the optimal treatment of KCOTs; nevertheless, most lesions are treated using enucleation with or without peripheral ostectomy followed by the application of a superficial chemical necrosing and tissue fixation agent, Carnoy solution, to remove any cyst wall epithelial remnants. Larger lesions are treated with marginal or segmental resection. Recurrence rates range from approximately 6%-30%,^{6,7} with recurrence rates generally higher for enucleation.

Ameloblastomas are the second most common benign odontogenic tumor and share a tendency for being locally aggressive and having a relatively high recurrence rate. Like the KCOT, Ameloblastomas arise from dental lamina and likewise are found within the tooth bearing areas of the alveolus similarly most prevalent in the posterior quadrants and having a predilection for the mandible. There are a number of histologic subtypes of ameloblastoma, with the multicystic

and unicystic follicular types most common; the less common desmoplastic, plexiform, and acanthomatous variants are generally indistinguishable on conventional imaging. Ameloblastomas are mixed cystic and solid lesions with the multicystic lesions generating the more classically known “bubbly” appearance produced by multiple intralesional septations ([Fig. 4A](#)); with contrast administration, these septations will typically enhance. The unicystic variants may contain a mural nodule that likewise enhance; identification of a mural nodule is key to differentiating this variant from the KCOT or the dentigerous cyst ([Fig. 4B](#)). The less common subtypes may have more aggressive appearing features, or like the desmoplastic subtype, may appear in more anterior alveolar locations ([Fig. 4C](#)).⁷ On MRI, the cystic elements will be T2 hyperintense, which helps to distinguish them from other benign mesenchymal odontogenic or malignant neoplasms. Moreover, although these lesions will appear cystic, the ameloblastoma is a more cellular lesion than the KCOT and thus the solid elements will generally restrict diffusion to a greater degree.⁸⁻¹⁰



Figure 4 Ameloblastoma. (A) Axial bone CT demonstrates the multiseptated or loculated “bubbly” appearance of the multicystic ameloblastoma. The septations are somewhat coarse and the expansion is more eccentric (arrow), rather than along the long axis. Adapted from with permissions from Mosier K: Ameloblastoma, in Harnsberger (ed): *Diagnostic Imaging Head and Neck*. Altona, Manitoba, CA, Amirsys, 2011, pp. 1-15, 30. (B) Axial contrast-enhanced CT of a unicystic ameloblastoma shows a cystic mass eccentrically expanding the buccal and lingual cortex; compare this with the KCOT in [Figure 3A](#). The enhancing mural nodule (arrow) is characteristic for ameloblastoma. (C) Axial bone CT of a desmoplastic variant of ameloblastoma. The expansile lobulated and loculated mass (long arrow) is typical for ameloblastoma; the more anterior location is less common. However, the location, aggressive sclerotic response and periosteal reaction (short arrow) are seen more often in this variant. CT, computed tomographic.

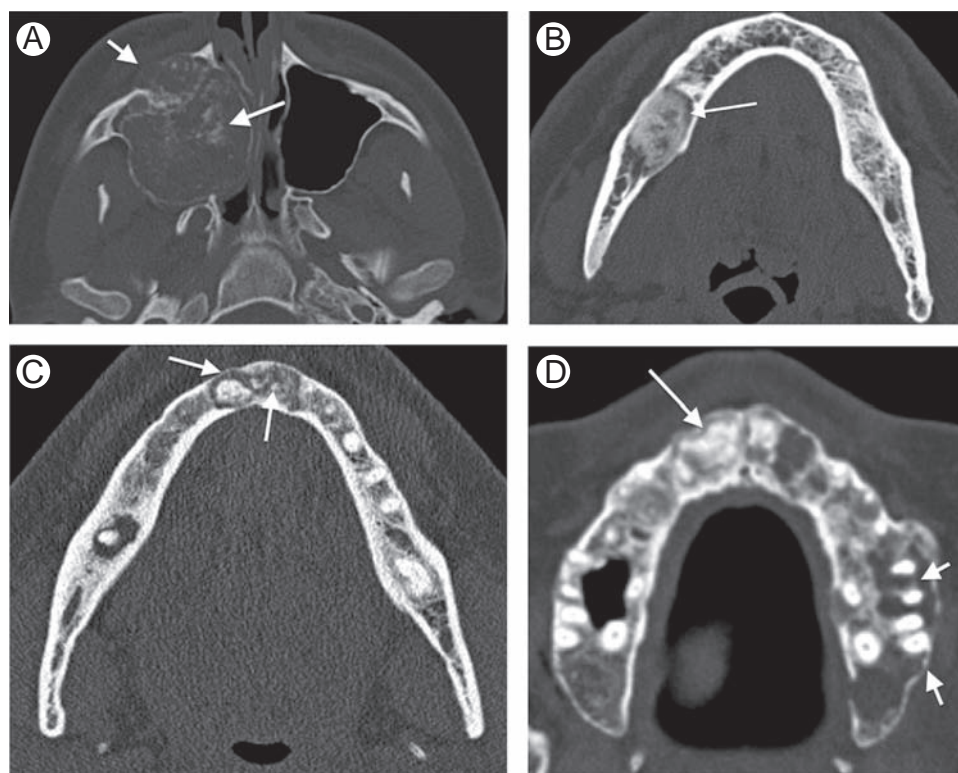


Figure 5 Fibro-osseous lesions. (A) Axial bone CT: ossifying fibroma. The presence of multiple internal foci of calcification within the cystic mass (long arrow) and gently lobulated borders (short arrow) should prompt consideration of benign calcifying/ossifying neoplasm. (B) Axial bone CT: ossifying fibroma. The heterogeneous but largely sclerotic mass represents a more mature fibroma. A key feature of these fibro-osseous lesions is the lucent rim (arrow) representing the fibrous capsule. (C) Axial bone CT: periapical cemento-osseous dysplasia. The multiple calcified masses inferior to the root apices of the anterior mandibular dentition and mild associated expansion (arrows) is typical of these lesions as well as the central sclerosis surrounded by a peripheral radiolucent zone. (D) Axial bone CT: florid osseous dysplasia. Multiple ossified masses are distributed throughout the maxillary alveolus (long arrow). Note the associated expansion, and lucent fibrous matrix and or simple bone cysts scalloping in between the roots of the dentition (short arrows). CT, computed tomographic.

Mixed Cystic and Sclerotic Lesions: Benign Fibro-Osseous Lesions

Bony expansion and septation of the alveolus represents the osteolysis, replacement and or remodeling of the cancellous trabeculation by a neoplastic mass and as such these findings are relatively nonspecific to the odontogenic neoplasms. Non-odontogenic neoplasms will similarly expand bone and may be septated. Ossifying fibromas (Cemento-ossifying fibromas) are among the most common nonodontogenic neoplasms to arise within the alveolus, but as their tissue of origin is not odontogenic, they are found distributed throughout the facial bones. Those arising within the alveolus are generally centered within the non-tooth bearing areas of the alveolus. Ossifying fibromas are the unique neoplastic manifestation of a diverse array of fibro-osseous lesions of the maxillofacial complex in which normal bone is replaced by a connective tissue matrix undergoing various degrees of mineralization.¹¹⁻¹³ These lesions are expansile even when small and varying rates of trabecular ingress at the tumor margins will result in septation, often having the characteristic of being thin and wispy.

The solid tumor and degree of intralésional mineralization, however, is what differentiates these lesions from the more common odontogenic lesions. Ossifying fibromas are expansile, often cystic appearing masses with varying degrees of calcification or ossification and as such these lesions may appear either cystic or largely sclerotic depending on the degree of internal calcification (Fig. 5A and B). Non-neoplastic fibro-osseous lesions are common in the jaws and although controversy prevails over the etiology of these lesions, they are believed to represent reactive lesions.^{7,14} Periapical cemento-osseous dysplasia is a benign fibro-osseous lesion that occurs around the root apices of the teeth. These lesions begin as lucent areas of fibrous tissue deposition that centrally ossify over time producing a sclerotic appearing mass with lucent rim, often with associated mild expansion of the alveolus (Fig. 5C). Notably the dentition will typically be intact without caries or periodontal disease; a key diagnostic feature to distinguish this lesion from the apical inflammatory lesions of apical periodontitis or condensing osteitis. Periapical cemento-osseous dysplasia most commonly presents in the anterior mandibular dentition, has a predilection for African Americans, and usually involves a single quadrant.

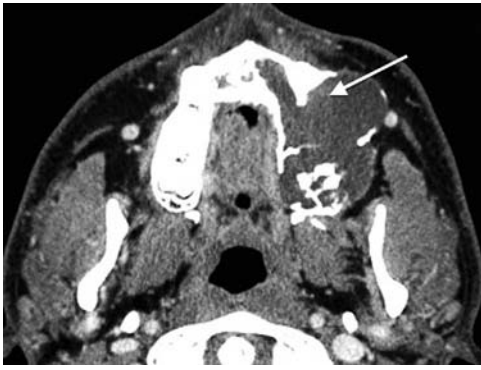


Figure 6 Odontogenic myxoma. Axial contrast-enhanced CT: the expansile lobulated cystic mass looks like an ameloblastoma; however, the diffuse areas of mild hyperdensity (arrow) reflecting the myxomatous stroma differentiate this lesion from the discrete mural nodule of the ameloblastoma. CT, computed tomographic.

Involvement of multiple quadrants by these lesions indicates the exuberant form known as florid osseous (or florid cemento-osseous) dysplasia (Fig. 5D).^{7,14-16}

Mixed Cystic and Sclerotic or Sclerotic Lesions: Benign and Malignant Tumors

The mixture of soft tissue neoplastic elements and cartilaginous or ossified neoplastic elements, or the osseous destruction of bone, will generate the appearance of lesions having a mixed cystic and sclerotic composition. Although the most common benign odontogenic neoplasms are typically cystic in appearance, more uncommon or rare lesions including the odontogenic myxoma, and the calcifying epithelial odontogenic cyst and calcifying epithelial odontogenic tumor will appear mildly dense or with intralesional calcifications, respectively (Fig. 6).

Malignant tumors of the jaws are very rare and arise principally from 4 sources: (1) osseous, cartilaginous, or neuroectodermal elements giving rise to sarcomas,

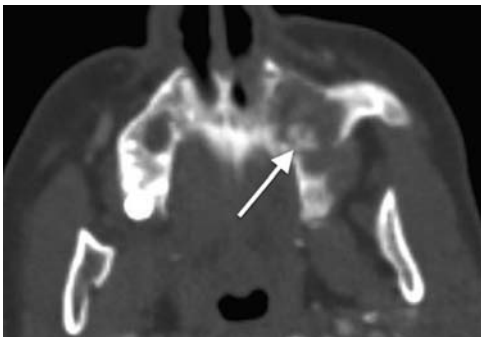


Figure 7 Chondrosarcoma. Axial bone CT shows an expansile mass in the left maxilla containing multiple “whorled” areas of calcification (arrow). The appearance of these calcifications, bone destruction, and the extra-alveolar extension differentiate this lesion from the ossifying fibroma in Figure 5A. CT, computed tomographic.

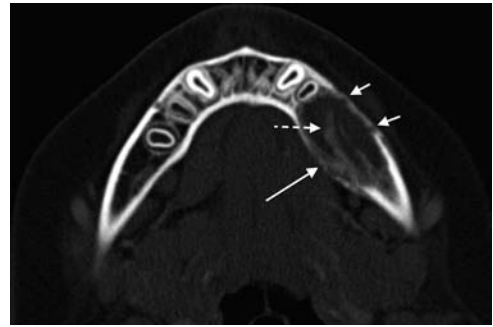


Figure 8 Osteosarcoma. Axial bone CT shows an expansile lytic mass with peripheral sclerosis and periosteal reaction (long arrow), as well as thickening and sclerosis of the inferior alveolar nerve canal (dashed arrow). The focal pockets of erosion in the buccal cortex (short arrows) reveal the aggressive or malignant nature of this lesion. CT, computed tomographic.

(2) malignant transformation of odontogenic epithelium, (3) malignant transformation of intraosseous squamous or salivary epithelial remnants, or (4) from metastatic disease.

Chondrosarcoma in the jaws represents less than 10% of all chondrosarcomas and occurs more commonly in the maxilla than in the mandible with the production of calcified matrix producing a lobulated mass (Fig. 7).¹⁷⁻¹⁹

Osteosarcoma of the jaws accounts for approximately 4% of all the primary malignant jaw lesions and approximately 5% of all osteosarcomas.²⁰⁻²² Osteosarcoma of the jaw typically presents later than those of the long bones with peak incidence in the third to fourth decade, and although most arise spontaneously from osteoid producing neoplastic cells, these lesions can occur following radiation to the face or jaws, with an average lag time of approximately 10 years.^{21,22} Depending on the histologic subtype, varying degrees of osteoid and chondroid matrix are produced, nevertheless, on imaging these are lytic destructive lesions typically with periosteal reaction (Fig. 8). MR imaging offers the benefit of determining the degree and extent of cancellous involvement and extra-alveolar extension. Osteogenic sarcomas are heterogeneous in their signal intensity depending on the amount of mineralized matrix; the mineralized components demonstrating low T1 and T2, whereas the solid tumor will demonstrate hypointense to intermediate T1 and hyperintense T2 signal. With gadolinium, these lesions will show variable enhancement.

The computed tomographic and MR appearance may further help to differentiate osteosarcomas from other sarcomas such as Ewing sarcoma. Ewing sarcoma is a small round cell sarcoma grouped among the primitive neuroectodermal malignant neoplasms (primitive neuroectodermal tumor²³⁻²⁵), and has a higher rate of distant metastases than the osteosarcomas. Ewing sarcomas typically present in childhood or adolescence as an expansile mass in the jaws, most frequently in the mandible (Fig. 9A). Owing to their histologic character, on MRI these lesions generally are more T2 hyperintense than osteosarcomas, and generally demonstrate greater, albeit variable, and enhancement (Fig. 9B).²⁶ Although Ewing sarcoma characteristically causes expansion of the alveolus, more rarely, they may present as a diffuse marrow replacing

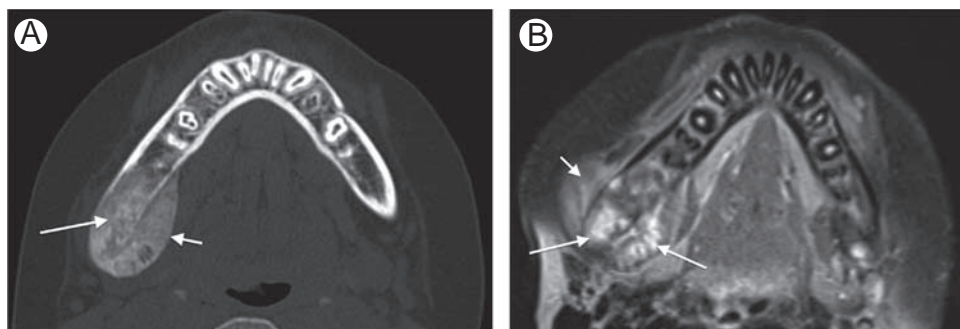


Figure 9 Ewing sarcoma. (A) Axial bone CT demonstrates a typical appearance of Ewing sarcoma. The expanded mandible is filled with heterogeneous but solid mass (long arrow) with a significant periosteal reaction (short arrow). (B) Axial contrast-enhanced MRI with fat saturation in the same patient shows the more avidly enhancing areas in the mandible and the periosteum (long arrows). Note the extra-alveolar extension into the masseter muscle (short arrow). CT, computed tomographic.

process, necessitating differentiation from osteosarcoma, osteomyelitis or osteonecrosis.

Malignant transformation of odontogenic epithelium is very rare and accounts for less than 1% of the malignancies involving the jaws.²⁷ Odontogenic carcinomas are ameloblastomas with histologic features of carcinoma including abnormal mitoses. The presence of benign ameloblastic or amelofibroma proliferation with accompanying malignant mesenchymal stroma is termed an odontogenic sarcoma. The combination of an ameloblastic carcinomatous component and a malignant spindle cell component is termed an odontogenic carcinosarcoma. Malignant ameloblastomas are distinct from odontogenic carcinomas, having features of a primary benign ameloblastoma and demonstrated locoregional or distant metastasis.²⁸⁻³² The broad overlap in histologic components renders the imaging nonspecific; the keys to the differential being an intra-alveolar tooth bearing location, relatively hyperenhancing components with accompanying aggressive extra-alveolar extension or lymphadenopathy (Fig. 10).

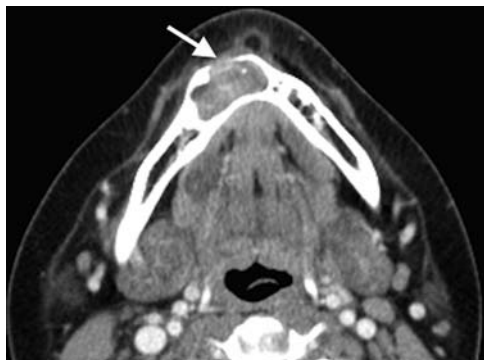


Figure 10 Odontogenic sarcoma. Axial contrast-enhanced CT shows a moderately enhancing destructive mass in the anterior mandible. The amount of enhancement together with the destruction of the buccal cortex and extra-alveolar extension (arrow) are the clues that suggest this is not a benign odontogenic neoplasm. CT, computed tomographic.

Finally, metastasis to the jaws is similarly very rare with the most common primary sites consisting of the breast, adrenal, colorectal, and thyroid for women, and lung, prostate, and kidney for men. These lesions are typically solitary lesions occurring anywhere in the jaws, more common in the mandible.³³⁻³⁶ Most are adenocarcinomas and as such will generally appear more solid and osteolytic than the benign odontogenic lesions. Metastatic renal cell is a hypervascular tumor and often will demonstrate flow voids; in these lesions the bone destruction, and intra- and extra-alveolar extension differentiates them from vascular malformations.

In summary, this article summarizes the variety of common benign and malignant lesions affecting the jaws that give rise to cystic or sclerotic appearing processes. An understanding of the relationship between the different tissues of origin and their associated pathophysiologic abnormalities allows more simplified approach to the differential diagnosis and ensures better patient management.

References

1. Avelar RL, Antunes A, Carvalho RWF, et al: Odontogenic cysts: A clinicopathological study of 507 cases. *J Oral Sci* 51(4):581-586, 2009
2. Henley J, Summerlin DJ, Tomich C, et al: Molecular evidence supporting the neoplastic nature of the odontogenic keratocyst: A laser capture microdissection study of 15 cases. *Histopathology* 47(6):582-586, 2005
3. Agaram NP, Collins BM, Barnes L, et al: Molecular analysis to demonstrate that odontogenic keratocysts are neoplastic. *Arch Pathol Lab Med* 128:313-317, 2004
4. Kaneda T, Minami M, Kurabayashi T: Benign odontogenic tumors of the mandible and maxilla. *Neuroimaging Clin N Am* 13(3):495-507, 2003
5. Manfredi M, Vescovi P, Bonanini M, et al: Nevoid basal cell carcinoma syndrome: A review of the literature. *Int J Oral Maxillofac Surg* 33(2):117-124, 2004
6. Chirapathomsakul D, Sastravaha P, Jansisanont P: A review of odontogenic keratocysts and the behavior of recurrences. *Oral Surg Oral Med Oral Pathol Oral Radiol Endod* 101(1):5-9, 2006
7. Regezi JA: Odontogenic cysts, odontogenic tumors, fibrous, and Giant Cell Lesions of the Jaws. *Mod Pathol* 15(3):331-341, 2002
8. Minami M, Kaneda T, Ozawa K, et al: Cystic lesions of the maxillomandibular region: MR imaging distinction of odontogenic keratocysts and ameloblastomas from other cysts. *Am J Roentgenol* 166(4):943-949, 1996
9. Sumi M, Ichikawa Y, Katayama I, et al: Diffusion-weighted MR imaging of ameloblastomas and keratocystic odontogenic tumors: Differentiation by

- apparent diffusion coefficients of cystic lesions. *AJNR Am J Neuroradiol* 29:1897-1901, 2008
10. Weissman JL, Synderman CH, Yousem SA, et al: Ameloblastoma of the maxilla: CT and MR appearance. *AJNR Am J Neuroradiol* 14:223-226, 1993
 11. Alwai F: Benign fibro-osseous diseases of the maxillofacial bones. A review and differential diagnosis. *Am J Clin Pathol* 118(suppl):S50-S70, 2002
 12. Brannon RB, Fowler CB: Benign fibro-osseous lesions: A review of current concepts. *Adv Anat Pathol* 8:126-143, 2001
 13. Toyosawa S, Yuki M, Kishino M, et al: Ossifying fibroma vs fibrous dysplasia of the jaw: Molecular and immunological characterization. *Mod Pathol* 20:389-396, 2007
 14. Slootweg PJ: Maxillofacial fibro-osseous lesions: Classification and differential diagnosis. *Sem Diag Pathol* 13(2):104-112, 1996
 15. Speight PM, Carlos R: Maxillofacial fibro-osseous lesions. *Curr Diagn Pathol* 12(1):1-10, 2006
 16. MacDonald-Jankowski DS: Florid cemento-osseous dysplasia: A systematic review. *Dentomaxillofac Radiol* 32:141-149, 2003
 17. Finn DG, Goepfert H, Batsakis JG: Chondrosarcoma of the head and neck. *Laryngoscope* 94(12):1539-1544, 1984
 18. Saito K, Unni KK, Wollan PC, et al: Chondrosarcoma of the jaw and facial bones. *Cancer* 76(9):1550-1558, 1995
 19. Prado FO, Nishimoto IN, da Cruz Perez DE, et al: Head and neck chondrosarcoma: Analysis of 16 cases. *Br J Oral Maxillo Surg* 47(7):555-557, 2009
 20. Chindia ML: Osteosarcoma of the jaw bones. *Oral Oncology* 37(7):545-547, 2001
 21. Laksar S, et al: Osteosarcoma of the head and neck region: Lessons learned from a single-institution experience of 50 patients. *Head Neck* 30(8):1020-1026, 2008
 22. Nissanka EH, Amaraturunge EAPD, Tilakaratne WM: Clinicopathological analysis of osteosarcoma of jaw bones. *Oral Dis* 13(1):82-87, 2007
 23. Poramate PA, Bellefqih S, Bertolus C, et al: Ewing's sarcoma of the jaw bones in adult patients: 10 Year experiences in a Paris university hospital. *J Craniomaxillofac Surg* 36(8):450-455, 2008
 24. Delattre O, Zuchman J, Melot T, et al: The Ewing family of tumors—A subgroup of small-round-cell tumors defined by specific chimeric transcripts. *N Engl J Med* 331:294-299, 1994
 25. Daw NC, Mahmoud HH, Meyer WH, et al: Bone sarcomas of the head and neck in children. *Cancer* 88(9):2172-2180, 2000
 26. Gorospe L, Fernandez-Gil MA, Garcia-Raya P, et al: Ewing's sarcoma of the mandible: Radiologic features with emphasis on magnetic resonance appearance. *Oral Surg Oral Med Oral Pathol Oral Radiol Endod* 91(6):728-734, 2001
 27. Ebenezer V, Ramalingam B: A cross-sectional survey of prevalence of odontogenic tumors. *J Oral Maxillofac Surg* 9(4):369-374, 2010
 28. Houston G, Davenport W, Keaton W, et al: Malignant (metastatic) ameloblastoma: Report of a case. *J Oral Maxillofac Surg* 51(10):1152-1155, 1993
 29. Inoue N, Shimojyo M, Iwai H, et al: Malignant ameloblastoma with pulmonary metastasis and hypercalcemia. Report of autopsy case and review of the literature. *Am J Clin Pathol* 90(4):474-481, 1988
 30. Slater LJ: Odontogenic sarcoma and carcinomasarcoma. *Semin Diagn Pathol* 16(4):325-332, 1999
 31. Slootweg PJ, Muller H: Malignant ameloblastoma or ameloblastic carcinoma. *Oral Surg Oral Med Oral Pathol* 57(2):168-176, 1984
 32. Verneuil A, Sapp P, Huang C, et al: Malignant ameloblastoma: Classification, diagnostic, and therapeutic challenges. *Am J Otolaryngol* 23(1):44-48, 2002
 33. Sánchez Aniceto G, García Peñín A, de la Mata Pages R, et al: Tumors metastatic to the mandible: Analysis of nine cases and review of the literature. *J Oral Maxillofac Surg* 48(3):246-251, 1990
 34. Bodner L, Sion-Vardy N, Geffen DB, et al: Metastatic tumors to the jaws: A report of eight new cases. *Med Oral Patol Oral Cir Bucal* 11(1):E132-E135, 2006
 35. D'Silva NJ, Summerlin DJ, Cordell KG, et al: Metastatic tumors in the jaws: A retrospective study of 114 cases. *J Am Dent Assoc* 137(12):1667-1672, 2006
 36. Hirsberg A, Leibovich P, Buchner A: Metastatic tumors to the jawbones: Analysis of 390 cases. *J Oral Pathol Med* 23(8):337-341, 1994